



ESAIL D41.2

Design Description of the Remote Unit

Work Package: WP 41

Prepared by: Sven Wagner, Johan Sundqvist, and Greger Thornell, Ångström Space Technology Centre, Uppsala University

Time: Uppsala, February 14th, 2012

Coordinating person: Pekka Janhunen, pekka.janhunen@fmi.fi

WP coordinator: Greger Thornell, greger.thornell@angstrom.uu.se

(List of participants:)

Participant no.	Participant organisation	Abbrev.	Country
1 (Coordinator)	Finnish Meteorological Institute	FMI	Finland
2	University of Helsinki	UH	Finland
3	University of Jyväskylä	UJ	Finland
4	German Aerospace Center	DLR	Germany
5	Ångström Space Technology Centre	ÅSTC	Sweden
6	Nanospace AB	Nanospace	Sweden
7	Tartu Observatory	Tartu	Estonia
8	University of Pisa	Pisa	Italy
9	Alta S.p.A.	Alta	Italy

Table of Contents

1. General description.....	3
1.1. Introduction.....	3
1.2. Applicable documents.....	3
1.3. Main design considerations.....	3
1.4. Overall Remote unit design.....	4
1.5. RU bus components design.....	10
1.6. Design justification.....	14
1.7. Conclusions.....	22
2. Auxiliary Tether Reel Design.....	23
3. Power System.....	25
3.1. Introduction.....	26
3.2. RU Power System design requirements.....	26
3.3. RU power system design concept	31
3.4. RU power system detailed design.....	33
3.5. Mechanical design.....	38
4. Controller and Telemetry.....	47
4.1. Introduction.....	49
4.2. Telemetry system design.....	50
4.3. Optical Beacon design	54
4.4. Control system design.....	57
4.5. Heat shield design.....	61
5. Tether Jettison Mechanism	74
5.1. Introduction.....	75
5.2. RU Tether jettison system design requirements.....	75
5.3. RU Tether jettison system design concept	76
5.4. RU Tether jettison system mechanical design.....	76
5.5. RU Tether jettison system electrical design.....	79
6. Gas Thruster.....	80
6.1. Introduction.....	83
6.2. Applicable documents.....	83
6.3. Requirements definition	83
6.4. Requirements for the Gas Thruster on the RU.....	83
6.5. Trade-off studies and critical design issues.....	87
6.6. Gas Thruster Design.....	97
7. FEEP Thruster.....	102
7.1. Introduction.....	104
7.2. Thruster system.....	106
7.3. Thruster unit configuration	107
7.4. Power and control unit.....	112
7.5. Remote Unit and thruster system Integration.....	116

1. General Description

1.1. Introduction

This document serves to describe the design of the entire Remote Unit (RU), which is to occur 50 to 100 times in the ESAIL spacecraft, and to provide a justification to its embodiment mainly through mechanical and thermal modeling.

Treating the RU as a spacecraft itself, the first part of the report (Chapter 1) can be considered a design description of the spacecraft bus, the purpose of which is to accommodate the RU's subsystems of propulsion, communication, power, etc., and shield them from mechanical and thermal ordeals, whereas other chapters address the design of the subsystems in a similar manner.

All designs have taken the requirement specification, AD-2, into account, and are to a large extent the result of iterative and collaborative work during the course of the project. Correspondence and meetings have been vital for this process, the outcome of which is summarized in Main design considerations.

Both the functionality and context of the RU subsystem are described in detail in AD-1-2.

1.2. Applicable documents

AD-1: "Part B: Description of Work" of final EU E-sail application (final version)

AD-2: D4.1 Requirements specification of the Remote Unit (project deliverable)

AD-3. Arian 5 launch manual

1.3. Main design considerations

Given the ESAIL propulsion principle and the multiplicity of the RU, an almost overwhelming design driver for the hardware is low mass. Adding to this, both the expertise asked for in the realisation of each subsystem, and the desire to be able to switch propulsion system, a concept based on modules or at least assembly is necessary. This limits the application of multifunctionality somewhat, and, in particular, increases the challenge with overall mechanical and thermal design. In addition, the latter aspect is made even more difficult given the minuteness of the RU (correspondingly low thermal mass) and the range of the missions anticipated (0.9 to 4 AU from Sun), which is also a challenge to the power supply. Further to this, the deployment and operation of the electric sail put constraints on the location of the RU's centre of mass and its points of attachment to the rest of the ESAIL craft. From this, and the functionality, stem the following main design-governing principles:

1. The RU design shall permit for implementation of both FEPP and gas thrust, but not simultaneously (ES1-RU-212, AD-2).
2. The two auxiliary tethers (ES1-RU-209, AD-2) shall be individually reeled.
3. The main tether (reeled on the main craft) connects with the RU through a jettison mechanism (ES1-RU-208, AD-2).
4. Energy is generated from solar panels and stored in batteries (ES1-RU-213, AD-2)
5. Parts sensitive to temperature extremes and fluctuations should be accommodated in a thermally controlled environment, henceforth denoted *thermal box* (ES1-RU-201--202, AD-2).
6. This thermal box shall be protected from sunlight with a plate, henceforth denoted *heat shield*, and extensions thereof, henceforth denoted *shading wings* conveniently carrying the solar cells (ES1-RU-201--202, AD-2).
7. The attachment of the thermal box to the heat shield shall provide mechanical support as well as thermal insulation, henceforth denoted *thermal spacers* (ES1-RU-201--202, AD-2).

8. As the RU must tolerate being inclined with respect to sun (ES1-RU-104, AD-2), the size and shape of the thermal shield depend heavily on the height of the thermal box and the length of the spacers.
9. The FEEP system shall be thermally insulated but not contained in the thermal box, whereas the gas thruster system is part of the thermal box.
10. The face of the thermal box opposite to the heat shield, as well as the end faces of the two reel motor housings (facing the same direction) shall be fixed to the main craft until deployment (cf. ES1-RU-204, AD-2).
11. The thermal box shall include a heating element (ES1-RU-201--202, AD-2).
12. Outside the thermal box, there shall be an excess heat dissipator (ES1-RU-201--202, AD-2).
13. With radiation tolerant electronics anticipated for the fulfilled version of the RU, radiation protection is not accounted for.
14. The centre of mass shall be close to the plane defined by the three points of tethering, and outside of the line between the two auxiliary tether connections viewed from centre of ESAIL craft (cf. ES1-RU-103, AD-2).
15. Communication with the ESAIL main craft is made with a beacon and a radio transmitter/receiver. The beacon and dipole antenna are located outside the thermal box and even the shaded part of the RU (ES1-RU-207, 215--217, AD-2).
16. The tether reels are only partly shielded from sunlight.
17. Attitude of RU to Sun is monitored with sun sensors (ES1-RU-215, AD-2).
18. The temperature at critical locations is monitored with thermal gauges (ES1-RU-214, AD-2).

1.4. Overall Remote unit design

The RU design depends on which of the two propulsion systems, Cold Gas or FEEP, it is configured for. Although taken from the former type, Figures 1.1-1.3 illustrate the concept for both. The design is divided into the heat shield with its shading wings and deployment reels, the thermal spacers and the thermal box. This general set up is similar for both systems. A main difference is that the Cold Gas system has been integrated to the thermal box, whereas the FEEP hasn't. This, together with the number, size and direction of the exhausts of the two propulsion systems, has called for tailoring of the framework of the thermal box and the shading wings, an adjustment of the height of the tethering points, and the inclusion of a separate electronics annex between the two reels to accommodate the FEEP electronics.

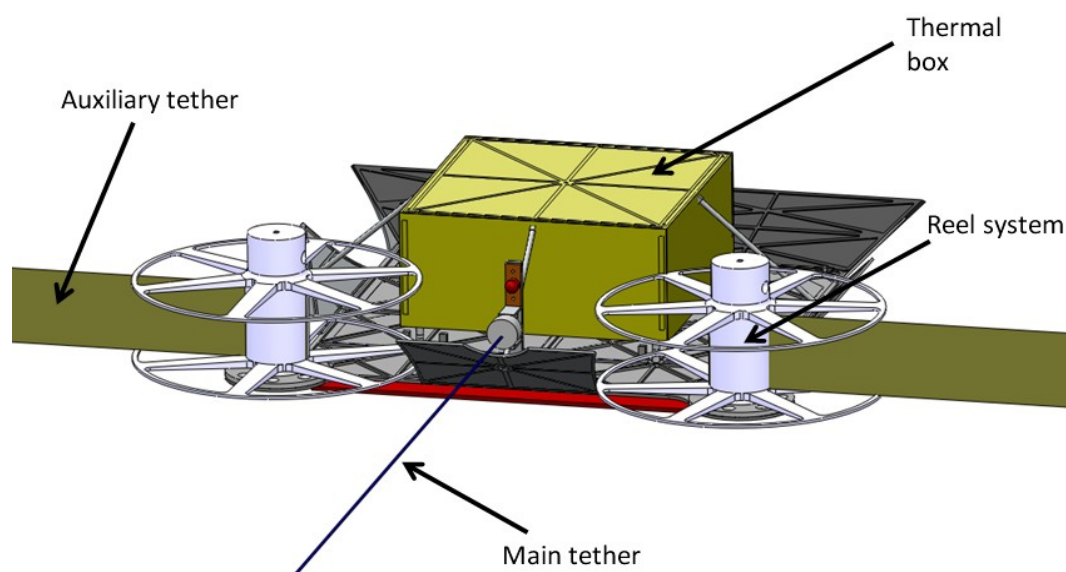


Figure 1.1: Overview of the RU (in Cold Gas propulsion configuration) from front side (side facing main craft), with completely deployed auxiliary tethers. The yellow cover of the thermal box represents the MLI, which insulates the system thermally.

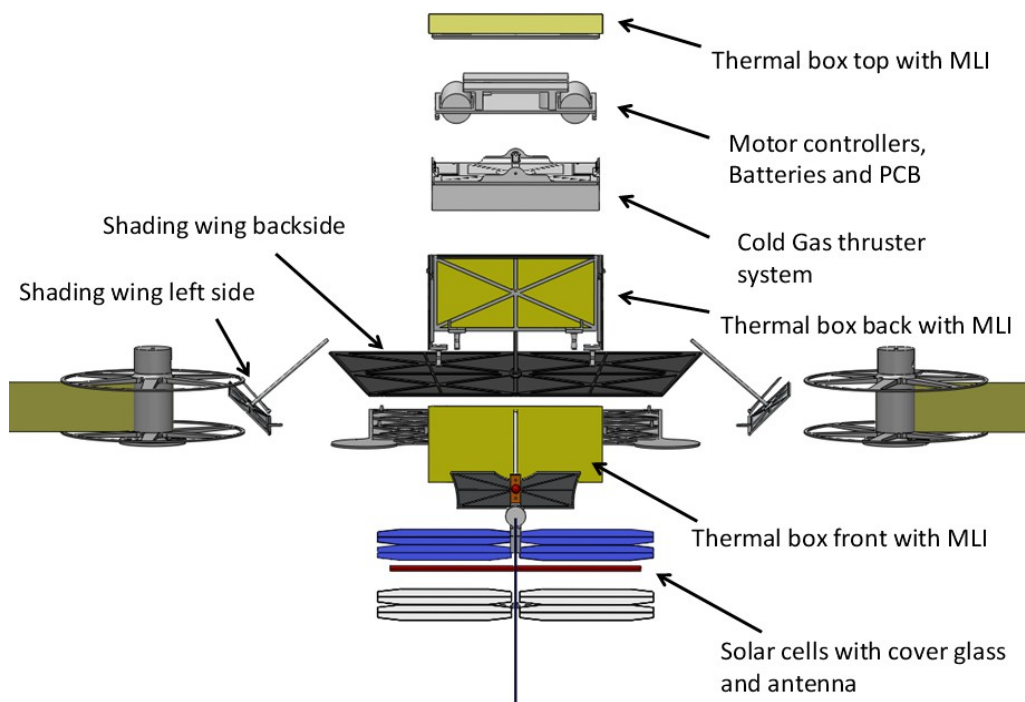


Figure 1.2: Exploded front view of RU showing all main parts of RU in Cold Gas configuration.

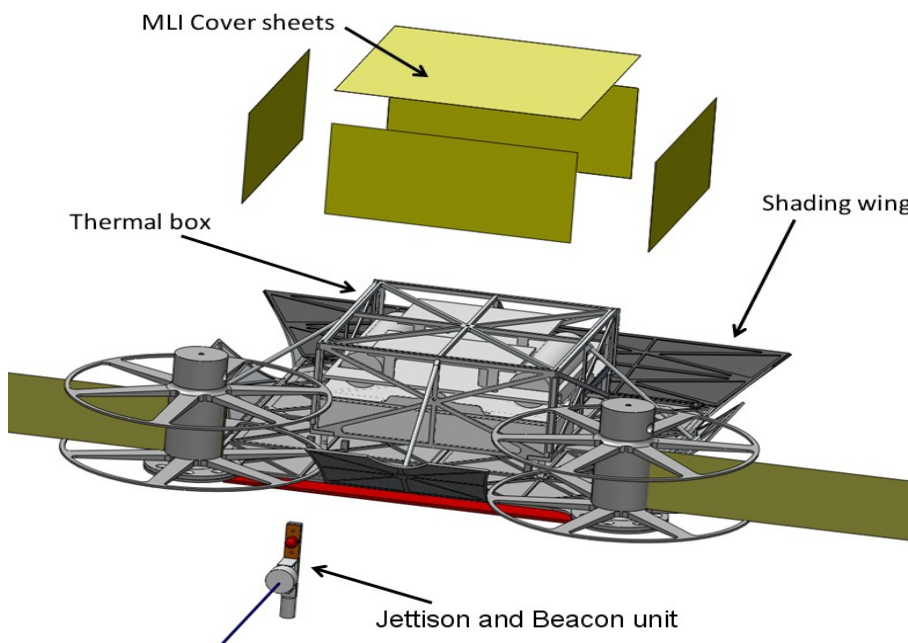


Figure 1.3: Partly exploded view of RU (Cold Gas configuration) showing thermal box in place and connection of wings to heat shield. (The thermal box is covered with MLI on all six faces.)

The arrangement of the solar cells, the sensors in the middle of the heat shield and the antenna are visible from the bottom, Figure 1.4. This view shows the shading wings for the Cold Gas-based assembly. For both configurations, it is necessary to cut a well-defined area from the wings to allow the propulsion system to work properly.

The purpose of those wings is to protect the thermal box from direct sunlight and therefore allow a good control of the temperature inside the box. The design of the them enables the RU to an inclination of up to 60° towards the sun.

The solar cells on top of the heat shield are protected by 0.10mm thick cover glass.

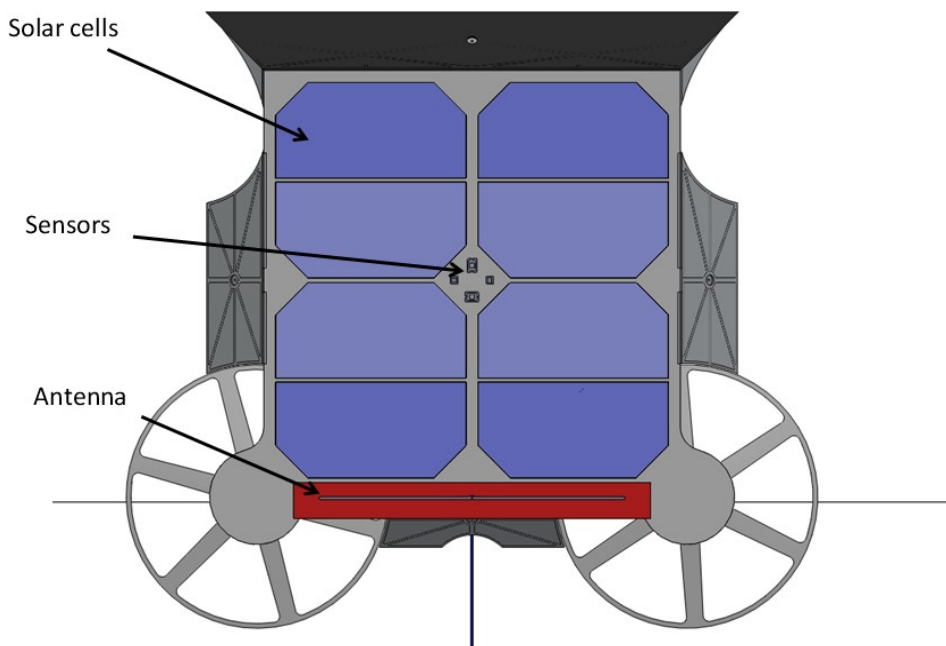


Figure 1.4: Bottom view of RU showing, in particular, heat shield with solar cells and wings (with cut-outs for Cold Gas thrusters), antenna, and protrusion with tether reels.

Figure 1.5 shows the thrusters plume for the FEEP-based system. Unlike the Cold Gas-based one, which has two symmetrical thruster plumes pointing in close to opposite directions, the FEEP system has only one, which is directed more to the side of the RU. The plume is elliptical, whereas the Cold Gas-based set-up has conical plumes with a half opening angle of 30°.

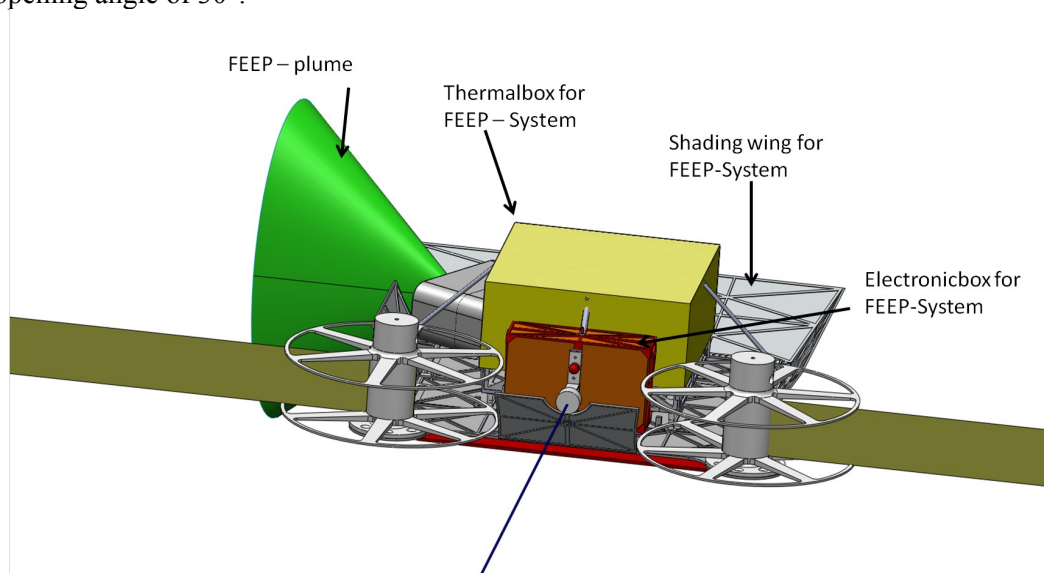


Figure 1.5: Location of FEEP thruster plume (green) on RU.

The exploded view below, Figure 1.6, shows the framework of the RU. The heat shield represents the base of the system and is surrounded by shading wings. On top of the heat shield are the thermal spacers, which separate and insulate the thermal box from the heat shield. These spacers are identical for the two propulsion system, and differ only by number.

The thermal box is an MLI-wrapped beam structure which holds all electronics and the propulsion system in the Cold Gas case.

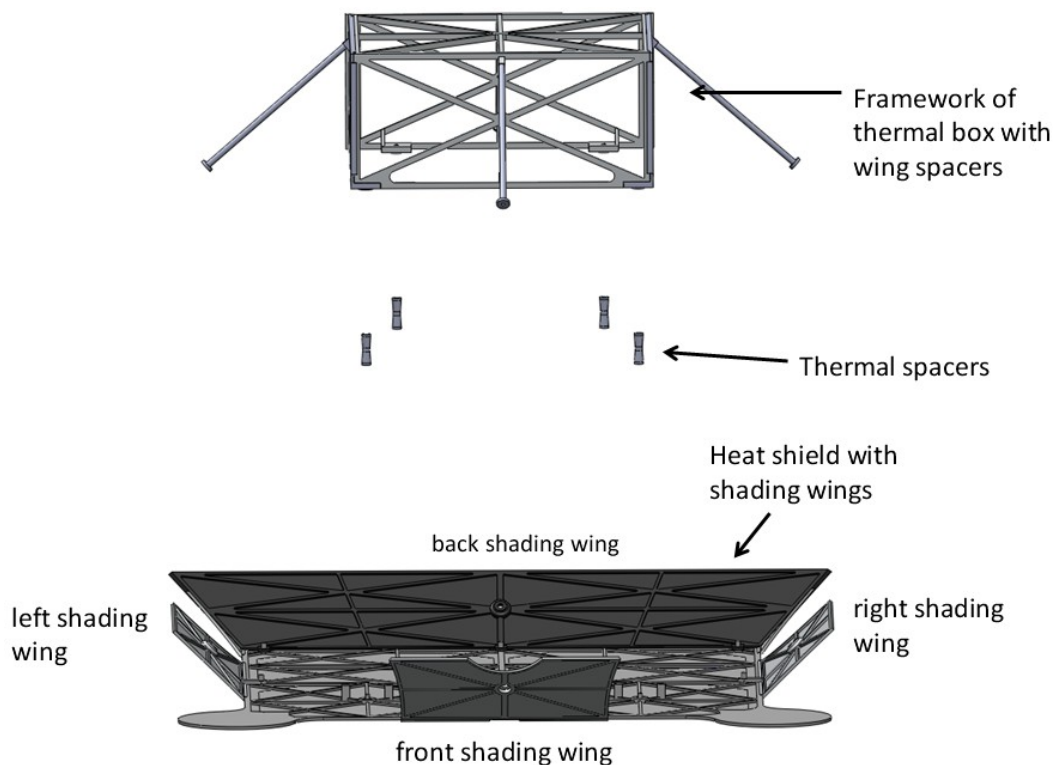


Figure 1.6: Exploded view of the thermal box beam structure for the Cold Gas configuration, and thermal spacers with respect to heat shield with wings.

The design of the beam structure, as well as the design of the shading wings depends on the installed propulsion system, as shown in Figure 1.7.

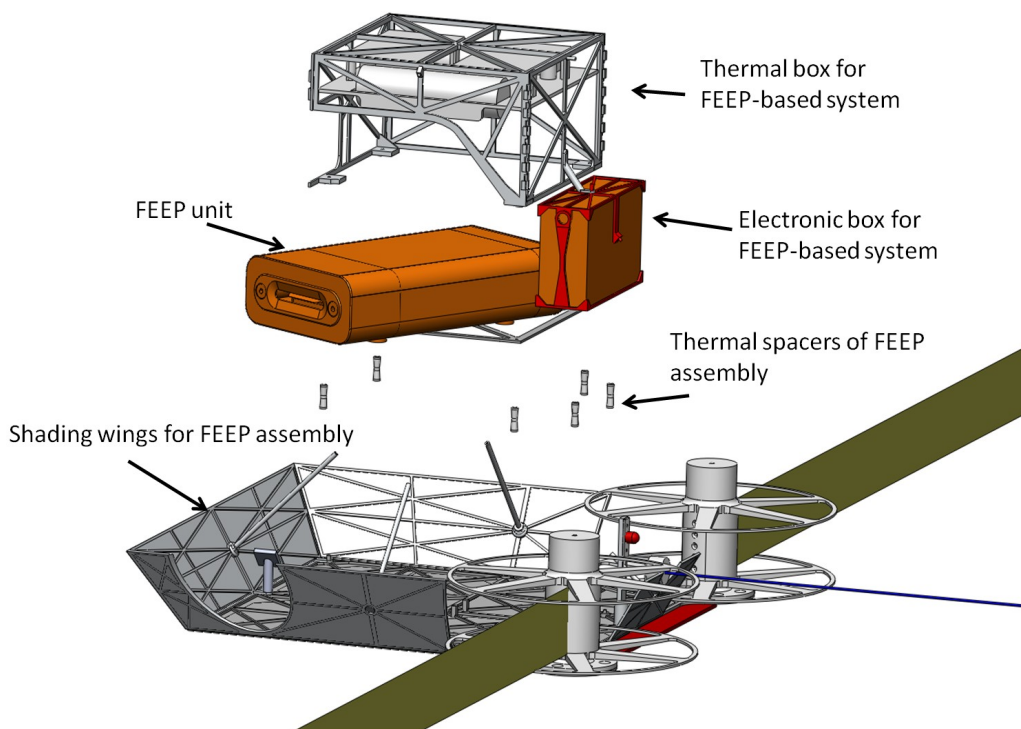


Figure 1.7: Adaptation of framework structure and heat shield wings for FEEP configuration.

Table 1.1 contains the overall size and mass, as well as centre of mass, of the two propulsion system configurations of the RU. The point of origin is in the centre of the heat shield. The x- axis is parallel to the auxiliary tethers, the y-axis is parallel to the reel rotational axis and the z-axis is parallel to the main tether facing towards the back shading wing.

Table 1.1: Size, dry mass and centre of mass (fully deployed) for dry and wet RU system.

Thruster system	Overall size L x W x H (mm)	Overall dry mass (g)	Centre of mass (coordinates in mm) for dry mass	Centre of mass (coordinates in mm) for wet mass
Cold Gas	287.4 x 294.7 x 57.7	560.92	X = 0.00 Y = 26.91 Z = -26.84	X=0.00 Y=26.02 Z=-24.95
FEEP	287.4 x 294.7 x 70.8	809.3	X = 2.13 Y = 32.07 Z = -30.21	X=0.05 Y=31.89 Z= -28.64

In order to adjust the centre of mass to the plane defined by the three tether connections, it is possible to raise the reels a few millimetres. This allows for adjustment within a range of 4 mm, but, of course, requires even further propulsion-specific design.

Tables 1.2 and 1.3 contain mass breakdowns of the masses for Cold Gas- and FEEP-based remote units, respectively. Tables 1.4 and 1.5 contain the mass breakdowns of the corresponding spacecraft bus.

Table 1.2: Components size and number of Cold Gas-configured RU.

Component	Mass (g)	Number	Total mass (g)
Heat shield & wings	73,2	1	73.2
Reel	67.4	2	134.8
Solar cells	2.4	8	19.2
Cover glass	0.78	8	6.24
Control unit	48.8	1	48.8
Thermal box	34.1	1	34.1
Jettison	5	1	5
Pin heater	0.4	1	0.4
Beacon	0.4	1	0.4
Batteries	48	2	96
Motor controller	18	2	36
Jettison beam	2.45	1	2.45
Thermal spacer	0.08	4	0.32
Cold Gas propulsion system (dry mass)	106	1	106
	Complete Mass	dry mass	562.91
		wet mass	612.91

Table 1.3: Components size and number of FEEP-configured RU.

Component	Mass (g)	Number	Total mass (g)
Heat shield & wings	90.36	1	90.36
Reel	67.4	2	134.8
Solar cells	2.4	8	19.2
Cover glass	0.78	8	6.24
Control unit	48.8	1	48.8
Thermal box	55.08	1	55.08
Jettison	5	1	5
Pin heater	0.4	1	0.4
Beacon	0.4	1	0.4
Batteries	48	2	96
Motor controller	18	2	36
Jettison beam	4	1	4
Thermal spacer	0.08	6	0.48
FEEP propulsion system (dry mass)	165	1	165
Fixture for electronic box	7.5	1	7.5
FEEP electronic box	140	1	140
	Complete mass	dry mass	809.26
		wet mass	879.26

Table 1.4: RU spacecraft bus mass breakdown for Cold Gas-based system.

Parts group	Component	Number	Mass per component (g)	Total mass (g)
Heat shield		1	41.90	41.90
	Shading wing front	1	2.70	2.70
	Shading wing side	2	3.30	6.60
	Shading wing back	1	13.00	13.00
	Nut – M1.6	6	1.5	9.00
Thermal box	Back side	1	4.67	4.67
	Left/Right side	2	4.22	8.44
	Front side	1	3.07	3.07
	Top	1	7.52	7.52
	Screw M1.4x3	4	1.50	6,00
	Brackets	6	0.20	1.80
	Wing spacer	4	0.50	2.00
	MLI	6	0.10	0.60
Thermal spacer		4	0.08	0.32

Table 1.5: RU spacecraft bus mass breakdown for FEEP-based system.

Parts group	Component	Number	Mass per component (g)	Total mass (g)
Heat shield		1	41.90	41.90
	Shading wing front	1	3.52	3.52
	Shading wing left	1	4.84	4.84
	Shading wing right	1	12.4	12.4
	Shading wing back	1	15.7	15.7
	Nut – M1.6	8	1.5	12.00
Thermal box	Back side	1	5.15	5.15
	Right side	1	4.6	4.6
	Left side	1	5.2	5.2
	Front side	1	3.59	3.59
	Top	1	7.52	7.52
	Screw M1.4x3	9	1.5	13.5
	Brackets	10	0.2	2.0
	MLI	6	0.12	0.72
	Wing spacer	4	0.9	3.6
	Fixture FEEP	1	9.2	9.2
Thermal spacer		6	0.08	0.48

1.5. RU bus components design

1.5.1 Heat shield

The heat shield, Figure 1.8, has a base area of 175x175 mm and consists of a continuous 0.2 mm thick sheet. The sheet is supported by a structure of beams in order to achieve a stiff layer for the fragile solar cells. The beams are 1.1 mm thick and 1.0 mm wide.

The purpose of the heat shield is for the mounting of the solar cells and sensors on the front side, and the assembly of the tether reels, shading wings, connectors and thermal spacers on the back side. The heat shield protects the electronics from overheating and radiation.

It is necessary to change the shading wing dimensions and shapes depending on the propulsion system. For the FEEP-based system it is necessary to cut an outlet only on one shading wing, whereas for the Cold Gas-based system it is necessary to cut an outlet in two shading wings. Therefore, and for the reel design and placement, it is not possible to create a closed wing area around to base shield.

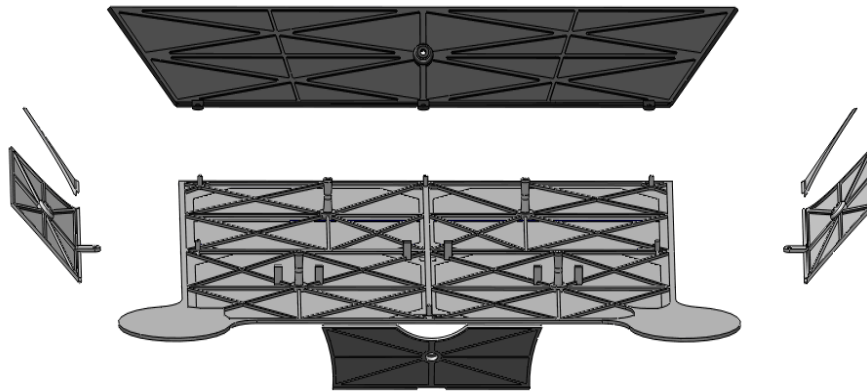


Figure 1.8: Heat shield with its four wings detached. (Thruster cut-outs close to the back edge of left and right wing are those for the Cold Gas case.)

The heat shield has an interface for the thermal spacers to allow a reliable and accurate assembly through use of a thread, Figure 1.9.

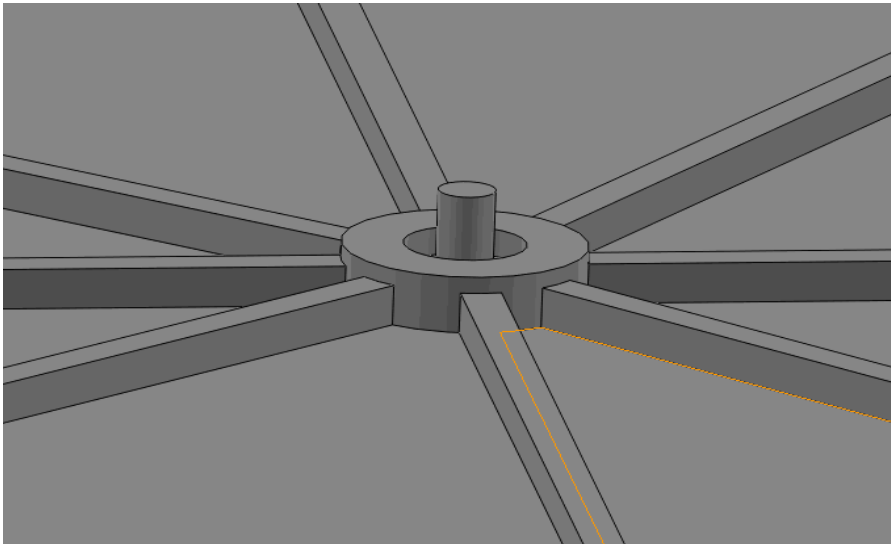


Figure 1.9: Threaded part of thermal shield connecting to a thermal spacer.

The total mass of the heat shield and wings is 90.36 g for the FEEP-based assembly, and 73.2g for the Cold Gas-based one.

The material is aluminium, Al 7075-T6.

1.5.2 Thermal box

The thermal box holds all sensitive parts, such as batteries, motor controllers, and printed circuit boards. It is an assembly of beam structures, which can easily be mounted and assembled, Figure 1.10 - 1.12. As with the shading wings, the design of the thermal box depends on the propulsion system implemented. However, the assembly of the box's faces, which the next figures serve to illustrate, is similar.

Starting with the thermal box for the Cold Gas type RU, the first step, Figure 1.10, is to assemble the side walls to the back wall with integrated teeth locking them sideways, and then to secure them with PEEK clamps. After this, components can be mounted in the box.

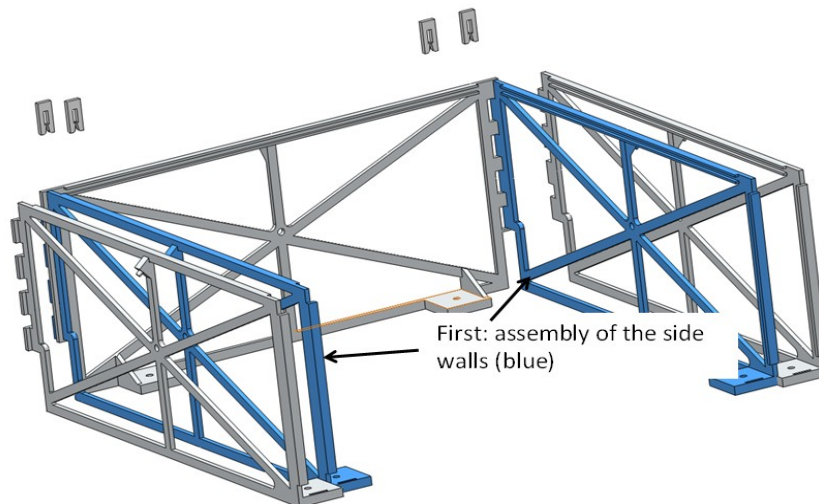


Figure 1.10: Side and back walls of thermal box. (Assembling step 1.)
Subsequently, the lid of the thermal box is slid into place, Figure 1.11.

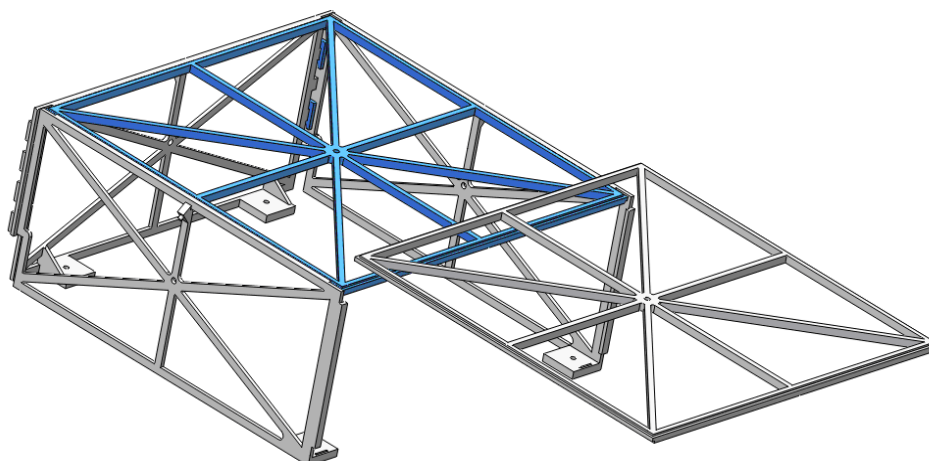


Figure 1.11: Lid of thermal box is slid into the partial frame of side and back walls. (Assembling step 2.)

As a last step, the front part is pushed downwards and fixed with a screw into place. By this, the framework part of the thermal box is completed, Figure 1.12.



Figure 1.12: Thermal box completed with its front part (blue) put into place. (Assembling step 3.)

The thermal box for the FEEP-based system has a different design, Figure 1.13.

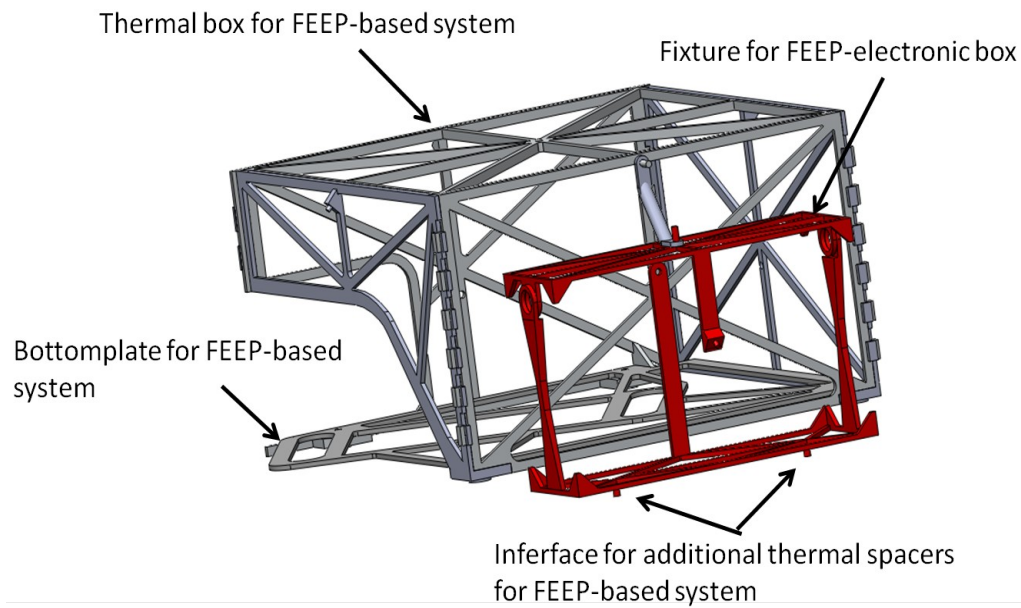


Figure 1.13: Thermal box and fixture for the FEEP electronics box (red).

The material for the thermal box is aluminium, Al 7075-T6, and the mass of the thermal box framework structure is 23.7 g for the Cold Gas-based system, and 35.3 g for the FEEP-based one, including the bottom on which the FEEP thruster resides

1.5.3 Thermal spacers

The 10.5 mm long thermal spacers separate the heat shield and the thermal box. The outer base diameter is 3 mm and the inner diameter is 1.4 mm. In order to minimize the thermal conductivity and mass, they are hollow with an inner thread. The thread is used to connect the spacer to the heat shield, as well as to the thermal box.

The thermal spacers, Figure 1.14, are made of PEEK, which is a mechanical, chemical and temperature resistant polymer, are rotationally symmetrical and weigh 0.08 g each.

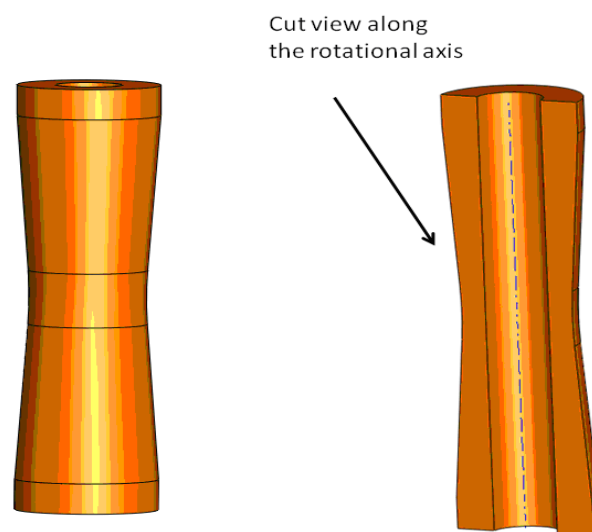


Figure 1.14: Shape of thermal spacer.

1.5.4 Connection with main craft

To minimize mass of the RU, it is assumed to be well supported to the main craft (and or launcher vehicle) during launch. The design of the actual docking (fixture) plate and the release mechanism are not within the scope of this work. However, it has been assumed that some kind of spring-loaded pins or cones shall attach at three or five pins to the RU, for the Cold Gas and FEEP configuration, respectively. In both cases there is one anchoring point at the upper back edge of the thermal box, and one at each reel hub. These should essentially fix the top plane of the RU, Figure 1.15. For the FEEP-equipped RU, there is one additional point at each side of the FEEP electronics cage.

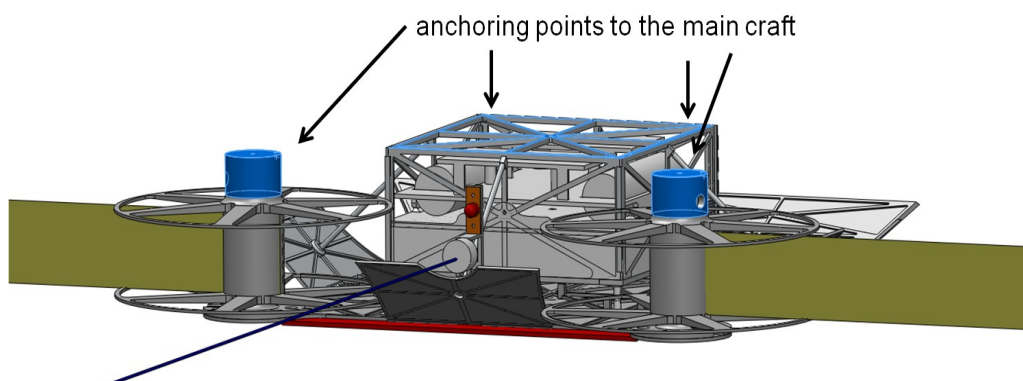


Figure 1.15: Assumed main craft anchoring locations (blue) for the Cold Gas-based RU.

1.6. Design justification

1.6.1 Mechanical modelling

To optimize the RU with respect to mass, extensive Finite Element Analysis (FEA) using Comsol Multiphysics software was conducted.

1.6.1.2. Static loading

The thermal spacers were individually tested under a static load of 10 N, and concurrently modelled thermally for minimum thermal conductivity for each design. (See below.)

The models had fixed constraints on one of the cylinder face sides. In Figure 1.16 the lower face is fixed.

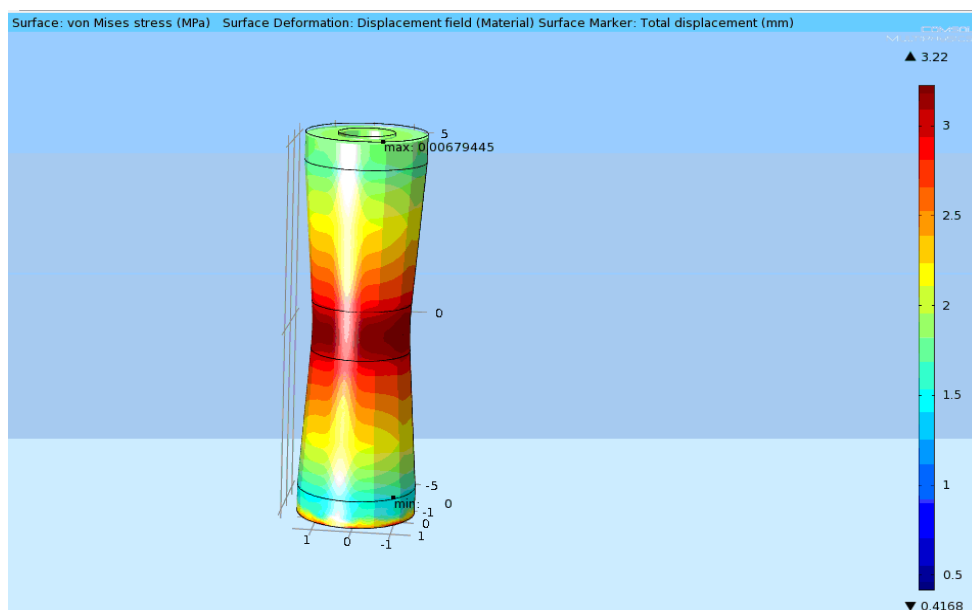


Figure 1.16: Example of von Mises stress FEA of single thermal spacer under 10 N of static loading.

The results for the hollow cylinder thermal spacers are:

- Thermal conductivity of 0.101 mW/K
- von Mises stress of 3.22 MPa and an axial deformation of 0.006 mm

The hollow cylinder design fulfils the requirements and are very light-weight as well.

1.6.1.3. Vibrational loading

Certain constrains had to be set for the vibrational simulation. The vibration was induced through the thermal box top part and through the reels, which are intended for attachment to main craft. The frequencies for the simulations were identical to the sinusoidal vibration levels of the Arian 5 launch manual, AD-3, Table 6.

Table 1.6: Frequency and amplitude of vibrational modelling.

Direction	Frequency band (Hz)	Sine amplitude (g)
Longitudinal	2 – 50	1.0
	50 – 100	0.8
Lateral	2 – 25	0.8
	25 – 100	0.6

The stress induced by longitudinal vibrations was always in an acceptable range of 1 to 9 MPa for the Cold Gas-based system and 5 to 50 MPa for the FEED-based one. For laterally induced vibrations along the z-axis, the results were tolerable for both system as well, but the vibrations along the x-axis locally created high stress areas in the centre point of the thermal box top part. Those results may be investigated separately, but can be neglected here since this point will be used to fix the RU to the main craft.

A graphical example of vibrational FEA von Mises stress results is given in Figure 1.17.

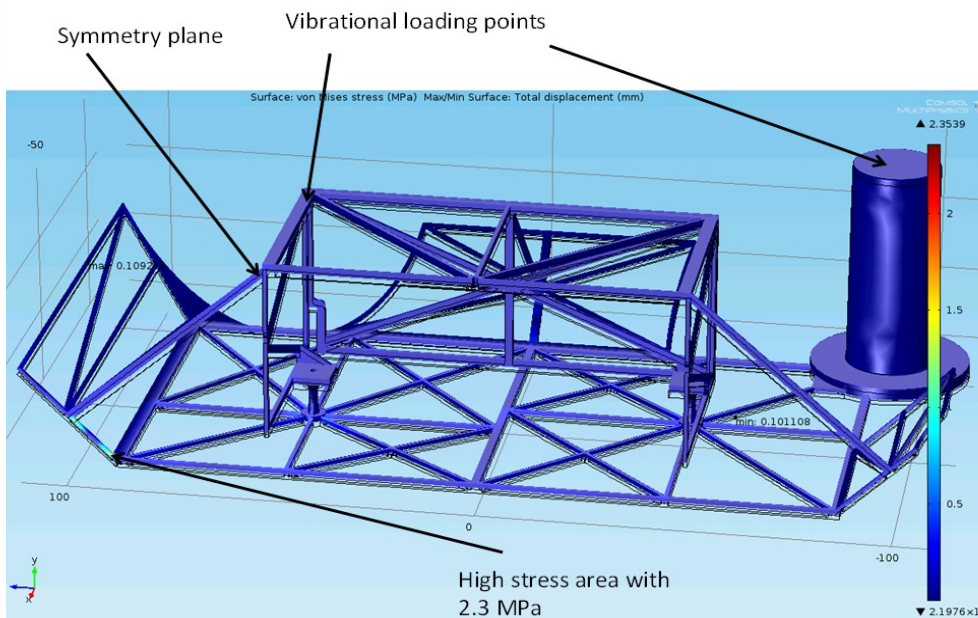


Figure 1.17: Example of FEA von Mises stress modelling indicating local stress at wing beam structure.

Through modelling, the eigenfrequency of the assembly was found to be 216 Hz for the Cold Gas-based system and 108.5 Hz for the FEED-based system.

1.6.1.4. Shock

The assembly was tested under a shock load, for which 1000 Hz and 1000 g was chosen, according to AD-3.

The results were similar with the vibration load along the x-axis. High-stress areas were located at the back shading wing. However, the model treats the interfaces between the heat shield and the shading wings as ideal, which means that it is a perfect connection, without any tolerances. The shock simulations show that it is useful to use a spring suspension to lower the influence of shock loads.

1.6.2 Thermal modelling

The purpose of this modelling is to verify that the requested temperature range of the RU and its subsystems can be maintained at both the extremes of the anticipated mission, i.e. avoiding overheating at maximum sun exposure 0.9 AU and detrimentally low temperatures at minimum sun exposure at 4.0 AU, and during an accidental flipping of the RU resulting in a belly side up for up to five minutes. In addition, the modelling shall indicate values on the internal heating power necessary to provide a warm enough interior of the thermal box far from Sun.

1.6.2.1 Description of model

For the thermal simulation a two-body lumped model is used, where the two heat sources/sinks are the main body (thermal box) and the heat shield. The model does not include subsystems such as reels, motors, or jettison mechanism.

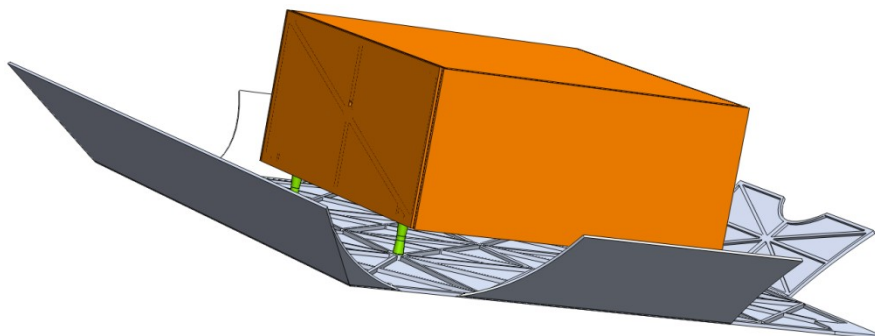


Figure 1.18: Two-body thermal model, showing the sun shield with shading wings, thermal spacers and main body.

A schematic of the two-body lumped model is shown in Figure 1.18. Facing the sun is the heat shield with solar cells. From a thermal perspective, the plate and main body are connected by heat flow through the thermal spacers and heat radiation exchange between the plate and one side of the main body. The plate provides part of the thermal control of the main body.

Thermal analysis

All physical constants and parameters used in the thermal model are shown in Table 1.7.

Table 1.7: Dimensions and thermal parameters used for the model.

Variable	Description	Unit
w_1	Main body lateral size	m
w_2	Sun shield lateral size	m
h	Main body height	m
A_w	Shading wing area	m ²
α_{21}	Absorptivity of sun shield, front	
α_{22}	Absorptivity of sun shield, back	
α_{23}	Absorptivity of shading wings	
ϵ_{21}	Emissivity of sun shield, front	
ϵ_{22}	Emissivity of sun shield, back	
ϵ_{23}	Emissivity of shading wings	
ϵ_{11}	Emissivity of main body, towards sun shield	
ϵ_{12}	Emissivity of main body, towards space	
T_1	Temperature of main body	°C
T_2	Temperature of sun shield	°C
Q_1	Energy storage main body	J
Q_2	Energy storage heat shield	J
κ	Thermal conductivity of spacers	W K ⁻¹
T_1	Main body temperature	°C
T_2	Sun shield temperature	°C
h_p	Heater power inside main body	W
v_f	View factor from heat shield to main body	
c_1	Main body heat capacity	J K ⁻¹
c_2	Sun shield heat capacity	J K ⁻¹
θ	Boresight angle of spacecraft	rad
r	Relative astronomical unit	
d	One Astronomical Unit	m
s	Solar constant	W m ⁻²
T_z	Absolute zero temperature	°C
σ	Stefan-Boltzmann constant	W m ⁻² K ⁻⁴

Given these parameters, the following system of differential equations are used to describe the heat flow to the thermal box:

$$\begin{aligned} \frac{dQ_{11}}{dt} &= h_p \\ \frac{dQ_{12}}{dt} &= -\epsilon_{11}\sigma (w_1^2 + 4w_1h) \left(\frac{Q_1}{c_1}\right)^4 \\ \frac{dQ_{13}}{dt} &= -\epsilon_{12}\sigma w_1^2 \left(\frac{Q_1}{c_1}\right)^4 \\ \frac{dQ_{14}}{dt} &= \kappa (T_2 - T_1) = \kappa \left(\frac{Q_2}{c_2} - \frac{Q_1}{c_1}\right) \\ \frac{dQ_{15}}{dt} &= v_f \epsilon_{11} \epsilon_{22} \sigma w_2^2 \left(\frac{Q_2}{c_2}\right)^4 \end{aligned}$$

The first equation describes power dissipation inside the box, the second and third equation describe emission towards and away from the heat shield, respectively, and the fourth and fifth equation express thermal transport from the heat shield, conducted through the spacers and as radiation, respectively.

In this model, it is assumed that the thermal box is never exposed to sunlight. In reality, the shading wings of the heat shield have cut-outs for the thruster plumes. This means that when the RU is tilted at a certain angle, corner parts of the thermal box can be exposed to sunlight.

Similar to the thermal box, the thermal flow to the heat shield is described by the following system of differential equations:

$$\begin{aligned}\frac{dQ_{21}}{dt} &= (\alpha_{21}w_2^2 + \alpha_{23}A_w \cos(\pi/4))\frac{s}{r^2} \cos(\theta) \\ \frac{dQ_{22}}{dt} &= -(\epsilon_{21}w_2^2 + \epsilon_{23}A_w)\sigma \left(\frac{Q_2}{c_2}\right)^4 \\ \frac{dQ_{23}}{dt} &= -(\epsilon_{22}w_2^2 + \epsilon_{23}A_w)\sigma \left(\frac{Q_2}{c_2}\right)^4 \\ \frac{dQ_{24}}{dt} &= -\kappa(T_2 - T_1) = -\kappa \left(\frac{Q_2}{c_2} - \frac{Q_1}{c_1}\right)\end{aligned}$$

Where the equations describe energy accepted from the sunlight, thermal radiation directed towards the sun, directed away from the sun, and heat flow through the thermal spacers, respectively. For simplicity reasons, the wings' effective area (the area which is seen by the sun) is assumed to be constant and a factor $\cos(45^\circ)$, or $\sim 70\%$, of the total area.

The final differential equation for the heat transfer between the two bodies is expressed as:

$$\begin{aligned}\frac{dQ_1}{dt} &= h_p - \sigma(\epsilon_{11}(w_1^2 + 4w_1h) + \epsilon_{12}w_1^2) \left(\frac{Q_1}{c_1}\right)^4 + \kappa \left(\frac{Q_2}{c_2} - \frac{Q_1}{c_1}\right) + v_f \epsilon_{11} \epsilon_{22} \sigma w_2^2 \left(\frac{Q_2}{c_2}\right)^4 \\ \frac{dQ_2}{dt} &= (\alpha_{21}w_2^2 + \alpha_{23}A_w) \frac{s \cos(\theta)}{r^2} - \sigma((\epsilon_{21} + \epsilon_{22})w_2^2 + 2\epsilon_{23}A_w) \left(\frac{Q_2}{c_2}\right)^4 - \kappa \left(\frac{Q_2}{c_2} - \frac{Q_1}{c_1}\right)\end{aligned}$$

The temperature of each body is calculated as:

$$\begin{aligned}T_1 &= \frac{Q_1}{c_1} + T_z \\ T_2 &= \frac{Q_2}{c_2} + T_z\end{aligned}$$

The Remote Unit must be designed to withstand a temporary flip-over, where the main body is fully exposed to sunlight for 5 minutes. Hence, the thermal equations above has been modified to properly describe this case and enable simulation of such an event. For this case, the final expression becomes:

$$\begin{aligned}\frac{dQ_1}{dt} &= h_p - \sigma(\epsilon_{11}(w_1^2 + 4w_1h) + \epsilon_{12}w_1^2) \left(\frac{Q_1}{c_1}\right)^4 + \kappa \left(\frac{Q_2}{c_2} - \frac{Q_1}{c_1}\right) + v_f \epsilon_{11} \epsilon_{22} \sigma w_2^2 \left(\frac{Q_2}{c_2}\right)^4 + \\ &\alpha_{11}w_1^2 \frac{s}{r^2} \\ \frac{dQ_2}{dt} &= (\alpha_{22}(w_2^2 - w_1^2) + \alpha_{23} \frac{A_w}{\sqrt{2}}) \frac{s}{r^2} - \sigma((\epsilon_{21} + \epsilon_{22})w_2^2 + 2\epsilon_{23}A_w) \left(\frac{Q_2}{c_2}\right)^4 - \\ &\kappa \left(\frac{Q_2}{c_2} - \frac{Q_1}{c_1}\right)\end{aligned}$$

1.6.2.2 Simulation parameters

The following section briefly describes and justifies the parameter values chosen for the thermal simulations. Parameter values that are common for all simulation cases are shown in Table 1.8.

Table 1.8: Parameter values used for simulations.

Variable	Description	Value	Unit
w_1	Main body lateral size	0.1	m
w_2	Sun shield lateral size	0.175	m
h	Main body height	0.05	m
A_w	Shading wing area	0.012	m ²
α_{21}	Absorptivity of sun shield, front	0.61	
α_{22}	Absorptivity of sun shield, back	0.88	
α_{23}	Absorptivity of shading wings	0.15	
ϵ_{21}	Emissivity of sun shield, front	0.88	
ϵ_{22}	Emissivity of sun shield, back	0.25	
ϵ_{23}	Emissivity of shading wings	0.07	
ϵ_{11}	Emissivity of main body, towards sun shield	0.004	
ϵ_{12}	Emissivity of main body, towards space	0.004	
$T_1(0)$	Initial temperature of main body	20	°C
$T_2(0)$	Initial temperature of sun shield	20	°C
κ	Thermal conductivity of spacers	4×0.101	mW K ⁻¹
v_f	View factor from heat shield to main body	0.3	
c_1	Main body heat capacity	179.4	J K ⁻¹
c_2	Sun shield heat capacity	35.88	J K ⁻¹
d	One Astronomical Unit	149.6×10^9	m
s	Solar constant	1366	W m ⁻²
T_z	Absolute zero temperature	-273.15	°C
σ	Stefan-Boltzmann constant	5.67×10^8	W m ⁻² K ⁻⁴

Material properties

The IR emissivity ϵ and the solar absorptivity α for the surface materials are shown in Table 1.9.

Table 1.9: Optical properties of chosen materials.

Material	IR emissivity ϵ	Solar absorptivity α
AAErotherm S10-190 (MLI)	0.004	0.17
Solar cell 3G30C	0.88	0.61
Aeroglaze A276 (white)	0.25	0.88
Aeroglaze Z306 (black)	0.95	0.89
Qioptiq CMX AR	0.88	
Aluminium 7075	0.15	0.07

Table 1.10 shows the heat conduction and thermal energy storage properties of the box and sun shield with wings (Aluminium 7075), and the thermal spacers (PEEK, Victrex 450G).

Table 1.10: Heat conduction and thermal energy storage properties of chosen materials.

Material	Density kg m ⁻³	Specific heat J kg ⁻¹ K ⁻¹	Thermal conductivity W m ⁻¹ K ⁻¹
Aluminium 7750	2700	960	237
PEEK Victrex 450G	1300	2160	0.25

The thermal spacer design, shown in Figure 1.14, gives a thermal conductance of 101 mW/K per spacer.

The weight of the sun shield with shading wings is estimated to be 40 g, solid aluminium. This gives a heat capacity of roughly 36 J/K. For the main body, a heat capacity of 180 J/K, corresponding to 200 g of aluminium, is chosen.

View factor - The energy transportation between the two bodies due to radiation depends on the view factor, defined as the fraction of the radiation leaving surface i that is intercepted by surface j , and can be expressed as:

$$dq_{i \rightarrow j} = I_{e+r,i} \cos\theta_i dA_i d\omega_{j \rightarrow i}$$

Assuming that surface i emits and reflects diffusely and the radiosity, J_i , is uniform over the surface A_i , the fraction of the radiation that leaves A_i and is intercepted by A_j is:

$$F_{ij} = \frac{1}{A_i} \int_{A_i} \int_{A_j} \frac{\cos\theta_i \cos\theta_j}{\pi R^2} dA_i dA_j$$

Solving this integral numerically for a heat shield of 175 x 175 mm and a thermal box 100 x 100 mm in size, the view factor is found to be approximately 0.3.

1.6.2.3 Thermal simulation results

The thermal model is simulated for a distance of 0.9 and 4.0 AU, both cases with 0 and 60 degree inclination. The simulated steady-state temperatures for the two bodies are shown in Table 1.11.

Table 1.11: Steady state temperatures of shield and main body at distances of 0.9 and 4.0 AU, 0 and 60° tilt, and reasonable heating powers.

Distance [AU]	Inclination [deg]	Heater power [mW]	Sun shield Temp. [°C]	Main body Temp. [°C]
0.9	0	40	85	26
0.9	60	60	29	21
4	0	100	-102	7
4	60	110	-128	7

The result from a simulation of the flipping case is shown in Figure 1.19. The flip lasts for 5 minutes and occurs during worst-case conditions, at 0.9 AU and no tilt, when the RU has reached steady state temperature with a 40 mW power dissipation inside the main body. A close-up of the temperature changes during the flip is shown in Figure 1.20, with the flipping occurring at $t=0$.

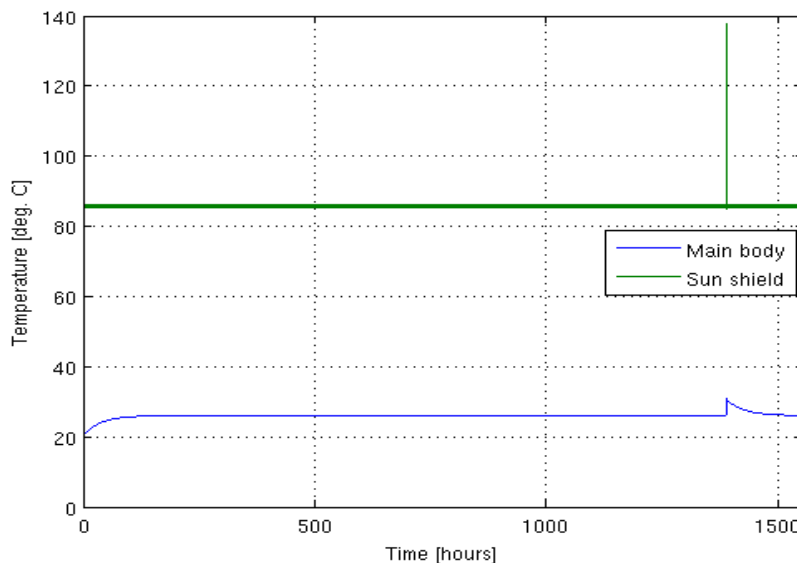


Figure 1.19: Temperatures when RU is flipped for 5 minutes at 0.9 AU. (Top graph is for sun shield, bottom graph is for main body.)

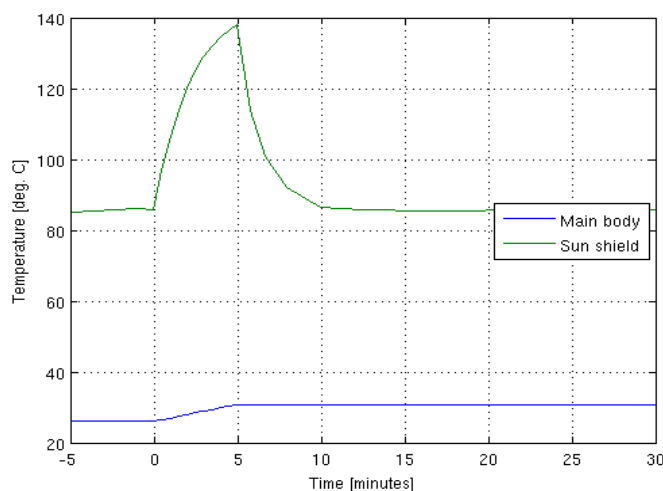


Figure 1.20: Close-up of 5-minute flip at 0.9 AU. (Top graph is for sun shield, bottom graph is for main body.)
At 4 AU, a 5-minute flip does not affect the temperatures much, as shown in Figure 1.21.

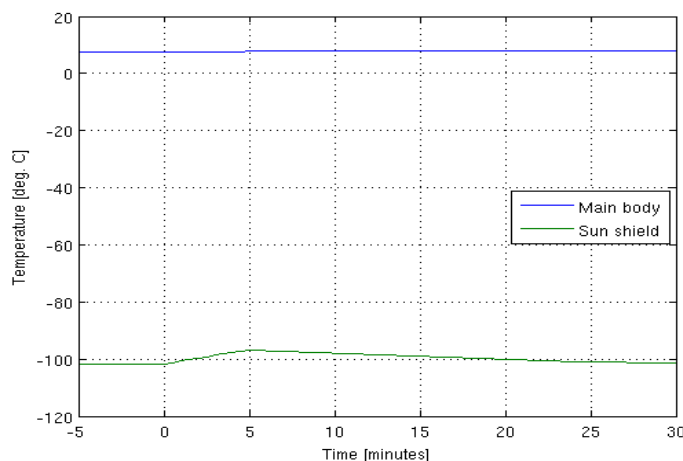


Figure 1.21: Close-up of 5-minute flip at 4 AU, no tilt and 100 mW heater. (Bottom graph is for sun shield, top graph is for main body.)

By these simulations, it has been shown that the thermal design of the Remote Unit is able to keep the all subsystems within the tolerable temperature ranges, mainly by adjusting the power dissipated inside the main body. At distances close to the sun, high power dissipation inside the main body will cause overheating. It is therefore likely that subsystems that dissipate much power must be duty cycled. The radiator, not included in the simulation, should also help to avoid overheating

1.7. Conclusions

Provided some care is taken in the design of the part of the attachment belonging to the main craft, especially with respect to damping, the Remote Unit and all its subsystems have been designed to fulfil the applicable requirements specification (AD-2), and to minimize mass. Modelling, analytical estimations and preliminary experimental results, have been used for a successful best-effort verification and justification of the design.

This marks the end of the project's design phase and allows for proceeding to manufacturing.

Final note:

For practical reasons, this document doesn't contain actual workshop drawings, but mostly illustrative 3-D CAD views. At any time, the full design material can be requested on disc by any of the ESAIL project members or by anyone reviewing the project.



2. Auxiliary tether reel

Prepared by:

**Roland Rosta, DLR,
Roland.Rosta@dlr.de**

&'3. Auxiliary tether reel design

In [RD-1] two different concepts are shown as the most suitable concepts. In both cases two separate reels are used in one remote unit.

During the remote unit component design review it was decided that the centre of gravity of the auxiliary deployment mechanism should be as low as possible [RD-02] and that the design “separate reel” design [RD-01] is chosen as the final design. These were adapted to a design with an attachment point for the main space craft as well as a lower centre of mass. The main space craft is attached to the top of the reel and during launch the reel is locked with a pin. The hole for the pin is placed in the reel as well as in the motor holder to lock the rotation of the reel.

To achieve a low centre of gravity the tether bay on the reel is placed as close as possible to the base plate of the remote unit. The centre of gravity for the deployment mechanism is at 26.6 mm above the base plate.

As described before the motor (colored blue) is placed congruent in the reels rotation axis. To fulfil the required torque of 58.13 mNm the Faulhaber brushless DC servomotor “M1226 12b” equipped with a planetary gear “10/1” (reduction 4096:1) “10/1” is selected [RD-01].

To mount the motor inside the reel a motor holder is needed. This holder is a small cylinder with an edge to mount the thin section ball bearing. This holder is shown in Figure 1 left panel (turquoise color) and has a weight of 7 g. It is mounted to the remote unit base plate with seven m3 screws. On this holder the thin section ball bearing is mounted (colored green). This thin section ball bearing bears the loads of the reel during launch and unreeling. It is fabricated from FAG Schaeffler and has a weight of 12 g as well as a total height of 12 mm with an external diameter of 19 mm. The motor is the brushless DC servo motor described before. The motor has an external diameter of 12 mm and a total length of 31 mm. The planetary gear 10/1 has a diameter of 10 mm and a length of 19 mm. In combination the total length is 45 mm. The tether reel is directly mounted on the motor axis with a press fit to transmit torque. The reel (colored grey) has an external diameter of 110 mm and a height of 34 mm. It is possible to reel 706 m tether on the reel. To build it lightweight, six pockets are countersunk of the side plates. The total weight of the reel in case of polyimide as material is 25 g. The length measurement is implemented in the motion control of the motor. The motion controller is not shown on Figure 1, it will be implemented on the remote unit data handling board to save mass and reduce the number of parts. It is chosen to agree to the motor specifications (Model: MCBL3003 S/C) and is equipped with a RS232 interface. As described before for the launch lock of the reel, the pin is used which locks the remote unit to the main space craft.

The overall system dimensions are the following: The total height is 57.3 mm with a mass of 67 g. See Table 2.1 for an overview of sizes and masses.

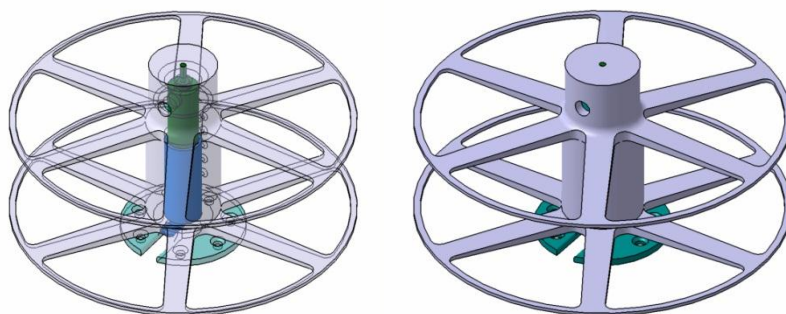


Figure 40I: Assembled separate reel deployment mechanism, on the right side the reel

and a holder are transparent to show the position of the motor and the sliding bearing.

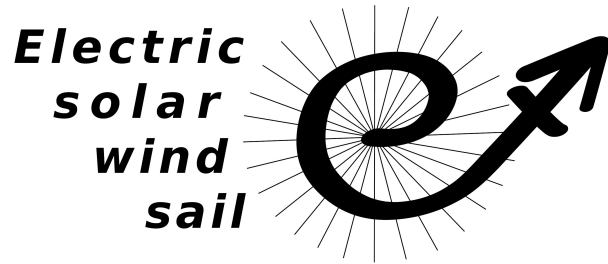
Quantity	Value
Tether capacity	706 m
Reel diameter	110 mm
Total height	57.3 mm
Total weight (material polyimide)	67 g
Motor (equipped gearbox)	Faulhaber 1226 12b (10/1)
Motor gear reduction	4096:1
Motor torque	100 mNm
Controller (Interface)	MCBL3003 S/C (RS323)

Table 40: Component Overview

Reference Documents:

RD-01: D3.3.2 Design description auxiliary tether reel

RD-02: MoM Remote unite component design review



3. Power System

Prepared by:

Tartu Observatory, Viljo Allik
viljo.allik@estcube.eu

Table of Contents

3.1. Introduction.....26
 3.2. RU Power System design requirements.....26
 3.3. RU power system design concept.....31
 3.4. RU power system detailed design.....33
 3.5. Mechanical design.....38
 References.....38
 Appendixes 1-7.....39-46

3.1. Introduction

This document describes the design of ESAIL Remote Unit (RU) electrical power generation and distribution subsystem (RU Power System).

3.2. RU Power System design requirements

3.2.1 Deduced design requirements from RU top level requirements

The RU Power System requirements are defined in document ^[1]. The most relevant applicable RU top level requirements are:

Requirement ID	ES1-RU-104
The Remote Unit must remain operational when the time-averaged angle between its pointing vector and the sun direction is 0-60°.	
Requirement ID	ES1-RU-201
The RU shall ensure the operational temperature range required by all its subsystems when these are operational. <i>Note: This is to be decided, but according to preliminary information, a range of 0 to +50°C is operational for all subsystems during operation. However, parts likely to be exposed to temperatures outside of this, tolerate approx. -25 to +85°C during operation.</i>	
Requirement ID	ES1-RU-202

<p>The RU shall ensure the tolerable temperature range required by all its subsystems when these are non-operational. <i>Note: This is to be decided, but according to preliminary information, a range of -30 to +60°C is tolerable for all subsystems. However, parts likely to be exposed to temperatures outside of this, tolerate approx. -40 to +85°C</i></p>	
Requirement ID	ES1-RU-213
<p>Throughout the mission, the RU must supply itself with power. <i>The amount is yet to be determined, but preliminary data indicate maximum continuous power consumption of 4.1, 2.1 and 0.1 W for MM I, MM II and MM III, respectively, if any need for heating power is neglected.</i></p>	
Requirement ID	ES1-RU-401
<p>Except for auxtether reeling mechanisms, the RU shall be designed to be fully operational for 5 years.</p>	
Requirement ID	ES1-RU-601
<p>Except for those relevant only for deployment, the RU shall be designed to fulfil all requirements after having been subjected to all environmental conditions anticipated from its deployment to completion of mission.</p>	
Requirement ID	ES1-RU-602
<p>The RU shall be tolerant to a total radiation dose of 100 krad assuming a 1-mm thick aluminium shielding, or its equivalent.</p>	
Requirement ID	ES1-RU-603
<p>The RU shall be fully operational when exposed to maximum heat radiation (sun at 0.9 AU, normal incidence, Earth albedo and Earth IR).</p>	
Requirement ID	ES1-RU-604
<p>Except for deployment-specific functions, the RU shall be fully operational when exposed to minimum heat radiation (sun at 4 AU and 60° incidence to spacecraft plane, no albedo and no other IR).</p>	
Requirement ID	ES1-RU-605
<p>During the mission life time, the RU shall withstand a vacuum level higher than 10⁻⁷ mbar without degradation.</p>	
Requirement ID	ES1-RU-606
<p>The Remote Unit must survive a turnover, i.e. a full reversal of its pointing vector, for up to 5 min without overheating or overcooling, and during this time maintain safe-mode functionality.</p>	
Requirement ID	ES1-RU-607
<p>The RU shall be tolerant to a total UV radiation dose corresponding to a worst case</p>	

scenario of 5 years at 0.9 AU.

3.2.2 Voltages and currents requirements from RU subsystems

The list of required voltage and current values is provided in Table 2.1:

Subsystem	Voltage(s) V	Pk Current(s) (A)
Aux. Tether Reel x 2	12	0.42
Control & Telemetry	2.5.12	0.05
LED Beacon	6.6 ... 8.4	0.65
Jettison	6.6 ... 8.4	1
Gas Thruster	12 / 2.5	0.14 / 0.24
FEEP Thruster	8 ... 12	0.25

Table 2.1: List of required currents and voltages.

Note: FEEP and Gas thrusters exist in two different RU configurations. Only one of them exists in a particular RU configuration.

3.2.3 RU Power budget

RU power budget has been calculated for two mission phases, most relevant to the power system design:

- Tether deployment phase at close to 1 AU (Table 2.2)
- Cruising phase at close to 4 AU (Table 2.3)

No of Solar Cells	8		
Solar cell output power @ 1AU	1.173		
Total Generated Power @ 1AU	9.384		
PPT Efficiency, %	85		
Total Available Power @ 1AU	7.9764		
Solar cell extra losses, %	7		
Mission Distance, AU	1		
Angle of incidence, deg	60		
DC/DC Converters Efficiency, %	85		
Available power, W	3.153		
Consumers	Peak Power	Duty Cycle	Average power
Aux Tether Reel(s)	5.04	0.50000	2.52
Control and Telemetry	0.1	1.00000	0.1
LED Beacon	4.4	0.00017	0.0007348
Thruster(s)	3	0.20000	0.6
Heaters	0.1	0.00000	0
Total Power Consumption	12.64		3.2207348
Power Balance, W			-0.0680627

Table 2.2: RU Power budget for tether deployment phase at 1 AU

No of Solar Cells	8		
Solar cell output power @ 1AU	1.173		
Total Generated Power @ 1AU	9.384		
PPT Efficiency, %	85		
Total Available Power @ 1AU	7.9764		
Solar cell extra losses, %	7		
Mission Distance, AU	4		
Angle of incidence, deg	60		
DC/DC Converters Efficiency, %	85		
Available power, W	0.197		
Consumers	Peak Power	Duty Cycle	Average power
Aux Tether Reel(s)	5.04	0.00000	0,0000
Control and Telemetry	0.1	1.00000	0,1000
LED Beacon	4.4	0.00017	0,0007
Thruster(s)	3	0.00000	0,0000
Heaters	0.1	0,73	0,0731
Total Power Consumption	12.64		0,1737
Power Balance, W			0,0233

Table 2.3: RU Power budget for cruising phase at 4 AU

The following limitations have been assumed for power budget tables above:

- Tether reel motors will operate at maximum 50% duty cycle in tether deployment phase due to their high current consumption. This has been accepted by ESAIL project team. It is acceptable to run both motors simultaneously but their average duty cycle has to be less or equal to 0.5.
- Thrusters and tether reel motors duty cycle has to be adjusted to keep total power balance of the RU positive.
- Heaters are not needed during tether deployment phase
- CG Thrusters consume the specified peak power of 3 W only during valve activation cycle for the duration of 1-2 ms. After that power consumption drops down to 0.6 W.
- When thrusters operation is needed at close to 4 AU they must operate at very low duty cycle to be able to maintain positive average power balance.
- Heaters apparent duty cycle have been decreased compensate for the actual dissipated power due to the heat dissipated by the power conversion circuits. Eventually some heat generated by the control subsystem can be added to the heating power as it dissipates within the RU electronics and thrusters enclosure. Any power saving here can increase the power available for operating thrusters at close to 4AU.

- Solar cell extra losses combine the loss from solar cell cover glass and solar cell ageing.

3.3. RU power system design concept

3.3.1 Primary power generation

Electrical power will be generated by using solar photovoltaic cells (solar cells). Typical efficiency of available space qualified triple junction GaAs solar cell is about 30%. Due to their relatively small physical size multiple cells will be needed to generate required amount of electrical power. Rigid flat surface area facing towards Sun is needed for mounting the solar cells. The best possible location for solar cells on the RU is the outer surface of its heat shield. To reduce the amount of heat transferred to the RU electronics and thrusters enclosure a cover glass layer may have to be added on top of solar cells. To be able to harvest highest possible amount of energy from a solar cell its load impedance has to match the load impedance. The optimum load impedance depends on the sunlight power density at solar cells. To be able to operate solar cells at their highest efficiency a special power conversion system is needed.

3.3.2 Secondary power generation (electrical energy storage)

As seen from RU power budgets it will be impossible to supply enough peak power to the RU subsystems during certain mission phases without energy storage device(s).

Lithium-Ion type rechargeable batteries are feasible alternatives to be used as energy storage devices on the RU. The main concern using Li-Ion battery cells in E-Sail missions is the lifetime of the battery cell. ESAIL top level requirements demand at least 5 years of continuous operation. To achieve such long life time of a commercially available battery cell its maximum charge level has to be kept below rated capacity. Battery cell temperature must be kept above 0 deg/C during its charging cycle. A number of space qualified battery cells are available commercially from companies like Sony, Panasonic, Saft and others. Cylindrical and some types of prismatic battery cells are most recommended to be used in vacuum. Typical Li-Ion battery cell voltage is between 3.2 and 4.1 V.

The battery charging system has to be able to supply constant electrical current until the voltage reaches the level corresponding to specified charge level.

It is recommended to include a dedicated battery protection circuit for protecting the battery against abnormal charge and discharge conditions and also enables to monitor the battery parameters during E-Sail space mission. It should be possible to adjust battery charging and discharging related parameters during the space mission.

3.3.3 Electrical power conversion

From the requirements above it is obvious that several electrical power conversion subsystems will be needed:

- Maximum Power Point Tracker circuit
The MPPT has to match the solar cells output impedance to the electrical load impedance of the RU power bus. It is implemented as a Maximum Power Point Tracker (MPPT) circuit. The MPPT controls the electrical power transferred from solar cells to the spacecraft power bus. MPPT

operational parameters can be adjusted and monitored by RU control and telemetry subsystem.

- Battery charging circuit
The battery charging circuit maintains constant battery charge current and disables battery charging after battery voltage reaches required level. Battery charge current cut-off voltage level can be adjusted by the RU control and telemetry subsystem.
- Secondary voltage regulators.
Secondary voltage regulators are necessary to be able to supply RU subsystems with voltages different from the RU power bus voltage. Secondary voltage converters should have high efficiency (>85%), low component count, over current protection (output current limiter), activation via logic signal, possibility to monitor output current and output voltage.

3.3.4 Additional circuitry that should be implemented by the RU power subsystem:

- RU jettison system activation and driver circuit.

This circuit is needed for reliable operation of the RU main tether jettison device. Its function is to supply electrical voltage at sufficient current to heat or melt the resistance wire used to release the main tether end from RU if needed. This circuit should have very low probability of false activation. It is highly recommended to require more than one logic signal to be activated when tether release has been initiated.

- Tether reel motors switch circuit

As it may be impossible to switch the tether reel motor motion unit into low power standby or sleep mode the 12 V supply voltage to the motion unit should be independently controllable by the control and telemetry system of the RU.

- RU heater device drivers

To maintain tolerable temperature within RU electronics and thrusters enclosure an active heater(s) may be needed. RU power system should include the necessary driver circuit(s) to control the state of heater(s).

To lower the amount of transmissive heat through solar panel and heat shield when RU power consumption is very low the unused electrical power should be radiated away by using a radiator device. The radiator driver is also included in the RU power system

- A/D converters and I/O expander for reducing the number of connections between RU power subsystem and RU control and telemetry subsystem.

To make the electrical interface between RU power and control subsystem simpler and interference tolerant, most of the RU power system A/D converters and I/O port expanders will be implemented within RU power system. Both devices will be operated using a single two-wire (I2C) compatible interface.

3.4. RU power system detailed design

3.4.1 RU power system block diagram

RU power system block diagram is presented on Figure 3.4.1:

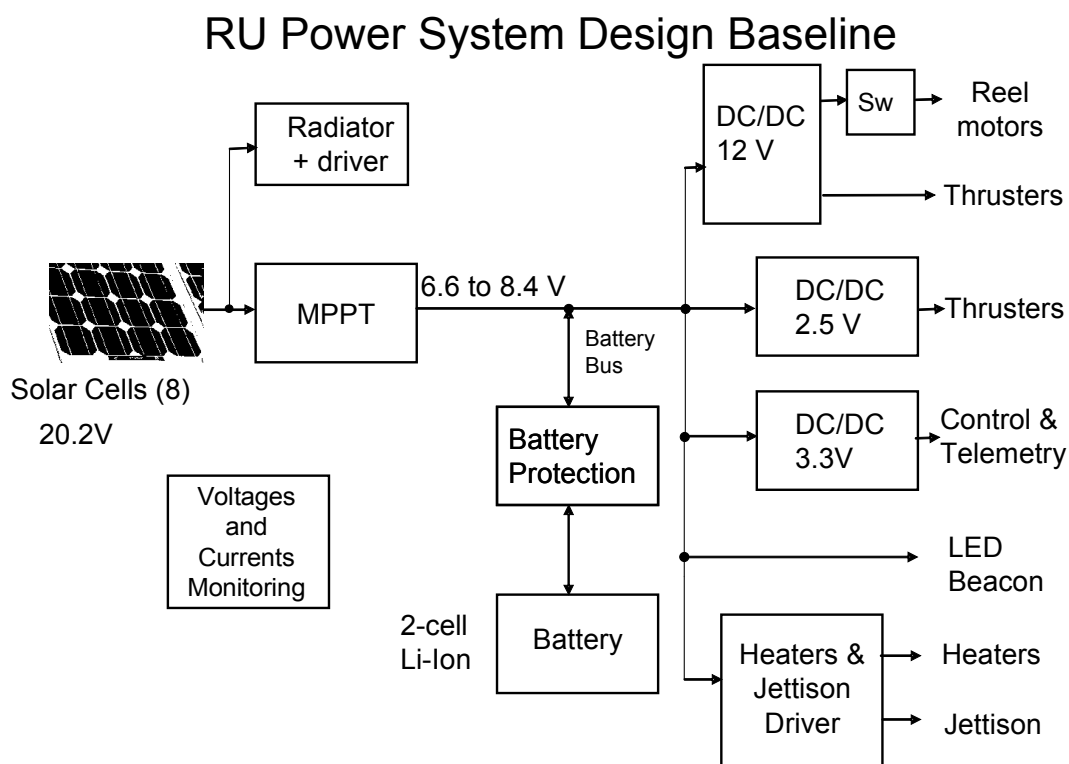


Figure 3.4.1: Block diagram of the RU power system

3.4.2 Primary power source (solar panel)

Azur Space 3G30C triple-junction GaAs solar cells have been selected as the primary power source of the RU. This solar cell has high efficiency, is space qualified and is readily available from the manufacturer with short lead time. The most relevant electrical and mechanical parameters of the solar cell are provided below:

- Physical area = 30.18 cm²
- Thickness = 150 ± 20 μm
- Voc = 2.7V (Open circuit voltage on cell at 1 AU)
- Current at max power = 505mA
- Average efficiency at BOL = 29.1%
- Cover glass may be needed for thermal balance of the RU

Mechanical layout and dimensions of the solar cell is presented on Figure 3.4.2.

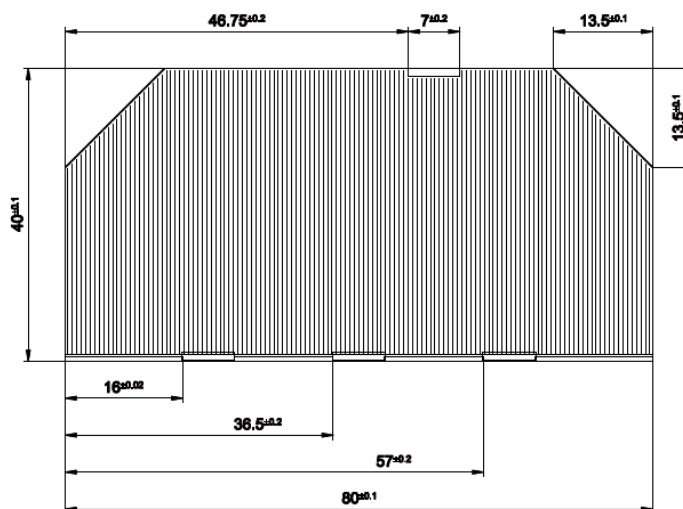


Figure 3.4.2: Mechanical layout of the Azur Space 3G30C solar cells

3.4.3 MPPT and battery charging circuit

MPPT and battery charging circuit block diagram is presented on Figure 3.4.3. The MPPT design is based on a solution initially proposed by Maxim Integrated Products Inc.^[2]

The actual design uses a single National Semiconductor Inc. (now Texas Instruments Inc.) LM26001 switched mode DC/DC converter to implement both MPPT and battery charging functionality.

The input voltage from solar panels is connected to the DC/DC converter input and an energy storage capacitor. As the output voltage corresponding to the maximum power output remains relatively constant at any given lighting condition of the solar cell it is possible to optimize the solar panel average load by switching the DC/DC converter on and off based on the voltage on energy storage capacitor. A n LMP7300 voltage comparator with adjustable hysteresis is used to compare the DC/DC converter input voltage against a reference voltage set by the MPPT control algorithm. If the voltage on the storage capacitor increases above the reference the DC/DC converter switches on and power is transferred to the load. The storage capacitor starts to discharge until the voltage on comparator input falls below the reference voltage switching the DC/DC converter off. The actual reference thresholds can be adjusted by the comparator hysteresis setting.

The DC/DC converter output voltage is controlled by a current feedback loop based on a current sense amplifier LMP8645 and an operational amplifier LMC6482A. The current sense amplifier output voltage is also used for battery charge current monitoring. An additional circuit (not shown on the block diagram) has been included to disable battery charging after the battery is fully charged. When battery voltage reaches the value corresponding to fully charged state the DC/DC converter switches into to voltage feedback mode to maintain constant voltage and prevent overcharging of the battery. Full schematic diagram of the MPPT and battery charging circuit is provided in Appendix 3.1.

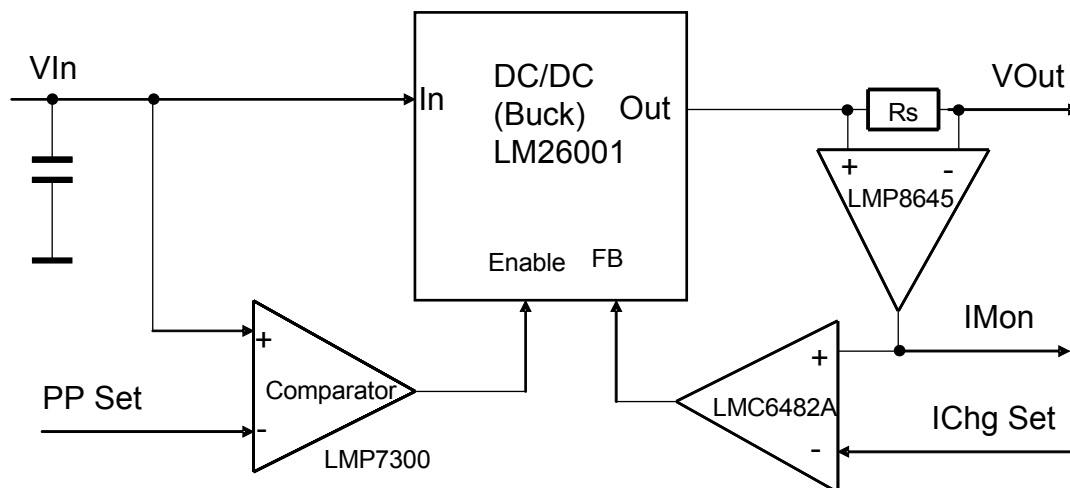


Figure 3.4.3: MPPT block diagram

3.4.4 Secondary DC/DC regulators

Secondary DC/DC regulator convert the RU battery bus voltage to the value needed by RU other subsystems. Three different voltages will be needed for the RU subsystems. One of the voltages is equal to the battery bus voltage which means no dedicated regulator is needed for it. For other voltages two separate DC/DC converters are used, one to generate 2,5 V needed by the control and telemetry subsystem and CG thrusters module, and another one for generating 12 V for tether reel motors and CG thruster activation. For the FEPP thruster configuration another 15-30 V regulator may be needed if the thruster cannot be supplied from 12V regulator.

As the battery bus voltage is higher than 2.5V an LM2674 “Buck” type regulator is used. For regulator output current monitoring a current sense amplifier LMP8645 is used.

Full schematic diagram of the 2.5V regulator is provided in Appendix 3.2.

To get +12 V DC voltage from the lower battery bus voltage (6.6...8.4V) an LM2700 “boost” mode DC/DC converter is used together with a current sense amplifier as in the +2.5V regulator section. Both regulators can be activated by the logic signals from the RU control and telemetry subsystem.

An additional 3.3V regulator is included to supply voltages to A/D converter and IO expander circuits of the RU power system. This regulator may also be used to supply the voltage to the RU control and telemetry system instead of the 2.5 V regulator it must stay switched on permanently.

Full schematics of the 12 V regulator is provided in Appendix 3.3. and 3.3 V regulator in Appendix 3.4.

To suppress high frequency switching noise at DC/DC converters input and output terminals feed-through capacitors are used.

3.4.5 Battery

Two commercially available Li-Ion battery cells will be used as energy storage devices on the RU. A primary battery cell candidate to be used is Sony 18650-HC space qualified Li-ion battery cell. This is a cylindrical cell, 18 mm diameter and 65mm long. The weight of the cell is 65 mm. The capacity of one battery cell is about 1.5 Ah and the battery has been used in many space missions with excellent reliability, safety and performance records. Some newer battery designs can also be considered for the future E-Sail missions as the battery technology advances very fast and many new high performance

batteries with extended life time may become available.

3.4.6 Battery protection circuit

To protect the battery from unexpected overloads and over voltages a battery protection circuit based on commercially available UCC3911 integrated circuit from Texas Instrument Inc. is used. This integrated circuit implements battery protection and monitoring functions independently for both battery cells. If needed the battery can be disconnected using a logic signal from RU control and telemetry system.

Full schematics of the battery protection circuit is provided in Appendix 3.5.

3.4.7 A/D circuit

The A/D circuit provides support for monitoring most of the RU power system voltage and current levels. It is implemented using an AD7291 A/D converter IC from Analog Devices Inc. A/D converter is interfaced to the RU control and telemetry system via I2C compatible interface.

Full schematics of the A/D converter section is provided in Appendix 3.4.

3.4.8 I/O expander, heater and jettison drivers

To minimize the number I/O signals between RU Control and telemetry system and power system an I/O expander is used. It is based on Texas Instruments Inc. TCA6408A I2C to 8 bit parallel interface converter IC. To protect the RU jettison system from unwanted activation caused by eventual software glitch or a single event latch-up problem the logic signal used to trigger the jettison system is combined from two separate signals by using 74LXG08 logic AND gate. One of its input signals (Jettison_arm) is connected directly to the RU control and telemetry I/O port. The second signal comes from the I/O expander. Both signals should be set active to trigger tether jettison event.

Heater and jettison system drivers are implemented using ST Microelectronics Inc. VNQ810-E high side driver IC. As both jettison and heaters do not require any regulated supply voltages the battery bus voltage is used. A spare driver output is available to power additional equipment on the RU if needed.

The full schematic diagram of the I/O expander, heater and jettison drivers is provided in Appendix 3.6.

3.4.9 RU power system interface signals

The RU power system interface signals are described in Table 3.4.1. below.

Signal Name	Signal Type	Signal Level	Signal Function
Vin	Power, Input	< 20.8 V	Power from solar cells
BAT_Bus	Power, Output	6.6 ... 8.4 V	Battery bus voltage
+12V_Out	Power, Output	12 V	Supply voltage to thrusters
+12V_RM	Power, Output	12 V	Supply voltage to reel motors
+2.5V_Out	Power, Output	2.5 V	Voltage to CG thruster
+3.3V_Out	Power, Output	3.3 V	Voltage to Control and telemetry
ICh_Mon	Analog, Output	0 ... 2.5 V	Charge current monitoring

Signal Name	Signal Type	Signal Level	Signal Function
IChCtrl	Analog, Input	0 ... 2.5 V	Charge current adjust
SDA	Digital, I/O	2.5 V	I2C bus data line
SCL	Digital, I/O	2.5 V	I2C bus clock line
VBat_En-	Digital, Input	2.5V	Battery enable, active low
LowBat_ind	Digital, Output	Open Drain	Low battery volt. Indication, active low
Jettison_arm	Digital, Input	2.5 V	Jettison system control
Radiator_En	Digital, Input	2.5 V	External heat radiator control, active high
+12V_FT_En	Digital, Input	2.5 V	+12V output to FEEP thruster enable, active high

Table 3.4.1: RU power system interface signals

Additional control and monitoring functions available via I2C interface are described in Table 3.4.2 below.

Signal Name	Signal Direction	Signal Function
Power Point Control	Input	MPPT power point adjustment
VIn Monitor	Output	Solar cell voltage monitoring
VOut Monitor	Output	Battery bus voltage monitoring
ICh	Output	Battery charge current monitoring
VBat	Output	Battery voltage monitoring
+12V Monitor	Output	+12V regulator output monitoring
+2.5V Monitor	Output	+2.5V regulator output monitoring
+3.3 V Monitor	Output	+3.3V regulator output monitoring
+12V Enable	Input	+12V regulator control
+12V_RM_Enable	Input	Reel Motor supply voltage control
+2.5V Enable	Input	+2.5 V regulator control
Jettison_Cmd	Input	Jettison event trigger control
ADC_Enable	Input	Local ADC enable control
Heater1_Enable	Input	Heater control
Heater2_Enable	Input	Heater control
Radiator_Enable	Input	Radiator control
+12V_FT_Adjust	Input	+12V output voltage adjustment

Table 3.4.2: RU power system control and monitoring signals available over I2C interface

3.5. Mechanical design

All components except solar cells can be mounted on a 4 or 6 layer printed circuit board (PCB). At least one routing layer of the PCB must be used as solid ground plane to be able to achieve good thermal and EMC related performance of the design. The PCB will be located in thermally controlled and partially radiation shielded compartment of the RU. It may be possible to assemble both RU power system and control and telemetry system on a single PCB. The approximate size of the PCB is 98 x 98 mm². Preliminary mass budget of the RU Power Subsystem components is provided in Table 3.4.3 . Note that the weight of heaters is not included in this mass budget. The list of all electronic components used in the RU Power Subsystem is provided in Appendix 3.7.

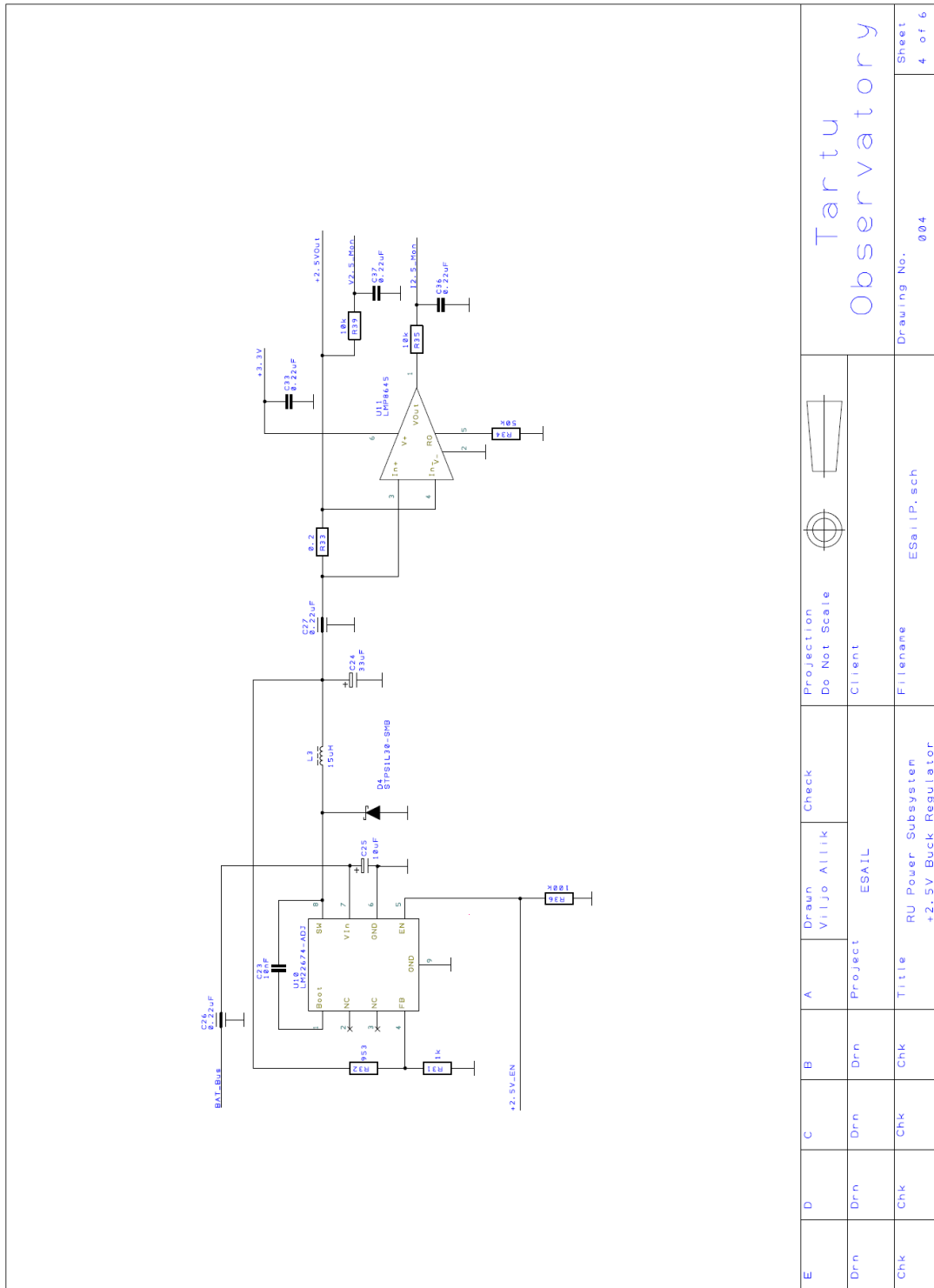
Item	Mass [g]
Unmounted PCB	34
Electronic components	10
Wiring	10
Batteries	85
Solar cells (including assembly materials)	25
Total:	164

Table 3.4.3: RU Power Subsystem preliminary mass budget

References

- 1 ESAIL D41 Requirements specification of the Remote Unit
- 2 Harnessing Solar Power with Smart Power-Conversion Techniques, AN484, Maxim Integrated Products Inc. Dec. 01, 2000

Appendix 3.2: +2.5 V regulator circuit diagram

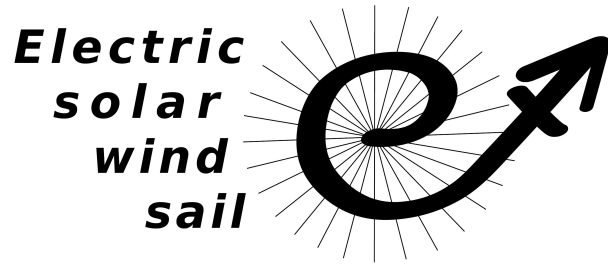


E	D	C	B	A	Drawn Viljo Allik	Check	Projection Do Not Scale		Tartu Observatory	Drawing No. 004 Sheet 4 of 6
Drn	Drn	Drn	Drn	Project ESAIL	Client	File name ESailIP.sch				
Chk	Chk	Chk	Chk	Title RU Power Subsystem +2.5V Buck Regulator	File name ESailIP.sch	Drawing No. 004				

Appendix 3.7: List of RU Power Subsystem electronic components

Ref Name	Component	Value	Qty
V1, V2	2N7002		2
U16	74LXG08		1
U6, U19	AD5259		2
U12	AD7291		1
D2	BAS21		1
BAT1, BAT2	BATT_SLPB603870H	4.1V Lilon	1
C3, C4, C44, C55	C0402	0.1uF	4
C13, C32, C33, C34, C35, C36, C37, C43	C0402	0.22uF	8
C6, C11, C12, C28, C29, C31, C45, C50, C51, C52, C57, C58, C60, C61	C0402	1uF	14
C16, C54	C0402	2.2uF	2
C17	C0402	2.7nF	1
C23, C38	C0402	10nF	2
C5, C15	C0402	10uF	1
C9	C0402	47nF	1
C10	C0402	47pF	1
C18	C0402	180pF	1
C14	C0402	330pF	1
C30	C0805	10uF	1
C25, C40	C7343	10uF	2
C24, C39	C7343	33uF	2
C2, C19, C20	C7343	100uF	3
C1	C7343	100uF*	1
1.1.12	DT3316_1	15uH	1
L2	DT3316_1	*	1
L3	DT3316_1	*	1
L4	DT3316_1	*	1
U8	LM2700		1
U10, U13	LM22674-ADJ		2
U1	LM26001Q		1
U4	LMC6482A		1
U2	LMP7300		1
U3, U9, U11	LMP8645		3
U7	LP2980-50		1
C7, C8, C21, C22, C26, C27, C41, C42, C46, C47, C48, C49, C53, C56, C59	NFM21_0805	0.22uF	15
R19, R20	R0402	*	2
R26	R0402	0	1
R12, R27, R33	R0402	0.2	3
R2, R7, R14, R15, R31, R42	R0402	1k	6
R6	R0402	1.2M	1
R24	R0402	1.3M	1

R43	R0402	1.6k	1
R3, R16, R18, R29, R35, R39, R44, R45	R0402	10k	8
R9	R0402	15k	1
R11	R0402	17.7k	1
R13, R28, R34, R41	R0402	50k	4
R23	R0402	68k	1
R1, R5, R8, R10, R30, R36, R38, R47, R48, R49, R50	R0402	100k	11
R17	R0402	100k*	1
R25	R0402	150k	1
R21, R22	R0402	220	2
R4	R0402	240k*	1
R40	R0402	250k	1
R37	R0402	260k	1
R46	R0402	750k	1
R32	R0402	953	1
D1, D3, D4, D5	STPS1L30-SMB		3
U15	TCA6408A		1
U5	UCC3911		1
U17, U18, U20	VN5160S-E		3
U14	VNQ810-E		1



4. Controller and Telemetry

Prepared by:

Ångström Space Technology Centre,
Johan Sundqvist

Coordinating person:

Greger Thornell,
greger.thornell@angstrom.uu.se

Table of Contents

4.1. Introduction.....	49
4.1.1 Requirements.....	49
4.2. Telemetry system design.....	50
4.2.1 Channel access control.....	50
4.2.2 Antenna design and simulation.....	50
4.2.3 Link budget.....	52
4.2.4 Mechanical, environmental and electrical specifications.....	53
4.2.5 Bill of Materials.....	53
4.3. Optical Beacon design.....	54
4.3.1 Estimation of required power.....	54
4.3.2 Mechanical, environmental and electrical specifications.....	56
4.3.3 Bill of Materials.....	56
4.4. Control system design.....	57
4.4.1 Reel motor driver interface.....	57
4.4.2 Power subsystem interface.....	57
4.4.3 Cold gas thruster interface.....	58
4.4.4 FEEP thruster interface.....	59
4.4.5 Mechanical, environmental and electrical specifications.....	59
4.4.6 Bill of Materials.....	60
4.5. Heat shield sensing.....	61
4.5.1 Mechanical, environmental and electrical specifications.....	61
4.5.2 Bill of Materials.....	61
Appendix.....	63 - 73

4.1. Introduction

This document describes the design of the ESAIL Remote Unit (RU) control and telemetry system. The purpose of the control subsystem is to control the various subsystems of the RU and to monitor the status of each subsystem as well as the overall RU status. The telemetry system is used to receive simple commands from the Main Craft (MC) and to transmit status data to the MC.

The main design drivers for the Control and Telemetry subsystem is high reliability, low power and low mass. Much effort has been put into minimizing power consumption and system size.

4.1.1 Requirements

In Table 4.1, derived from document D41, *Requirements specification of the Remote Unit*, requirements affecting the control and telemetry subsystem are shown.

Req. ID	Description
ES1-RU-104	<i>The Remote Unit must remain operational when the time-averaged angle between its pointing vector and the sun direction is 0-60°.</i>
ES1-RU-201	<i>The RU shall ensure the operational temperature range required by all its subsystems when these are operational.</i>
ES1-RU-202	<i>The RU shall ensure the tolerable temperature range required by all its subsystems when these are non-operational.</i>
ES1-RU-207	<i>Within angular ranges of $\pm 3^\circ$ azimuthal, and $\pm 15^\circ$ in the bulging direction of the sail with respect from a flat sail, the RU shall be able to reveal its position to the main craft by an optical beacon, either at a predetermined schedule or on request.</i>
ES1-RU-210	<i>During deployment, the RU shall control the reeling out of the auxetethers and adjust the pace to that of the reeling out of the main tether. The amount of auxetether reeled out shall be monitored with 5-mm accuracy.</i>
ES1-RU-214	<i>The RU shall monitor its temperature and communicate this with main craft either at a predetermined schedule or on request.</i>
ES1-RU-215	<i>The RU shall monitor its angle to the sun and communicate this with main craft either at a predetermined schedule or on request.</i>
ES1-RU-216	<i>The RU shall be able to communicate via radio with main craft.</i>
ES1-RU-217	<i>At all times, the RU shall maintain the command and data handling required for its internal functions as well as communication with main craft.</i>
ES1-RU-501	<i>In case of detection of an onboard anomaly, the RU shall automatically enter a Safe Mode. The Safe Mode shall:</i> <ul style="list-style-type: none"> - ensure power supply to relevant subsystems - maintain operational temperature - provide necessary communication capacity

Table 4.1: RU Requirements relevant to the Control and Telemetry system.

4.2. Telemetry system design

A single low-power transceiver chip handles all Radio-Frequency communication between RU and Main Craft. All circuitry is placed inside the thermally controlled box, mounted on a four or six layer PCB. In order to save space and weight, the telemetry electronics should be placed on the same PCB as the control subsystem.

A coaxial cable connects the transceiver chip to a Printed Circuit Board (PCB) half-wave dipole antenna that is mounted on the heat shield. The antenna PCB also holds a surface-mount balun. Communication takes place on the 869 MHz band.

Commands and data are sent to the RF chip using an SPI interface. An on-chip buffer stores received bytes and triggers an interrupt signal when a transmission is completed, allowing the Microcontroller to sleep and wake up when data is received. Address-based packet filtering and automatic CRC checksum calculations makes certain that only intended and valid commands are received.

4.2.1 Channel access control

Both the forward links (MC to RUs) and the return links (RUs to MC) will share the same channel. Hence, with one MC and 100 RUs, some kind of channel access scheme must be implemented.

A simple and reliable solution is to let the MC initiate all transmissions over the medium. The MC will then act as a Master, and all RUs as Slaves. This makes the protocol rather deterministic and easy to implement. The drawback is that an RU can not signal immediately when a critical error is detected, as it must await its turn.

Given a bitrate of 12000 bps, 10 bytes MC → RU and 30 bytes RU → MC and a 3 ms response time, the total time required to complete one transmission will be approx. 30 ms. In the case of 100 RUs, one full transmission cycle would take 3 s, which would also be the worst-case latency. This is in compliance with the requirements.

4.2.2 Antenna design and simulation

The dipole antenna has a width of 129.44 mm and is manufactured on a 1.57 mm thick Nelco N4000-29 substrate with a copper thickness of 17.5 μm. The design of the antenna is shown in Fig. 4.1.

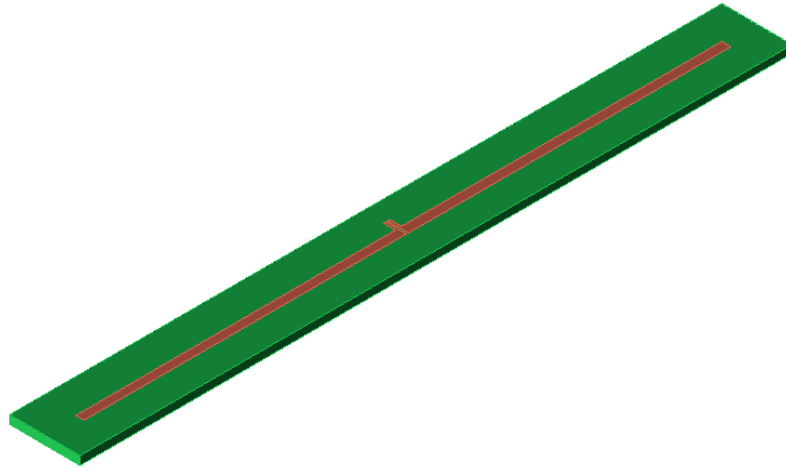


Figure 4. 1: Dipole antenna design.

The length and width of the antenna PCB is 140 mm and 12 mm, respectively. Not shown in Fig. 4.1 is the balun, which will be placed close to the dipole.

A simulation of the design, made in Agilent ADS, is shown in Fig. 4.2. It can be seen that the antenna has been matched to the 869 MHz and has a bandwidth large enough for the FSK modulation.

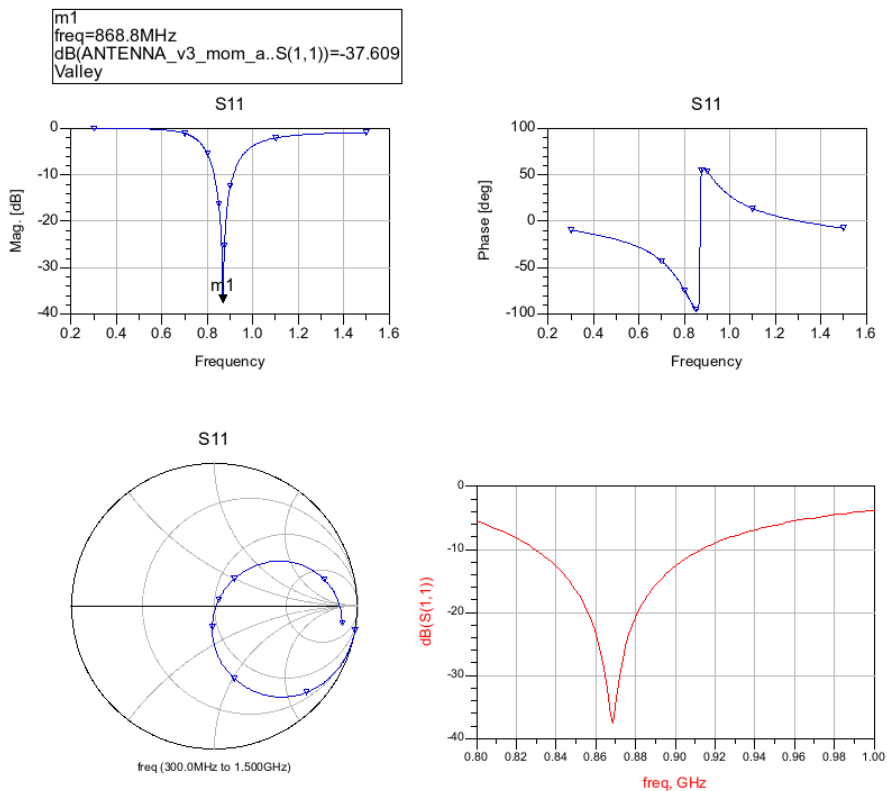


Figure 4.2: Agilent ADS simulation of Printed Circuit Board antenna

4.2.3 Link Budget

The link budget for the telemetry system is shown in Table 4.2.

Parameter		Value	Unit
Frequency	f	0.87	GHz
Transmitter Power	P	0.0100	Watts
Transmitter Power	P	-20.0	dBW
Transmitter Line Loss	L_l	-1.0	dB
Transmit Antenna Beamwidth	θ_t	128.0	deg
Peak Transmit Antenna Gain	G_{pt}	2.16	dBi
Transmit Antenna Diameter	D_t	0.2	m
Transmit Antenna Pointing Offset	e_t	0.2	deg
Transmit Antenna Pointing Loss	L_{pt}	0.00	dB
Transmit Antenna Gain (net)	G_t	2.16	dBi
Equiv. Isotropic Radiated Power	EIRP	-18.8	dBW
Propagation Path Length	S	20.0	km
Space Loss	L_s	-117.3	dB
Propagation & Polarization Loss	L_a	-1.0	dB
Receive Antenna Diameter	D_r	0.20	m
Receive Antenna Efficiency		0.52	
Peak Receive Antenna Gain (net)	G_{rp}	2.37	dBi
Receive Antenna Beamwidth	θ_r	120.7	deg
Receive Antenna Pointing Error	e_r	25.0	deg
Receive Antenna Pointing Loss	L_{pr}	-0.5	dB
Receive Antenna Gain	G_r	1.9	dBi
System Noise Temperature	T_s	614.0	K
Data Rate	R	12000.0	bps
Eb/No	E_b/N_o	24.2	dB
Carrier-to-Noise Density Ratio	C/N_o	65.0	dB-Hz
Bit Error Rate	BER	1.00E-005	
Required E_b/N_o	Req E_b/N_o	13.0	dB
Implementation Loss		-2.0	dB
Margin		9.2	dB

Table4.2: RF link budget

4.2.4 Mechanical, environmental and electrical specifications

Mechanical data

Main PCB dimensions	20 x 20 x 2	mm [L x W x H]
Antenna dimensions	140 x 15 x 1.6	mm [L x W x H]
Total weight	12	g

Temperature range

Min. operating temp.	-40	° C
Max. operating temp.	+85	° C

Electrical specifications

Supply voltage	2.5	V
Receive current	3	mA
Transmit current	25	mA
Average power dissipation	10	mW
Output RF power	10	dBm
Maximum input RF power	0	dBm
Sensitivity	-105	dBm (typ.)

4.2.5 Bill of materials

A complete Bill of Materials for the telemetry system is shown in Table 4.3.

REF	MFG	PART/VAL	TOL	PKG
SAW1	EPCOS	B3715		SMD
U2	SEMTECH	SX1211		QFN-32
XFMR1	MINI-CIRC.	TCN-1-10		FV1206-1
XTAL3		12.8 MHz		SMD
C1		680 pF	5%	0402
C10		220 nF	10%	0402
C11		1 μ F	15%	0402
C12		1 μ F	15%	0402
C13		22 pF	5%	0402
C14		1.8 pF	0.2 pF	0402
C27		10 nF	10%	0603
C7		10 nF	10%	0402
C8		100 nF	10%	0402
L1		8.2 nH	0.2 nH	0402
L2		8.2 nH	5%	0402
L3		100 nH	5%	0402
L4		8.2 nH	5%	0402
R1		6.8 k Ω	1%	0402
R2		1 Ω	1%	0402
R35		100 k Ω	5%	0402

Table 4.3: Bill of Materials for the Telemetry subsystem

4.3. Optical Beacon design

The optical beacon resides outside the thermally controlled box, where it is placed on a short boom close to the jettison mechanism. The Beacon itself consists of a single High-Brightness Light Emitting Diode (HBLED). Inside the thermally controlled box, a driver circuit supplies the HBLED with a constant current. A single binary signal, connected to the Control Unit, is used to toggle the optical beacon on and off.

The driver circuitry is mounted on a four or six layer PCB. In order to save space and weight, the optical beacon driver electronics should be placed on the same PCB as the control subsystem.

4.3.1 Estimation of required power

To make certain that the Main Craft camera will be able to detect the beacon pulse, transmitted power must be estimated. A typical COTS CCD camera for the main craft is likely to have specifications close to those shown in Table 4.

Parameter	Value	Unit
Dark current	0,001	electrons/pixel/sec
Readout Noise	8,5	electrons
Quantum Efficiency	75%	
Full well capacity	90 000	electrons

Table 4.4: Specifications of Spectral Instruments 850-series CCD Camera

A few basic assumptions are made, namely: (1) At distance d from the RU, the output power will be spread uniformly over a spherical cap. (2) The MC camera will have a narrow-band optical filter, suppressing background light. (3) All light that enters the MC camera lens will hit a single pixel on the CCD chip.

Given a distance of 10 km between MC and RU, a LED optical power output of 100 mW at a wavelength of 470 nm and a MC lens diameter of 56 mm, the number of photons detected per second as a function of the opening angle of the LED is shown in Fig. 4.3.

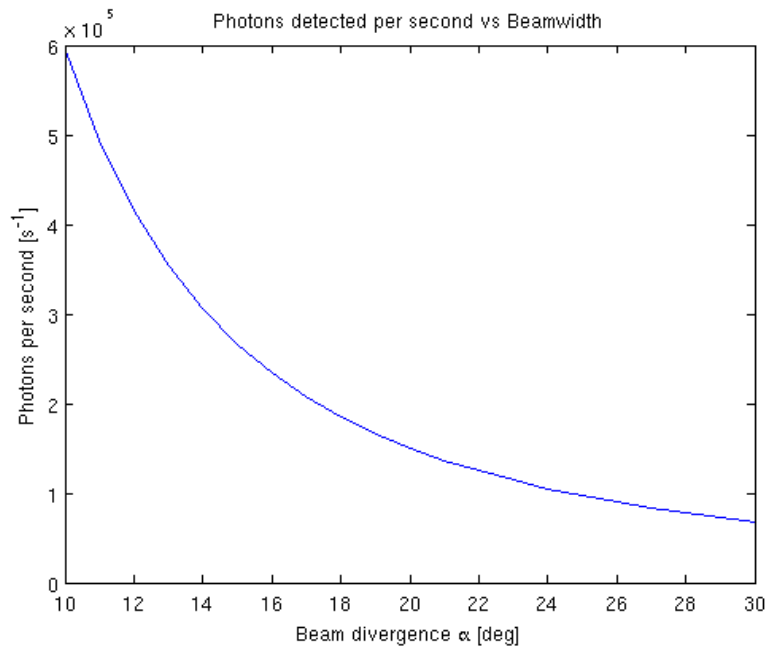


Figure 4.3: Number of photons detected per second versus beam width.

It can be seen that, for a beam divergence of 30 degrees, approximately 8 000 photons per second will enter the lens. This is several orders of magnitude greater than both the dark current and readout noise of the COTS camera. Hence, it should be no problem to detect the optical beacon even for integration times much shorter than one second.

In Fig. 4.4, the SNR of the image captured at the MC is plotted versus beam divergence for a worst-case scenario with a very poor camera. Here, a quantum efficiency of 50%, dark noise of 1 electron per pixel and second, and a readout noise of 10 electrons is assumed. The integration time is set to 10 ms and distance between RU and MC is 10 km.

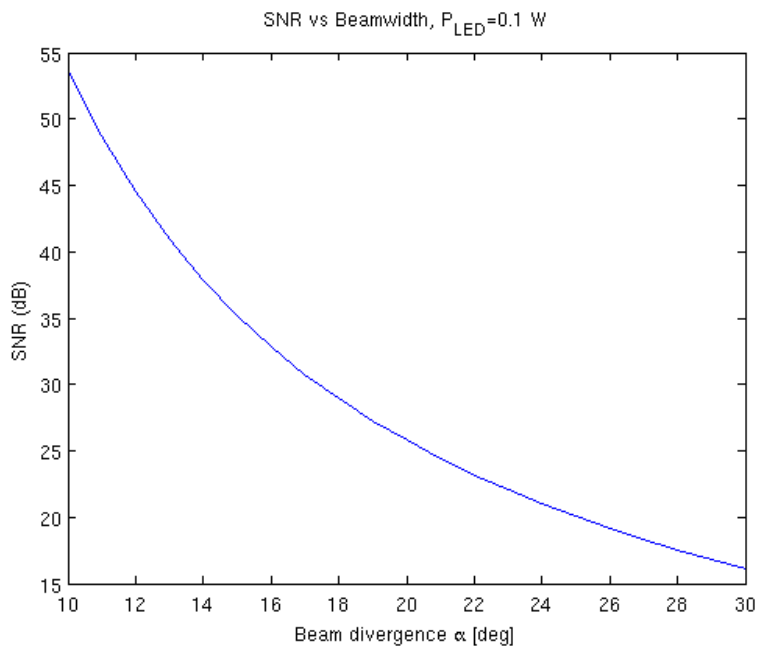


Figure 4.4: SNR of captured image versus beam divergence for a 10 ms beacon pulse.

By choosing a High-Brightness LED with a maximum output power of 350 mW, a good design margin is achieved.

A LED of lower power would reduce the peak current consumption, but it must also be lit for longer periods of time and will, hence, not decrease the average power consumption of the optical beacon.

It is of utmost importance that a narrow-band (5-10 nm passband) optical filter is mounted on the Main Craft camera to ensure that stray light is sufficiently suppressed.

4.3.2 Mechanical, environmental and electrical specifications

Mechanical data

Main PCB dimensions	20 x 20 x 5	mm [L x W x H]
LED PCB dimensions	10 x 10 x 2	mm [L x W x H]
Total weight	12	g

Temperature range

Circuitry Min. operating temp.	-40	° C
Circuitry Max. operating temp.	+125	° C
LED Min. operating temp.	-40	° C
LED Max. operating temp.	+100	° C

LED specifications

Output power (optical)	350	mW
Output wavelength	450	nm

Electrical specifications

Supply voltage	6 - 42	V
Current consumption, LED ON	700	mA ⁽¹⁾
Current consumption, LED OFF	100	µA
Average power dissipation	1	mW

¹ Typical value. Actual current consumption will vary with input voltage.

4.3.3 Bill of Materials

A complete Bill of Materials for the optical beacon is shown in Table 4.5. Part references are according to the schematics, appendix 4.1.

REF	MFG	PART/VAL	TOL	PKG
U9	NAT.SEMI	LM3404		PSOP-8
HBLED1	CREE	C450EZ1000		DIE
Q3	FAIRCHILD	FDC6401N		SSOT-6
L5	TDK	SLF10145T		10x10 mm
RC1	CENTR.SEMI	CMSH2-40		SMB
C23		100 nF	10%	0603
C24		10 nF	10%	0603
C25		3.3 µF 25 V	10%	0603
C26		1 µF 25 V	10%	0603
R32		100 kΩ	5%	0402
R33		133 kΩ	1%	0603
R34		0.33 Ω	1%	0603

Table 4.5: Bill of Materials for the Optical Beacon subsystem.

4.4. Control system design

The control system will monitor the status of all subsystems and will, upon detection of on-board anomalies, take appropriate action (shut down subsystems, keep temperatures within limits by activating/deactivating heaters, etc). All other subsystems will be activated only upon request from Main Craft.

The control system is based on a low-power micro-controller unit (MCU) from the Energy Micro Gecko family. Given the amount of I/O needed, a 64-pin QFN device with 54 General-Purpose I/O (GPIO) was chosen.

Following sections will briefly describe the electrical interfaces between the MCU and all subsystems of the Remote Unit that are external to WP 4.3. Schematics, shown in Appendix, should be used in reference to the text.

The electronics are mounted on a four or six layer PCB. In order to save space and weight, effort should be made to share PCB with the power subsystem.

4.4.1 Reel Motor driver interface

The reel motor motion control circuits are controlled via a RS232 asynchronous serial data interface. The signals required to be connected to the MCU is shown in Table 4.6, where signals to and from the MCU are inputs and outputs, respectively.

Signal name	Description	Dir., Voltage
MOTOR1_RX	RS232 Data	Output, 12 V
MOTOR1_TX	RS232 Data	Input, 12 V
MOTOR2_RX	RS232 Data	Output, 12 V
MOTOR2_TX	RS232 Data	Input, 12 V
MOTOR1_SGNL	Pulses/rev	Input, Open collector
MOTOR2_SGNL	Pulses/rev	Input, Open collector

Table 4.6: List of signals between the Reel Motion controller and Control subsystem.

Since the communication interface is rather slow, the 12 V signals are level shifted using standard MOSFETs. The two open-collector signals are connected to the 2.5 V bus with pull-up resistors and connected to the MCU's pulse counter pins.

By configuring the motion controller so that it outputs a certain number of pulses for each turn of the motors, the length of each unreeled tether can be measured.

4.4.2 Power subsystem interface

The signals required to interface to the power subsystem are shown in Table 4.7. Signals to and from the MCU are inputs and outputs, respectively.

Signal name	Description	Type, direction
I2C_SDA	I2C Bus Serial Data	Dig. Input/Output
I2C_SCL	I2C Bus Serial Clock	Dig. Input/Output
VBAT_ENABLEn	Battery bus enable	Dig. Output
JETTISON_ARM	Jettison mechanism	Dig. Output
3.3V_SHDN	3.3 V bus shutdown	Dig. Output
LOWBAT_IND	Battery low indicator	Dig, Input
ICH_CNTRL	Charge current control	Analog Output
BATTERY_TEMP	Battery thermistor	Analog Input
RADIATOR_EN	Radiator enable	Digital Output

Table 4.7: List of signals between the Power and Control subsystems

All digital signals operates at the same voltage level as the MCU and are connected directly to the MCU GPIO pins. The analog output is generated by the Digital-to-Analog Converter (DAC) peripheral inside the MCU, whereas the analog input is connected to an operational amplifier and sampled by the MCU ADC.

4.4.3 Cold Gas thruster interface

Some external circuitry is required in order to control and read temperature data from the CG thrusters. The signals involved are shown in Table 4.8.

Signal name	Description	Dir., Voltage
CG_VALVE_A	Thruster A valve	Output, 12 V pulse → 2.5 V DC
CG_VALVE_B	Thruster B valve	Output, 12 V pulse → 2.5 V DC
CG_HEATER_A	Thruster A heater	Output, Battery bus voltage
CG_HEATER_B	Thruster B heater	Output, Battery bus voltage
CG_TEMP_A	Thruster A temp.	Analog I/O, NTC thermistor
CG_TEMP_B	Thruster B temp.	Analog I/O, NTC thermistor
CG_TEMP_TANK	Tank temperature	Analog I/O, NTC thermistor

Table 4.8: List of signals between the Cold Gas Thruster and Control subsystems.

Thruster valve operation

The valve is opened by a short 12 V pulse, and is kept open by a 2.5 V DC power signal.

The low side of each valve is connected to a MOSFET that is normally off. A positive pulse from the MCU turns the FET on so that the valve is connected to ground. The high side of the valve is connected to an opto-relay that switches between the two different voltage supplies.

A RC-network connected to a comparator is used to create a logic '1' pulse approximately 1 ms after the FET has been turned on. This signal triggers the relays and the

Thruster heater operation

The thruster heaters are turned on by a low-side MOSFET switch. The battery voltage bus is used to power the heaters.

Temperature sensing

Operational amplifiers are used to interface to the three NTC thermistors that measures the temperature of the gas tank and of each thruster. The current through each thermistor is approximately 200 μA to avoid self-heating effects.

4.4.4 FEFP thruster interface

The FEFP thruster will carry a Power and Control unit (PCU). All communication between the PCU and MCU will use a standard digital low-speed interface, I2C, SPI or similar.

Thrust level is set by changing the input voltage to the High-Voltage converter. This implies adjusting the voltage of the 12 V (nominal) supply of the power system, which is made via the I2C bus. The FEFP tank heater is controlled by the RU MCU.

4.4.5 Mechanical, environmental and electrical specifications

Mechanical data

Dimensions	30 x 30 x 2	mm [L x W x H]
Total weight	6	g

Temperature range

Min. operating temp.	-40	$^{\circ}\text{C}$
Max. operating temp.	+85	$^{\circ}\text{C}$

Electrical specifications

Supply voltage	2.5	V
Active current consumption	4	mA ⁽¹⁾
Sleep mode current consumption	500	μA
Average power dissipation	5	mW ⁽²⁾

¹ MCU running at full speed at a clock frequency of 16 MHz.

² Assuming sleep mode cycling.

4.4.6 Bill of Materials

A complete Bill of Materials for the interface circuitry and the MCU is shown in Table 4.9 and Table 4.10, respectively.

REF	MFG	PART/VAL	TOL	PKG
U12	MAXIM IC	MAX9618		SC70
U13	MAXIM IC	MAX9618		SC70
U14	MAXIM IC	MAX9618		SC70
U10, U11	CLARE	LBA710S		SMD
U8	MAXIM IC	MAX9618		SC70
Q1, Q2	FAIRCHILD	FDC6401N		SSOT-6
Q4, Q5	FAIRCHILD	FDC6401N		SSOT-6
C20, C22		TBD	5%	0603
C21		100 nF	15%	0603
C32		100 nF	15%	0603
C33		10 nF	15%	0603
C34		100 nF	15%	0603
R22, R27		TBD	1%	0603
R23, R26		TBD	1%	0603
R24, R25		TBD	1%	0603
R28, R53		47 k Ω	5%	0402
R29, R45, R55		TBD	1%	0402
R30, R31		100 k Ω	5%	0402
R36, R37		100 k Ω	5%	0402
R38, R39		270 Ω	1%	0402
R40, R41		270 Ω	1%	0402
R42, R46, R54		TBD	1%	0402
R49, R50		TBD	1%	0402
R51, R52		TBD	1%	0402
R56		133 k Ω	1%	0402
R57		47 k Ω	1%	0402
R58, R59		47 k Ω	5%	0402

Table 4.9: Bill of Materials for interface circuitry.

REF	MFG	PART/VAL	TOL	PKG
U3	ENRGY MICRO	EFM32G230		QFN-64
XTAL1		32.768 kHz		SMD
XTAL2		16 MHz		SMD
C30, C31		13 pF	10%	0402
C28, C29		19 pF	10%	0402
R61, R62		47 k Ω	5%	0402
R60		47 k Ω	5%	0402
C2, C6		100 nF	10%	0603
C4, C5		10 nF	10%	0603
C3		1 μ F		0603

Table 4.10: Bill of Materials for MCU circuitry.

4.5. Heat shield sensing

The heat shield sensors monitors the RU's inclination relative to sun and the heat shield temperature. The sensors are placed at the center of the heat shield, while the electronics are placed inside the thermally controlled box, mounted on a four or six layer PCB. In order to save space and weight, the heat shield sensor electronics should be placed on the same PCB as the control subsystem.

The temperature sensing consist of two platinum Resistive Thermal Devices (RTDs). Each RTD is connected to a Wheatstone bridge and the output is amplified by an Instrumentation amplifier. The signal is then fed to the Analog-to-Digital converter in the MCU. Sampled voltages are translated to a corresponding temperature by the MCU, which adjusts for RTD nonlinearities.

Two photodiodes are used as sun inclination sensors. The photodiodes are reverse-biased and operated in a photoconductive mode where the output photocurrent is proportional to the illuminance. A shunt resistor creates a voltage drop that is amplified by an operational amplifier. These amplified signals are sampled by the MCU ADC.

4.5.1 Mechanical, environmental and electrical specifications

Mechanical data

Dimensions	20 x 30 x 2	mm [L x W x H]
Total weight	5	g

Temperature range

Circuitry Min. operating temp.	-40	° C
Circuitry Max. operating temp.	+125	° C
RTD Min. operating temp.	-125	° C
RTD Max. operating temp.	+150	° C
Photodiode Min. operating temp.	-40	° C
Photodiode Max. operating temp.	+125	° C

Sensor specifications

Temperature range	-125 to +100	° C
Temperature accuracy	±2	° C
Inclination range	TBD	°
Inclination accuracy	TBD	°

Electrical specifications

Supply voltage	2.5	V
Current consumption	2	mA
Average power dissipation	5	mW

4.5.2 Bill of Materials

A Bill of Materials for the heat shield sensors is shown in Table 4.11.

U5	MAXIM IC	MAX9618		SC70
U6, U7	ANALOG DEV.	AD8227		MSOP-8
U4	MAXIM IC	MAX9618		SC70
PD1, PD2	HAMAMATSU	S9674		SMD
RTD1, RTD2	IST	P1K0.161.6W		
C15		1 μ F	15%	0603
C16		2.2 μ F	15%	0603
C17		10 nF		0603
C18		1 μ F		0603
C19		1 μ F		0603
R10		TBD		0402
R11		TBD		0402
R12, R13		133 k Ω	1%	0402
R14, R15, R16		1 k Ω	1%	0603
R17, R20, R21		1 k Ω	1%	0603
R18, R19		TBD	1%	0603
R3, R6		TBD		0402
R4, R5		1 k Ω	1%	0402
R7, R8		TBD		0402
R9		2.7 k Ω	5%	0402

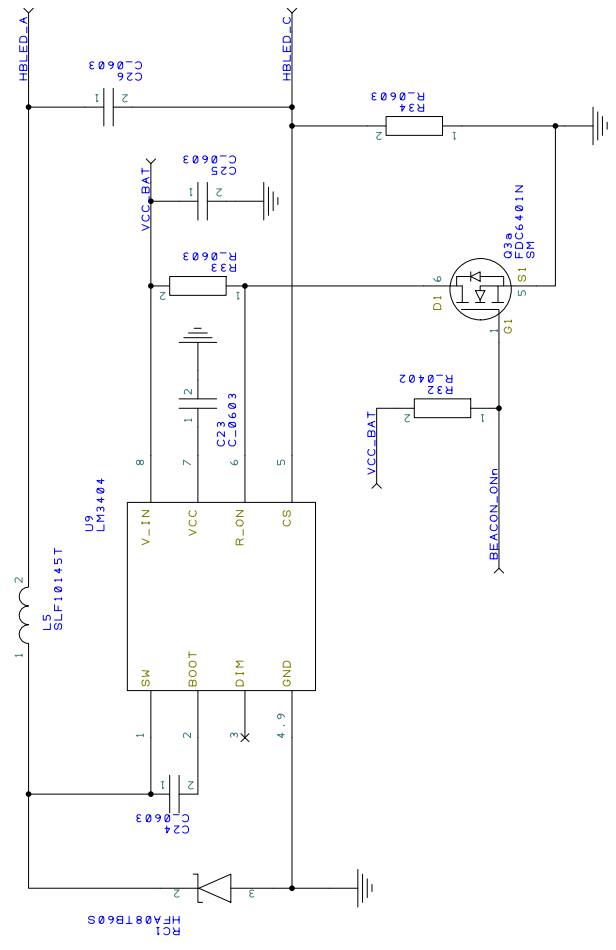
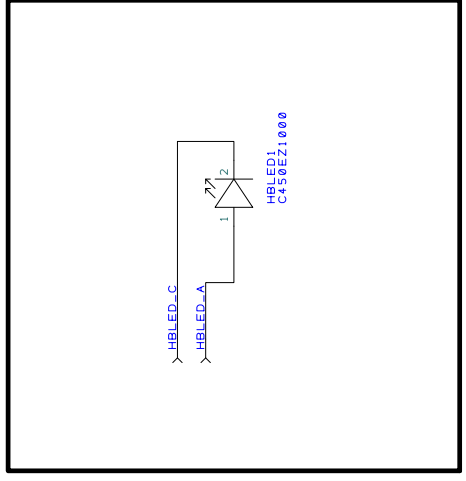
Table 4.11: Bill of Materials for heat shield sensor circuitry.

Appendix

Appendix to Chapter 4 of D41.2, Schematic drawings of controller and telemetry subsystem.

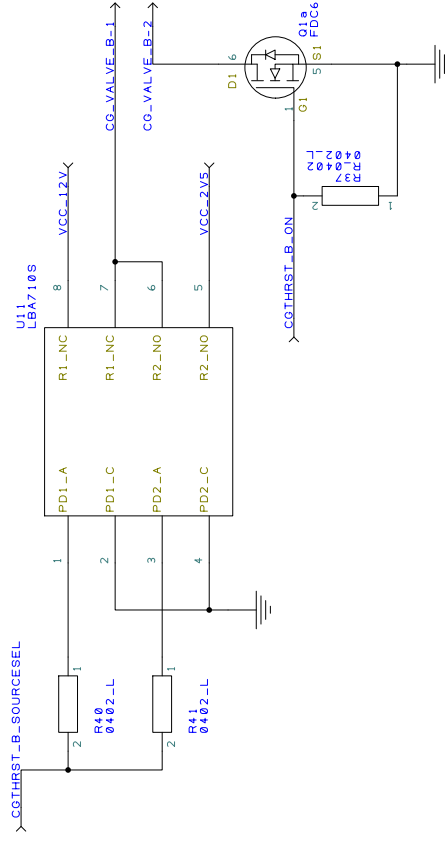
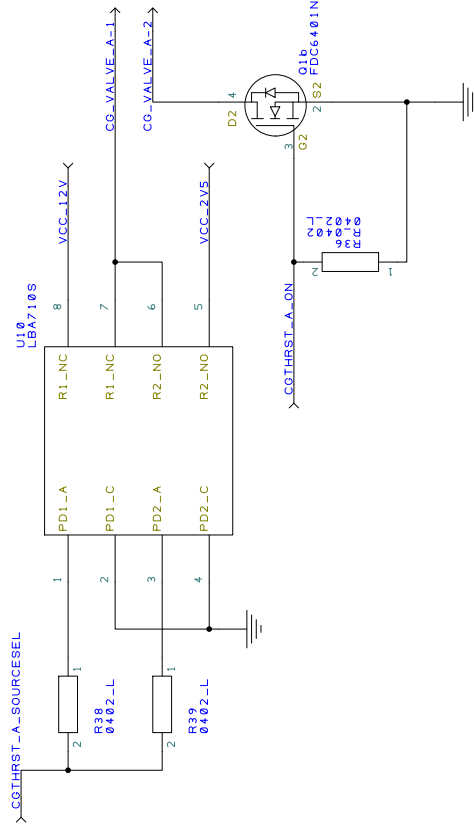
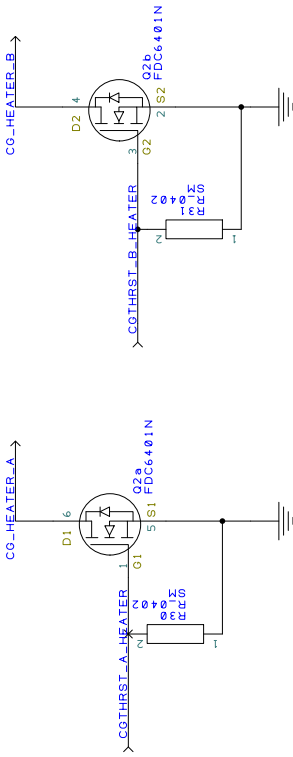
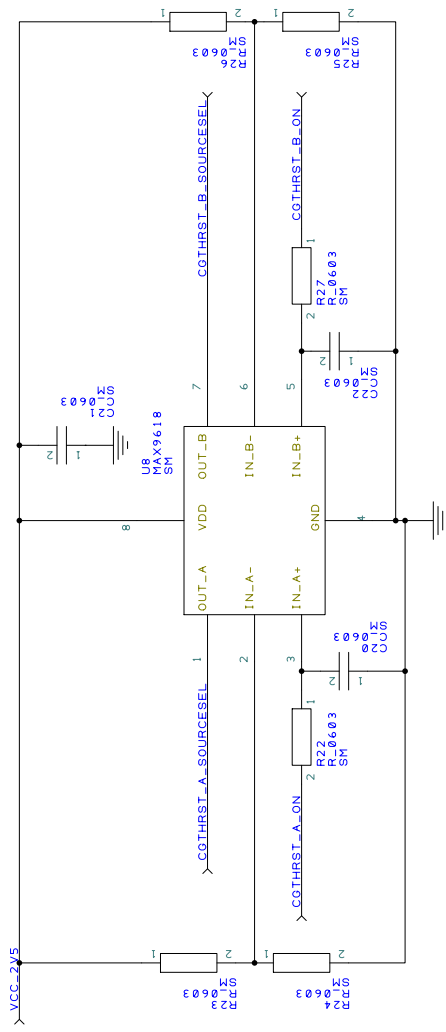
OPTICAL BEACON

OUTSIDE THERMAL BOX



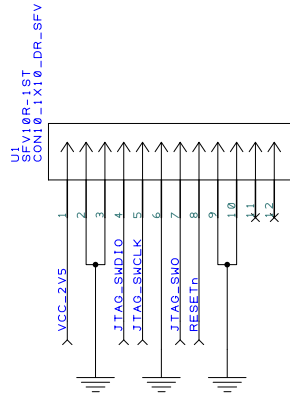
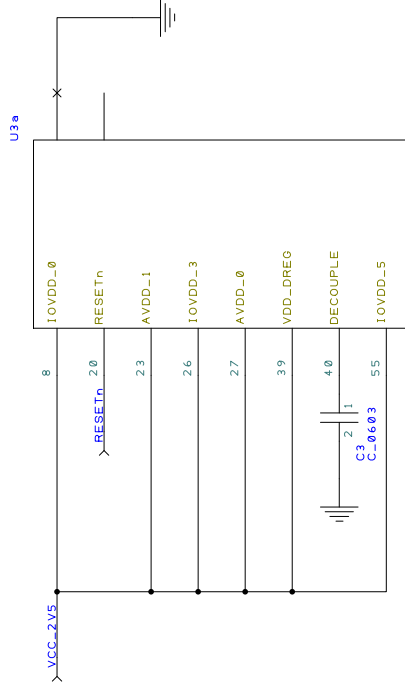
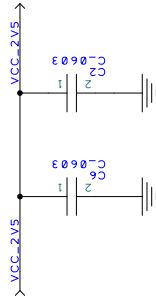
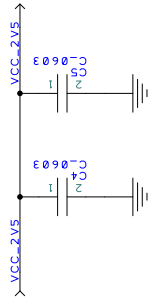
E	D	C	B	A	Drawn	Check	Projection Do Not Scale		Sheet of
Drn	Drn	Drn	Drn	Project		Client	Filename	Drawing No.	
Chk	Chk	Chk	Chk	Title					

CG INTERFACE



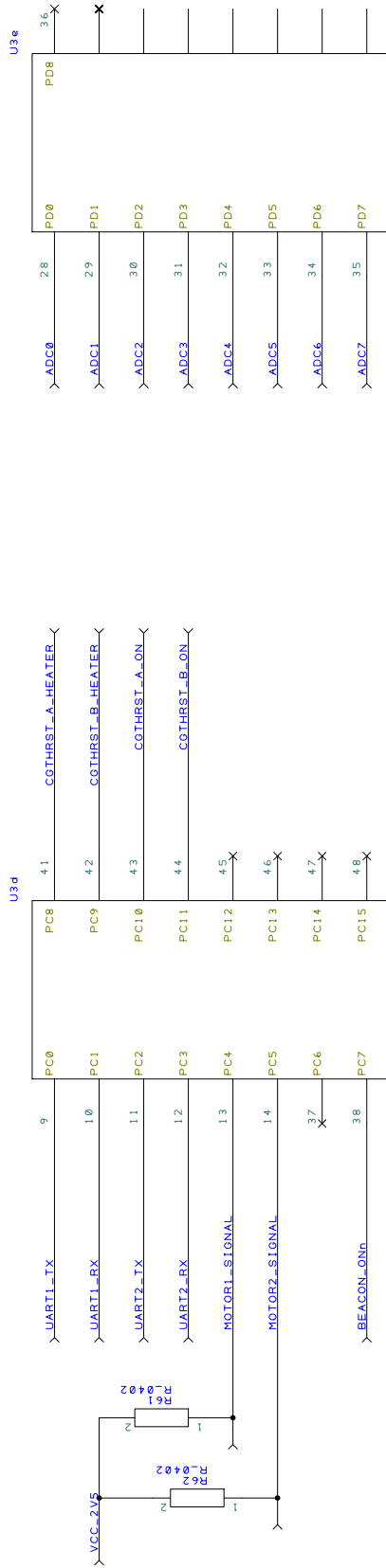
E	D	C	B	A	Drawn	Check	Projection Do Not Scale		Sheet of
Drn	Drn	Drn	Drn	Project	Client	Filename	Drawing No.		
Chk	Chk	Chk	Chk	Title					

MCU PWR & DEBUG



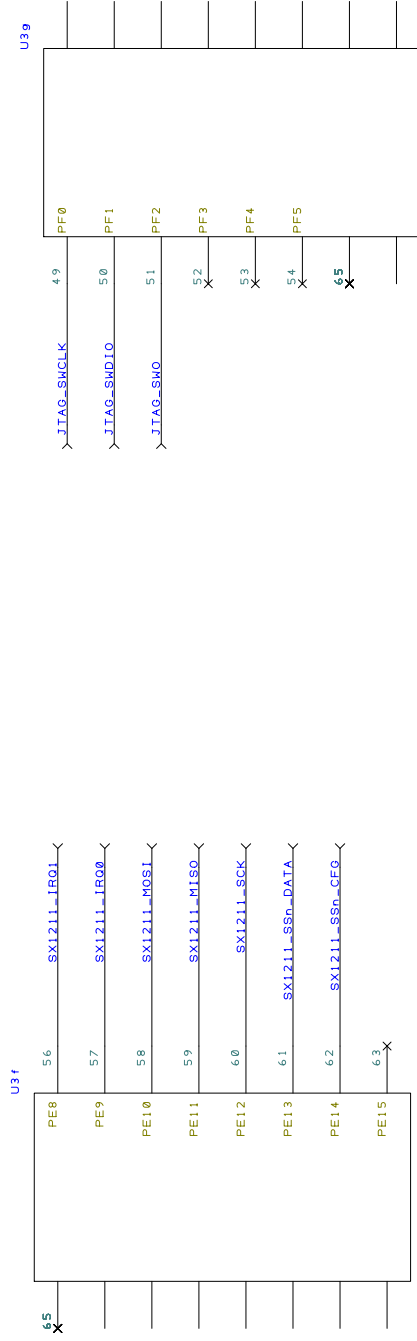
E	D	C	B	A	Drawn	Check	Projection Do Not Scale	Client	Sheet of
Drn	Drn	Drn	Drn	Project					
Chk	Chk	Chk	Chk	Title			Filename	Drawing No.	

PORTC & PORTD



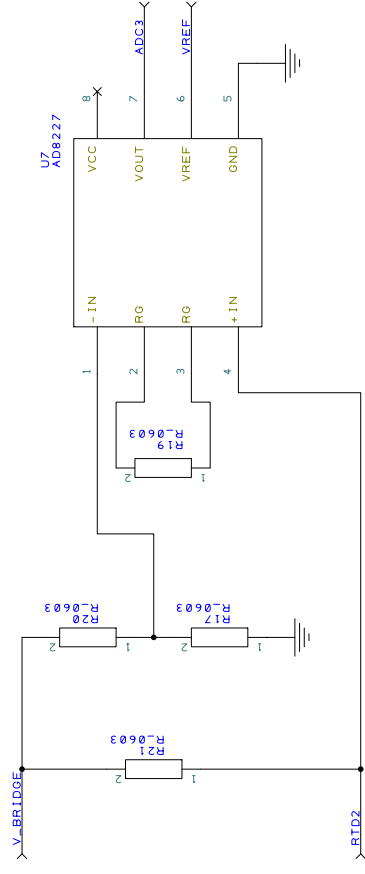
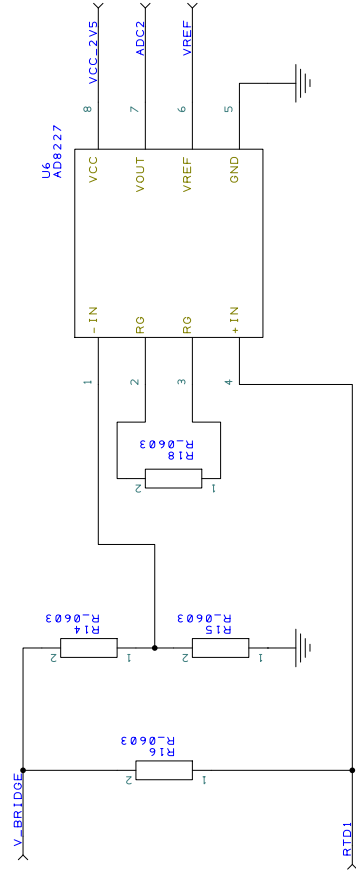
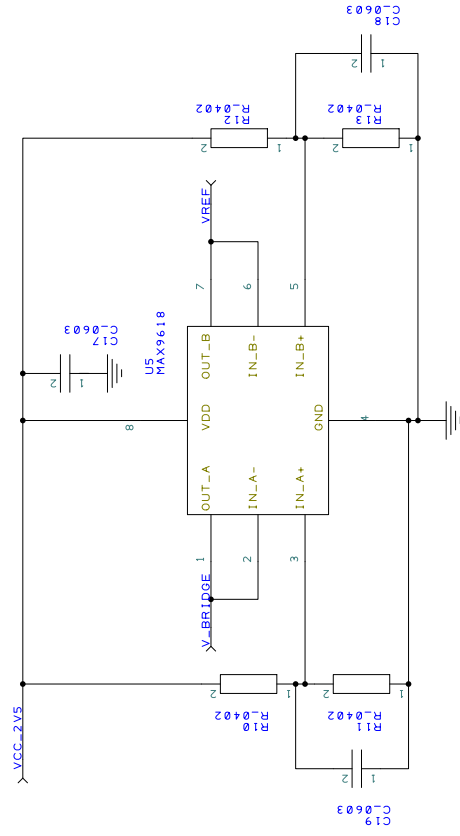
E	D	C	B	A	Drawn	Check	Projection Do Not Scale		
Drn	Drn	Drn	Drn	Project			Client		
Chk	Chk	Chk	Chk	Title			Filename	Drawing No.	Sheet of

PORTE & PORTF

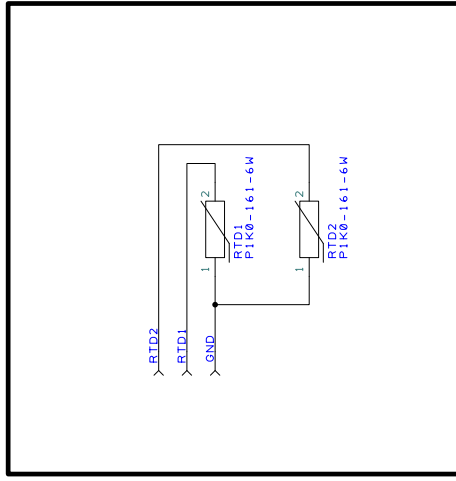


E	D	C	B	A	Drawn	Check	Projection Do Not Scale		
Drn	Drn	Drn	Drn	Project			Client		
Chk	Chk	Chk	Chk	Title			Filename	Drawing No.	Sheet of

HEAT SHIELD TEMPERATURE



AT HEAT SHIELD

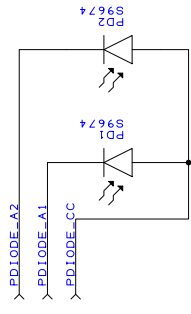
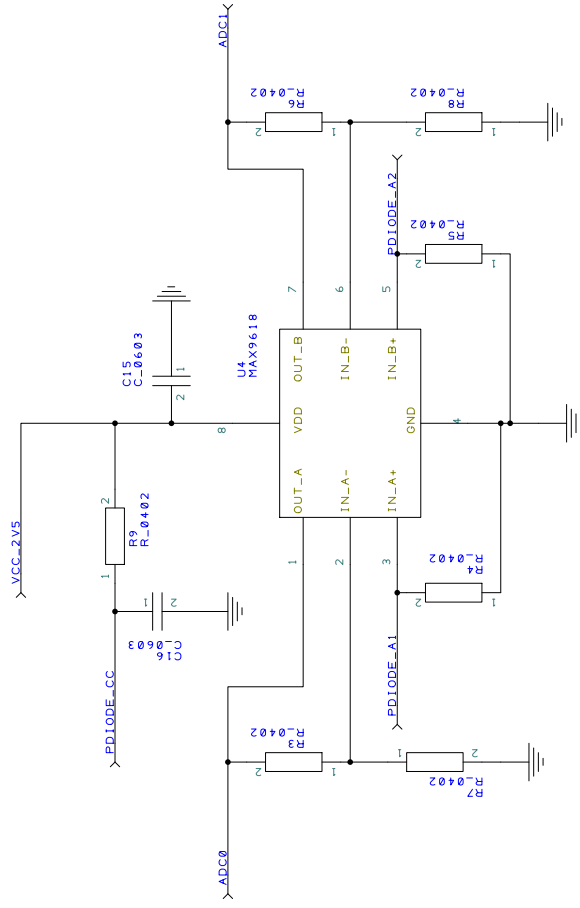


E		D		C		B		A		Check		Projection		Client		Drawing No.		Sheet	
Drn	Do Not Scale	Do Not Scale	Do Not Scale	Do Not Scale	Client	Client	Filename	Filename	of	of									

SUN SENSORS

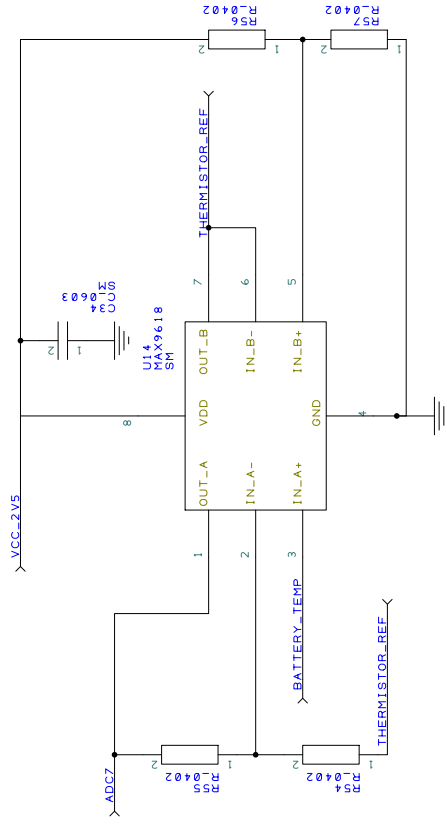
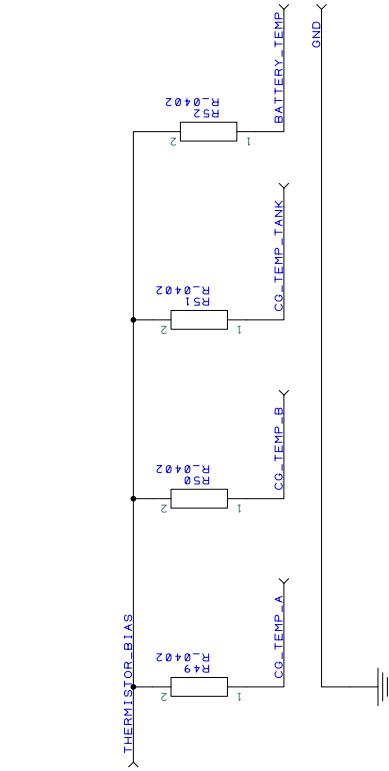
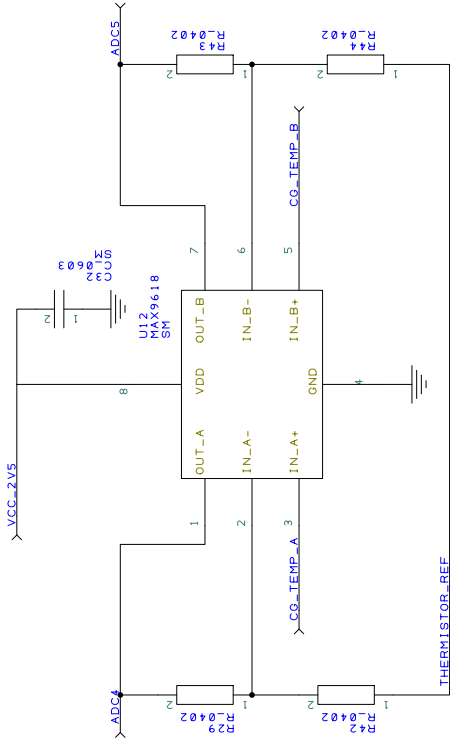
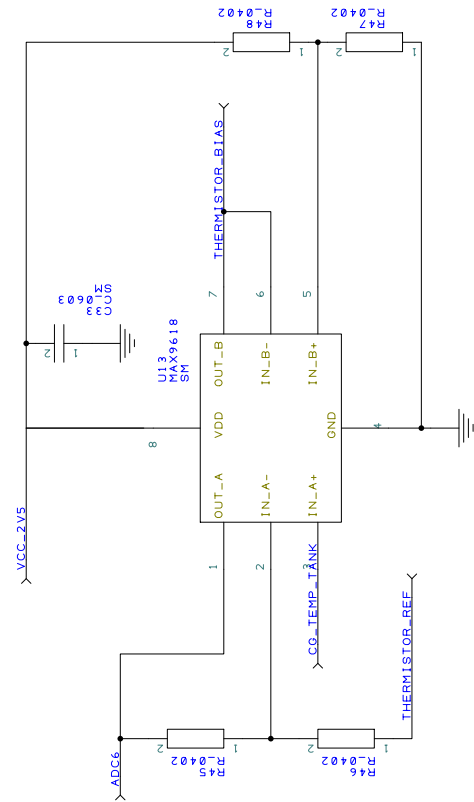
AT HEAT SHIELD

71



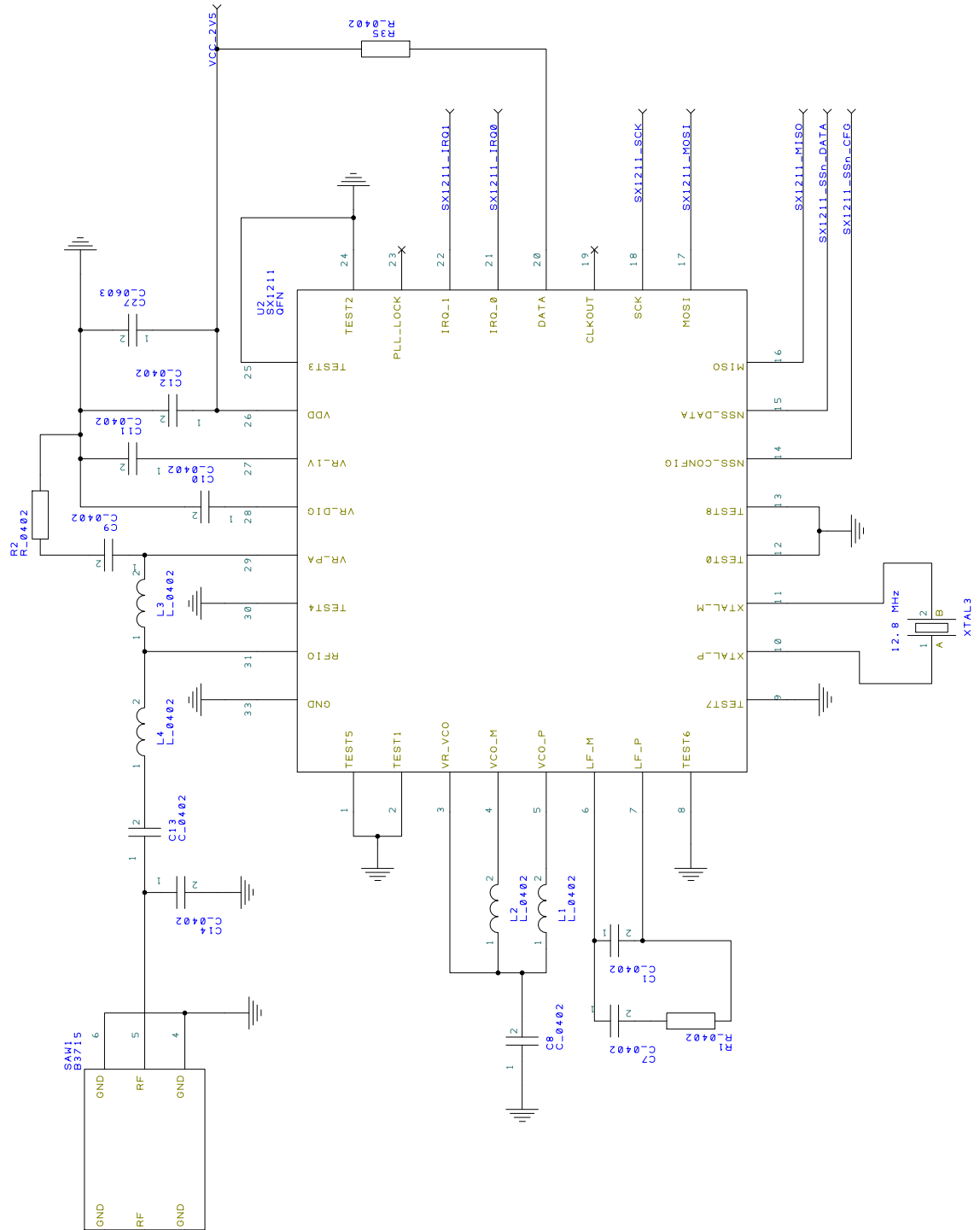
E	D	C	B	A	Drawn	Check	Projection Do Not Scale			Drawing No.	Sheet of
Drn	Drn	Drn	Drn	Project			Client				
Chk	Chk	Chk	Chk	Title			Filename				

THERMAL BOX TEMPERATURE

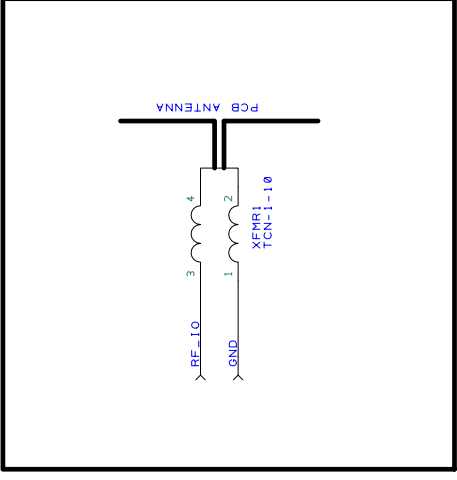


E	D	C	B	A	Check	Projection Do Not Scale	Client	Sheet of
Drn	Drn	Drn	Drn	Project	Filename		Drawing No.	
Chk	Chk	Chk	Chk	Title				

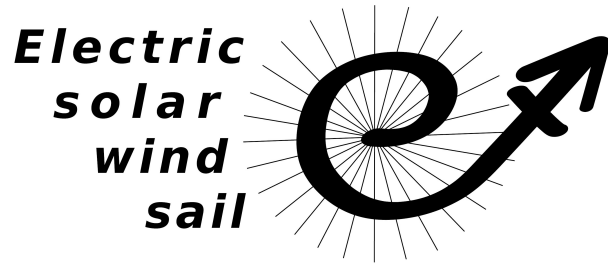
TELEMETRY



AT HEAT SHIELD



E	D	C	B	A	Drawn	Check	Projection Do Not Scale	Client	Filename	Drawing No.	Sheet 1 of 11
Drn	Drn	Drn	Drn	Project							
Chk	Chk	Chk	Chk	Title							



5. Remote Unit Tether jettison mechanism

Prepared by:

Tartu Observatory, Viljo Allik, Ants Agu
Viljo.allik@estcube.eu

5.1. Introduction

This document describes the design of ESAIL Remote Unit (RU) electrical power generation and distribution subsystem (RU Power System).

5.2. RU Tether jettison system design requirements

Design, build and test a pyrotechnic device, which can be used to jettison a tether if needed. The device will be placed at the outer end of each tether, in contact with the Remote Unit. The device will provide the thrust needed for the jettisoning of the tether, and it will also serve as an end mass to help the controlled removal of the tether. The jettisoning device may be used only under abnormal conditions, e.g., if a main or auxiliary tether reel gets stuck during deployment or if a main tether breaks during deployment or flight.

5.2.1 Deduced design requirements from RU top level requirements

The RU tether jettison system requirements are defined in document [1]. The most relevant applicable RU top level requirements are:

Requirement ID	ES1-RU-104
The Remote Unit must remain operational when the time-averaged angle between its pointing vector and the sun direction is 0-60°.	
Requirement ID	ES1-RU-201
The RU shall ensure the operational temperature range required by all its subsystems when these are operational. <i>Note: This is to be decided, but according to preliminary information, a range of 0 to +50°C is operational for all subsystems during operation. However, parts likely to be exposed to temperatures outside of this, tolerate approx. -25 to +85°C during operation.</i>	
Requirement ID	ES1-RU-202
The RU shall ensure the tolerable temperature range required by all its subsystems when these are non-operational. <i>Note: This is to be decided, but according to preliminary information, a range of -30 to +60°C is tolerable for all subsystems. However, parts likely to be exposed to temperatures outside of this, tolerate approx. -40 to +85°C</i>	
Requirement ID	ES1-RU-401
Except for aux-tether reeling mechanisms, the RU shall be designed to be fully operational for 5 years.	
Requirement ID	ES1-RU-601
Except for those relevant only for deployment, the RU shall be designed to fulfil all	

requirements after having been subjected to all environmental conditions anticipated from its deployment to completion of mission.	
Requirement ID	ES1-RU-603
The RU shall be fully operational when exposed to maximum heat radiation (sun at 0.9 AU, normal incidence, Earth albedo and Earth IR).	
Requirement ID	ES1-RU-604
Except for deployment-specific functions, the RU shall be fully operational when exposed to minimum heat radiation (sun at 4 AU and 60° incidence to spacecraft plane, no albedo and no other IR).	
Requirement ID	ES1-RU-605
During the mission life time, the RU shall withstand a vacuum level higher than 10 ⁻⁷ mbar without degradation.	
Requirement ID	ES1-RU-606
The Remote Unit must survive a turnover, i.e. a full reversal of its pointing vector, for up to 5 min without overheating or overcooling, and during this time maintain safe-mode functionality.	
Requirement ID	ES1-RU-607
The RU shall be tolerant to a total UV radiation dose corresponding to a worst case scenario of 5 years at 0.9 AU.	
Requirement ID	ES1-RU-208
At any time, and on confirmed request from main craft, the RU shall be able to free itself from its main tether by jettisoning it. <i>As this relates to minimizing the risk of the tether interfering with the rest of the spacecraft, the procedure must be carefully tailored from simulation data.</i>	
Requirement ID	ES1-RU-107
The RU:s connection to the main tether shall handle the same peak load as the main tether without yielding. <i>In theory, the anticipated peak load is 6 g, and the strength per stressed main tether member 16 g (gram forces).</i>	
Requirement ID	ES1-RU-106
The RU and its attachment to its tethers must be designed with proper HV spacecraft engineering practices (AD-5).	

5.3. RU Tether jettison system design concept

The main goal was to design, build and test a pyrotechnic device, which can be used to jettison a tether if needed. Pyrotechnic solution was abandoned as it was discussed during project meetings and replaced by a mechanical concept of simple cutting function of the tether.

The jettison system consists of a body, printed circuit board (PCB), fuse wire connection wires and mounting bolts. Tether end section, made of a dyneema or similar plastic fibre, will be attached to the fuse (resistance wire). Under abnormal conditions, when tether jettison is requested the fuse will be heated by electric current. The fibre will melt or vaporize releasing the main tether from RU.

The main tether may be attached to the jettison system in two configurations:

- Using a small loop of tether that wraps around the fuse wire.
In this configuration tether will be attached only to the fuse wire and if the fuse wire breaks mechanically during normal operation without actual jettison request then tether will be released from the RU.
- Using a designated anchor point on the RU where tether end is attached after looping around the fuse wire.
In this configuration tether will not be released if fuse wire breaks mechanically. If this happens only the jettison capability will be lost but tether remains attached, improving the reliability during normal operation of the RU.

5.4. RU Tether jettison system mechanical design

Based on the component specifications shown in section 2.1, the whole Jettison System has been designed following the idea to develop a lightweight, reliable and easy to produce device. The main properties of the Jettison System are summarized in Table. 5.1. and component descriptions are provided in Table. 5.2. The values in both tables should be considered as preliminary values and may be changed according to the future design refinements.

Table 5.1: Jettison system mechanical properties

Main properties	
Diameter	12 mm
Length	7 mm
Length	13 mm
Mass	5 g
Volume	1.47cm ³

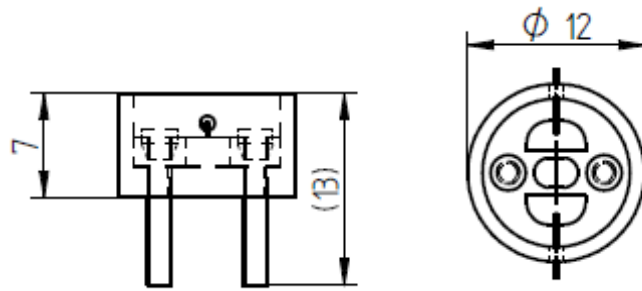


Figure. 5.1: Principal views of the Jettison Unit with overall dimensions.

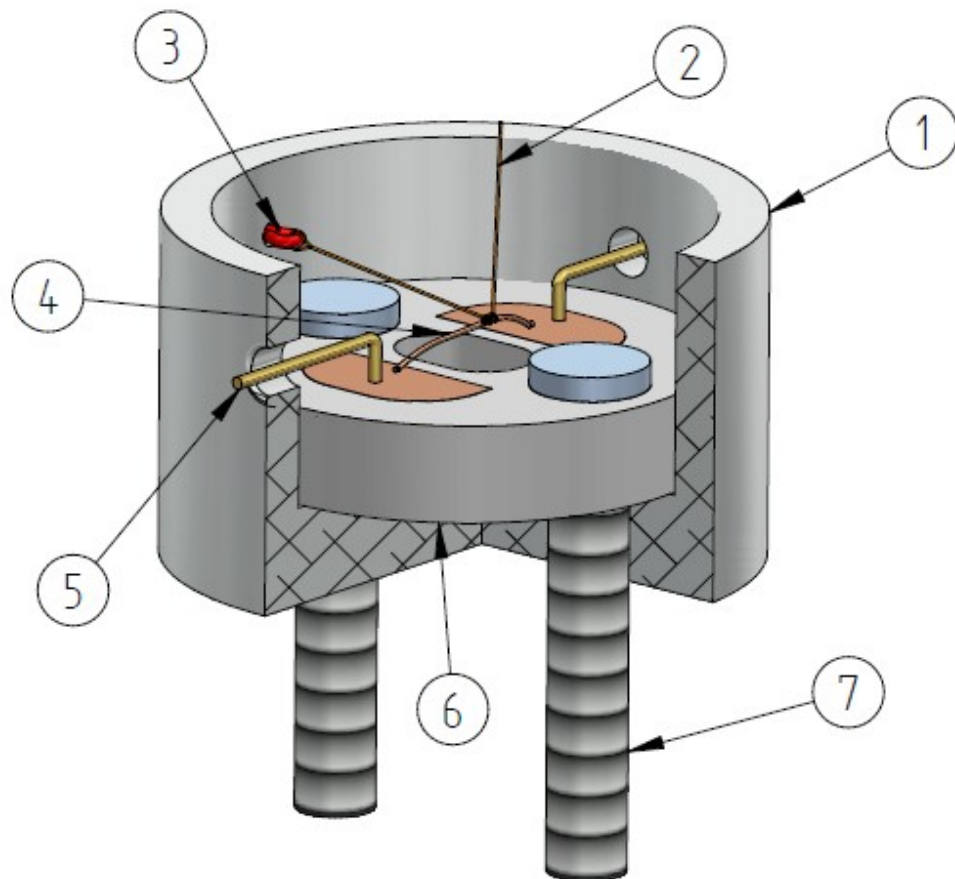


Figure. 5.2: Isometric view of the Jettison System with part numbers.

Table. 5.2. Parts description

Nr.	Name	Description
1.	Body	Body made from Aluminium
2.	Dyneema fiber	Tethers end piece attached to a fuse.
3.	Anchor	A safety measure, in case the fuse wire breaks up without jettison request.
4.	Fuse wire	When jettison is triggered current will heat up the wire as well as vaporize it. . Fuse wire will be positioned in the centre of the PCB as a bridge between two copper pads. Materials considered: Konstantan, diameter yet to be determined. Soldered to the PCB
5.	Power supply	Teflon coated wires, supply current to the fuse if required. Soldered to the PCB.
6.	PCB	A printed circuit board, whit a hole in the centre. Power supply and fuse wire are soldered to the copper pads. The PCB itself is fixed with two bolts to the Body.
7.	Bolts	Two countersunk bolts: M1.6 x 0.25 10mm tall; material-Titanium

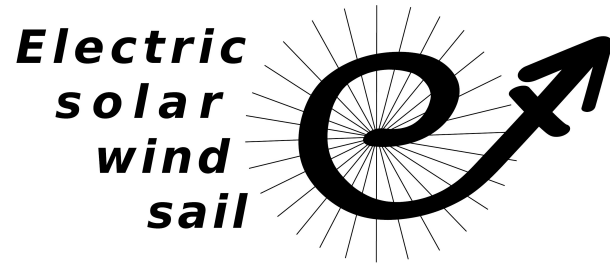
5.5. RU Tether jettison system electrical design

The resistance wire (fuse) will be heated up by electrical current generated and activated by the RU power system. The expected peak current value is between 0.5 and 2 A. The voltage source for the jettison system is the RU battery bus which is capable to deliver required current with good margin.

A special driver circuit is included within RU power system. For increased reliability two independent active logic signals are needed to initiate a jettison event.

References

1. ESAIL D41Requirements specification of the Remote Unit



6. Gas Thruster

Prepared by:

Håkan Johansson, NanoSpace AB

Table of Contents

6.1. Introduction.....	83
6.2. Applicable documents.....	83
6.3. Requirements definition.....	83
6.4. Requirements for the Gas Thruster on the RU.....	83
6.4.1 Mass, size, shape and connectivity.....	84
6.4.2 Functionality.....	84
6.4.3 Launcher compatibility.....	85
6.4.4 Lifetime.....	86
6.4.5 Dependability & Autonomy.....	86
6.4.6 Environment.....	86
6.5. Trade-off studies and critical design issues.....	87
6.5.1 Gas Thruster contribution to the general mass budget equation to the RU.....	87
6.5.1.1 Propellant trade off.....	87
6.5.1.2 Propellant selection.....	90
6.5.1.3 Basic micropropulsion subsystem description and configuration trade-off....	90
6.5.1.4 MEMS Thruster module configuration selection.....	92
6.5.2 Result for the Gas Thruster contribution to the remote unit general mass budget equation.....	92
6.5.3 Mechanical analysis of the propellant tank.....	92
6.5.3.1 Design Description.....	93
6.5.3.2 Static Analysis.....	94
6.5.3.3 Results.....	96
6.6. Gas Thruster Design.....	97
6.6.1 Interfaces.....	99
6.6.3.1 Mechanical IF.....	99
6.6.3.2 Thermal interface.....	110
6.6.3.3 Electrical interface.....	110
6.6.2 Components/parts.....	110
6.6.2.1 The propellant tank.....	110
6.6.2.2 MEMS Thruster module.....	111
6.6.3 Massbreakdown.....	112

6.1. Introduction

This is the design description document of the gas thrusters to the Remote unit in the ESAIL project.

The overall objectives of the Gas thruster propulsion subsystem are to extend the electric sail and control its position during flight. In detail this means that a propulsion system is needed on each Remote Unit (RU) to produce an angular momentum to deploy the tethers of the sail and also have the capability to modify the spin rate of the tethers if needed.

6.2. Applicable documents

- AD1 ESAIL D41 Requirements specification of the Remote Unit
- AD2 ESAIL MoM RU Component Specification, Uppsala 2011-08-29
- AD3 ECSS-E10-03A

6.3. Requirements definition

From the top level requirements defined as level 0 (Mission requirements), level 1 (System level) and level 2 (subsystem requirements) in AD1, requirements for the Gas thruster is defined on a subsystem level, also defined as level 3 requirements in AD1. From these requirements a set of unit level requirements can be established defined as level 4 requirements in AD1.

The requirement id format defined in AD1 for the gas thruster level is ES1-RU-GTH-xxx, where GTH is the format definition of the Gas Thruster subsystem.

By setting the requirements for the Gas thruster derived from the top level requirements, trade-off studies of critical design issues such as propellant selection, thruster configuration and assessment of interfaces (mechanical, electrical and thermal) can be performed.

6.4. Requirements for the Gas Thruster on the RU

The requirements on the Gas thruster level is categorized in the same way as defined in AD1 with the categories, Mass, size, shape and connectivity, Functionality, Launcher compatibility, Lifetime, Dependability & Autonomy and Environment.

6.4.1 Mass, size, shape and connectivity

Requirement Id	Title	Value	Parent document	Parent requirement Id	Version
ES1-RU-GTH-101	Mass (Dry)	<150"g	AD1	ES1-RU-101	1
ES1-RU-GTH-102	Dimension	97mm*97mm*15 mm	AD1	ES1-RU-102	1
ES1-RU-GTH-103	Voltage flow control valve (operating)	12V (Pull-in), 2.5 V (Hold)	AD1	ES1-RU-213	1
ES1-RU-GTH-104	Voltage heater	12"V	AD1	ES1-RU-213	1
ES1-RU-GTH-105	Power, flow control valve	< 3W (pull in for 50ms), < 0,6W (hold)	AD1	ES1-RU-213	1
ES1-RU-GTH-106	Power heater	< 1W	AD1	ES1-RU-213	1

6.4.2 Functionality

Requirement Id	Title	Value	Parent document	Parent requirement Id	Version
ES1-RU-GTH-201	Total impulse	40 Ns	AD1	ES1-RU-212	1
ES1-RU-GTH-202	Number of thrusters	2 Thrusters on each RU	AD1 AD2	ES1-RU-212	1
ES1-RU-GTH-203	Thrust direction	>15 degree outwards from the tangential direction of the spin	AD1 AD2	ES1-RU-212	1
ES1-RU-	Thrust range	1"mN (@	AD1	ES1-RU-212	1

GTH-204		nominal pressure and 25C)	AD2		
ES1-RU-GTH-205	Operating fluids	Gaseous Butane	AD1 AD2	ES1-RU-212	
ES1-RU-GTH-206	Operating pressure (nominal)	1.8-5 bar (2.5 bar@25C) Nominal)	AD1 AD2	ES1-RU-212	

6.4.3 Launcher compatibility

Requirement Id	Title	Value	Parent document	Parent requirement Id	Version
ES1-RU-GTH-301	Acceleration (all directions)	15g	AD3	ES-RU-203	1
ES1-RU-GTH-302	Resonance search	5 – 2000 Hz at 0.5 g and 2 octave/min	AD3	ES-RU-203	1
ES1-RU-GTH-303	Sinusoidal vibration, qualification level	5 – 21 Hz: 11 mm 21 – 60 Hz: 20 g 60 – 100 Hz: 6 g	AD3	ES-RU-203	1
ES1-RU-GTH-304	Random Vibration, qualification levels	20 –100 Hz: +3dB/octave 100 –300 Hz: 0.05 g ² /Hzx(M+20kg/M+1kg) (Parallell) 0.12 g ² /Hzx(M+20kg/M+1kg) (Perpendicular) 300 –2000 Hz: -5 dB/octave	AD3	ES-RU-203	1
ES1-RU-GTH-305	Shock	Hz g [Q=10]	AD3	ES-RU-203	1

		20 20 100 20 600 1080 2000 3000 10000 3000			
ES1-RU-GTH-305	Radiation	Total dose: 60 kRad (Si)	AD3	ES-RU-203	1

6.4.4 Lifetime

Requirement Id	Title	Value	Parent document	Parent requirement Id	Version
ES1-RU-GTH-301	Mission life	5 years	AD1	ES1-RU-401	1

6.4.5 Dependability & Autonomy

N/A

6.4.6 Environment

Requirement Id	Title	Value	Parent document	Parent requirement Id	Version
ES1-RU-GTH-601	Mass (Dry)	<170"g	AD1	ES1-RU-101	1
ES1-RU-GTH-602	Temperature range - Non operating	-30 to +60 °C	AD1	ES1-RU-202	1
ES1-RU-GTH-603	Temperature range - Operating	15 to +50 °C	AD1 AD2	ES1-RU-201	1
ES1-RU-GTH-604	Mounting plate temperature	15 to +50 °C	AD1	ES1-RU-201	1
ES1-RU-GTH-605	Thermal conductance	TBD	AD1	ES1-RU-201	1

6.5. Trade-off studies and critical design issues

From the requirements a number of trade-off studies and design issues can be derived. The main issue for the RU is the total mass requirement and an equation for the mass contribution of each subsystem/part on the RU is wanted. This equation is defined as the mass contribution for the Gas Thrusters as a function of the total impulse requirement for the RU. To set the parameters in this equation the propellant selection, main functionality and configuration of the micropropulsion subsystem needs to be investigated. The propellant tank design will be the most critical design issue from a mass aspect, as it will have a mayor part of the total mass for the gas thruster module. A trade off analysis of mechanical strength vs. mass has been performed to optimize the design of the tank for the pressure requirements and from a mass saving point of view. The result of the mechanical analyze of optimized tank design is described in chapter 6.5.3.

6.5.1 Gas Thruster contribution to the general mass budget equation to the RU

From the requirements of the RU the inputs are given for the further trade-off studies and critical design choices. The result from these studies and choices shall be the parameters in the mass contribution equation.

The general mass budget equation for the Gas thruster contribution to the RU=
 $M0_thruster + \alpha * \text{total impulse requirement}$

The input requirements are:

- Total impulse: 40 Ns (Δv 80m/s)
- Maximum weight (S/C): 500 g (Volume < 0.5-1U cubesat)

The output parameters in the mass budget equation is:

- $M0_Thruster$
- α

6.5.1.1 Propellant trade off

The propellant trade-off is performed by listing a number of optional propellants and also their specific parameters and then set up and mass and volume requirement list for each propellant using the RU requirements on total impulse and weight. From this list a number of suitable candidates can be used for a more detailed consideration.

A list of the most common and optional propellants considered for the Gas Thrusters is listed in table 6.1. Their basic parameters and theoretical vacuum specific impulse is also listed there.

Table 6.1: List of considered propellant with their basic parameters and theoretical vacuum specific impulse

Name	Gas	Molw. (g/mol)	R	γ	T [K]	$I_{sp} = \sqrt{\frac{2 \cdot g_0 \cdot P_c}{\rho}}$ [Ns/kg]	$I_{sp} = \sqrt{\frac{2 \cdot g_0 \cdot P_c}{\rho}}$ [s]
Hydrogen	H2	2	4157	1,41	273	2793,9	284,8
Helium	He	4	2079	1,66	273	1689,5	172,2
Neon	Ne	20,4	408	1,67	273	744,7	75,9
Nitrogen	N2	28	297	1,4	273	753,3	76,8
Argon	Ar	40	208	1,67	273	531,9	54,2
Xenon	Xe	131	63	1,7	273	290,1	29,6
Methane	CH4	16	520	1,3	273	1108,8	113,0
Ammonia	NH3	17	489	1,31	273	1062,3	108,3
Nitrous Oxide	N2O	44	189	1,3	273	668,6	68,2
Carbon Dioxide	CO2	44	189	1,3	273	668,6	68,2
Propane	C3H8	41,1	202	1,3	273	691,8	70,5
Butane	C4H10	58,1	143	1,09	273	972,8	99,2

In Table 6.2 the melting point, boiling point and density of the listed gases is shown. For alternatives with vapor pressure less than 250 bars, these are given, and liquid phase densities are used in the continued analysis.

Table 6.2: Melting point, boiling point and density of gases

Name	Gas	Tm (1bar) [C]	Tb (1bar) [C]	ρ [kg/dm3] (T=50 °X, P=120 Bar)	ρ [kg/dm3] (T=50 °X, P=250 Bar)	ρ [kg/dm3] (T=50 °X, P=550 Bar)	Vap. Pres 0C [bar]	Vap. Pres 50C [bar]	Tcrit [C]
Hydrogen	H2	-259	-253	0,008	0,016	0,030			
Helium	He	-272	-269	0,017	0,033	0,065			
Neon	Ne	-249	-246	0,083	0,164	0,319			
Nitrogen	N2	-210	-196	0,118	0,228	0,397			
Argon	Ar	-189	-186	0,177	0,359	0,659			
Xenon	Xe	-112	-108	1,238	1,918	2,324			
Methane	CH4	-182	-161	0,077	0,157	0,257			
Ammonia	NH3	-78	-33	0,559	0,575	0,602	4,3	20,3	30
Nitrous Oxide	N2O	-91	-88	0,528	0,792	0,921	31	72	36
Carbon Dioxide	CO2	N/A subl.	-78	0,436	0,777	0,952	34,8	72,1	
Propane	C3H8	-188	-42	0,474	0,504	0,546	4,75	17,1	
Butane	C4H10	-138	-0,5	0,555	0,574	0,607	1,3	4,89	

To use the propellant parameters and set up an list of the mass and volume requirements the equation of, $\Delta V = \text{Propellant mass} \cdot \text{Propellant Specific impulse} / \text{Spacecraft mass}$ is used.

RU requirements:

S/C mass [kg]	1
Total Impulse:	40
delta - V [m/s]	40

By putting in the requirements of the RU in the equation and calculate the needed propellant mass and volume for each propellant, we get a list of the propellant mass and volume requirements that is needed for each propellant, see Table 6.3.

Name	Gas	Prop. Mass [kg]	Prop. Vol [dm ³]
Hydrogen	H ₂	0,014	0,89774
Helium	He	0,024	0,72240
Neon	Ne	0,054	0,32836
Nitrogen	N ₂	0,053	0,23339
Argon	Ar	0,075	0,20961
Xenon	Xe	0,138	0,07191
Methane	CH ₄	0,036	0,22927
Ammonia	NH ₃	0,038	0,06550
Nitrous Oxide	N ₂ O	0,060	0,07558
Carbon Dioxide	CO ₂	0,060	0,07701
Propane	C ₃ H ₈	0,058	0,11466
Butane	C ₄ H ₁₀	0,041	0,07168

From this list and the parameters listed in Table 6.1 and 6.2 considered, there are two propellants that are especially attractive to consider.

Nitrogen is a good candidate to use as propellant due to our earlier experience with nitrogen on the PRISMA mission, as well as our laboratory test heritage made before the mission. The disadvantage of this is the fact that it need to be stored at very high pressures which will have a great impact on the tank mass properties. If we consider having a propellant that can be stored as a liquid instead, the best candidate could be butane, as it has such a low and very suitable vapor pressure in the temperature interval of 15-50°C, see Figure 6.1, which can be directly used as feeding pressure for the thrusters.

From a handling and safety aspect, Butane is beneficiary compared to for example Ammonia, which would require a high level of safety requirements.

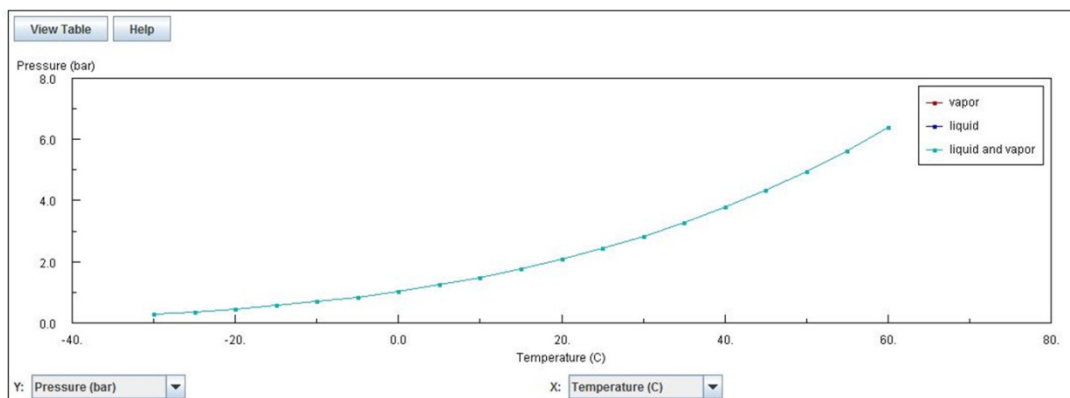


Figure 6.1. Pressure vs temperature for Butane

Comparison between the two optional propellants in respect of the needed mass, volumn and estimated tank mass for the ESAIL requirements:

Propellant mass: ~ 53 g, N₂, stored at 250 bar
 ~ 41 g Butane, stored as liquid

Propellant volume: ~ 233cm³ N₂, stored at 250 bar
 ~ 71cm³ Butane, stored as liquid

Propellant tank mass: ~ 200 g N₂, stored at 250 bar
 ~ 55 g Butane, stored as liquid

6.5.1.2 Propellant selection

The mass requirement for the complete RU is the driving requirement that will be the most important parameter to take into account for the choice of propellant. When summarizing the properties of propellant mass, volume, pressure and estimated propellant tank mass, Butane is the most suitable selection from a mass saving requirement view. It also has a very suitable vaporizing pressure in the temperature range 15-50°C for the thruster design requirement. With the pressure range in this region the tank material thickness is minimized as well as the fact that no pressure regulator is needed which also would have added extra weight to the system.

6.5.1.3 Basic micropropulsion subsystem description and configuration trade-off

The MEMS-based micropropulsion subsystem developed for the PRISMA satellites is in principle similar to a conventional cold gas system – though with the functional difference that the thrust can be chosen to be modulated proportionally in the sub milli-Newton range or through on/off modulation.

The micropropulsion subsystem consists of the following major components:

- a propellant tank
- a propellant fill/vent valve
- a micro isolation valve (incl filter)
- one pressure transducers
- one MEMS thruster module

The micropropulsion subsystem intended for the ESAIL project could be reduced to:

- a propellant tank
- a propellant fill/vent valve
- two MEMS thruster modules

With this reduced micropropulsion configuration we can also choose the level of functionality of the MEMS thruster module. This will also have an impact of the total mass of the micropropulsion system.

Do we need continuous thrust control on RU for spin rate modification? Only on/off thrust for spin up and unreeling aux tether?

Two optional thruster configurations with different thruster functionality can be further investigated.

6.5.1.3.1 Option 1. MEMS Thruster Module with the functionality of on/off modulation of the thrust

Main specifications:

- Two 1mN thrusters:
- Pulsed on/off thrust (no regulation of sail spin rate)
- Power requirement: ~ 600 mW + power thermal control (TBD)

With this option the thruster module is run in by on/off modulation. Only one normally closed valve is used to either run the thruster with valve open or valve closed. Short pulses of thrust can be run in the millisecond-region. The thrust is either 0 or 1mN, and small impulse bits can be achieved by commanding short pulses with 1mN thrust.

The MEMS thruster module contains of the following components and sensors:

- Normally closed valve
- Temperature sensor
- Heater
- Two thuster nozzles

6.5.1.3.2 Option 2. MEMS Thruster Module description on/off modulation + Proportional thrust (incl thrust feedback)

Main specifications:

- Two 1mN thrusters:
- Pulsed on/off thrust
- Proportional thrust (incl thrust feedback) for fine adjustment of RU position and sail spin rate
- Power requirement: 2W + power thermal control power (TBD)

With this option the thruster module can be run with both on/off modulation and proportional thrust control (incl thrust feedback). Only one normally closed valve is used to either run the thruster with valve open or valve closed. Short pulses of thrust can be run in the millisecond-region. The thrust is either 0 or 1mN, and small impulse bits can be achieved by commanding short pulses with 1mN thrust. The thrust can also be modulated proportionally in the range 0 - 1mN with thrust feedback control.

The MEMS thruster module contains of the following components and sensors:

- Normally closed valve
- Temperature sensor
- Normally open valve
- Massflow sensor (incl electronics)
- Heater
- Two thuster nozzles

The estimated micropropulsion mass requirements for the two different MEMS thruster module configurations are:

Option 1:

Micropropulsion thruster pod option 1 (incl two thrusters): ~ 20 g

Electronical card: ~10g
 Propellant tank (max tank volume 110cm³): ~100g
 Propellant: ~41g
 Total mass: ~171g

By assuming that the tank weight will be constant (this is under the consideration that the requirement of the total impulse is not highly increased and that the same tank volume can be used for the propellant required) we can receive an value of the $m_{0_thruster} = 130$ g and $\alpha = 0,97$.

Option 2:

Micropropulsion thruster pod option 2 (incl two thrusters): ~60g
 Electronical card: ~60g
 Propellant tank (max tank volume 110cm³): ~100g
 Propellant: ~41g
 Total mass: ~261g

By assuming that the tank weight will be constant (this is under the consideration that the requirement of the total impulse is not highly increased and that the same tank volume can be used for the propellant required) we can receive an value of the $m_{0_thruster} = 220$ g and $\alpha = 0,97$.

6.5.1.4 MEMS Thruster module configuration selection

When having a mass requirement for the complete RU as the driving requirement the choice of configuration for the MEMS Thruster module is the described option 1. Due to the fact that mass requirement is the most important one and the requirement of a total impulse can still be achieved with the option 1 configuration this is the best suitable option for the ESAIL application.

6.5.2 Result for the Gas Thruster contribution to the remote unit general mass budget equation

With the propellant selection of butane and the MEMS Thruster module configuration 1, we achieve the equation of the mass contribution of the Gas Thruster to:

General mass budget equation for the Gas thruster contribution to the RU = $m_{0_thruster} + \alpha * \text{total impulse requirement [gram]}$

$m_{0_thruster} = \sim 130$ g (without propellant)
 $\alpha = 0.97$

6.5.3 Mechanical analysis of the propellant tank

A trade off analysis of mechanical strength vs. mass has been performed to optimize the design of the tank for the pressure requirements and from a mass saving point of

view. The result of the mechanical analysis of optimized tank design is described in chapter 6.5.3.

6.5.3.1 Design Description

The cad model of the propellant tank can be seen in Figure 6.2.

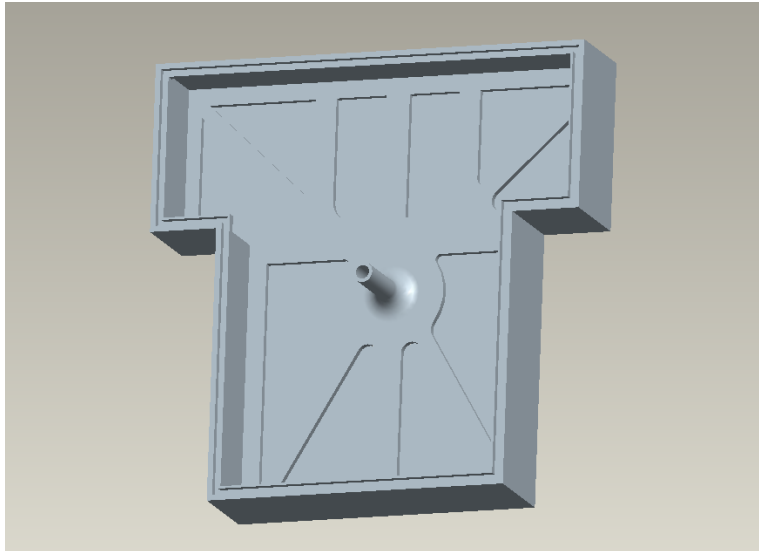


Figure 6.2. 3D cad model of tank bottom part design.

Technical Requirements and Model Data

a) Pressure Loads

Parameter	Requirement
MEOP	0.5 MPa
Proof Pressure (MEOP x 1,5)	0.75 MPa
Burst Pressure (MEOP x 2,5)	1.2 MPa

b) Dimensions

Parameter	Requirement
Dimensions	100 x 100 x 17 mm
Thickness	1 mm aprox (0.5/1.5mm)
Minimum inside volume	100 cm ³

c) Model Data

The following software packages are used for the structural analysis:

Static Analysis	Pro/ENGINEER Wildfire 4.0 ProE/Mechanica
-----------------	---

d) Material Properties for Aluminum alloy 7075

Parameter	Value	Units
Young's Modulus	71000	MPa
Yield, $\sigma_{0.2\%}$	470	MPa (Tensile)

σ_{ult}	540	MPa (Tensile)
Poisson's Ratio	0.33	
Density, ρ	2.81	g/cc

6.5.3.2 Static Analysis

All the above analyses are carried out using ProE/Mechanica. All models are generated using the following units: length (mm), Force (N), Stress (N/mm^2). [$1 \text{ N}/\text{mm}^2 = 1 \text{ MPa}$]

Load cases for MEOP, Proof and Burst were performed on the bottom part of the tank.

Pressure Boundary:

For the operating loads the percentage margin of safety must be calculated using the following formula:

$$\begin{aligned} \text{Where} &= \text{Yield Marging of Safety} \\ &= \text{Yield Strength of material, 0,2\% proof} \\ &= \text{Limit Stress in the model at Operating Pressure} \\ &= \text{Safety Factor for Yield, taken to be 1.1} \end{aligned}$$

$$\begin{aligned} \text{Where} &= \text{Tensile Marging of Safety} \\ &= \text{Tensile Strength of the material} \\ &= \text{Limit Stress in the model at Operating Pressure} \\ &= \text{Safety Factor for Yield, taken to be 1.25} \end{aligned}$$

MEOP, Proof and Burst loads were applied on the Bottom Tank part. In Figure 6.3-4 the result for the Maximum Principal Stress and the Equivalent Stress (von Mises) for the burst case can be seen. The burst case shows the maximum stress above yield, but only in specific points like corners or the central ribs, which have been neglected for being punctual sharp areas which will not have any mayor impact on the overall strength. A lower value, hence more realistic, has been selected for this analysis. In Figure 6.5 the equivalent stress for the proof pressure load case is shown, and in Figure 6.6 for the MEOP pressure load case.

6.5.3.2.1 Burst Case

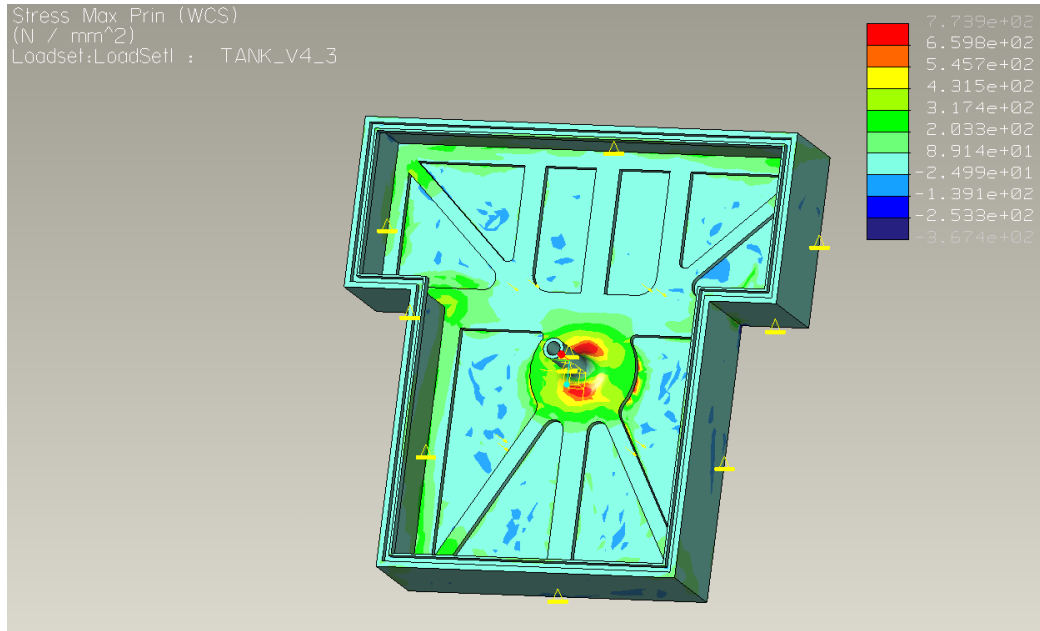


Figure 6.3. Maximum Principal stress (main area of the tank surface): 400

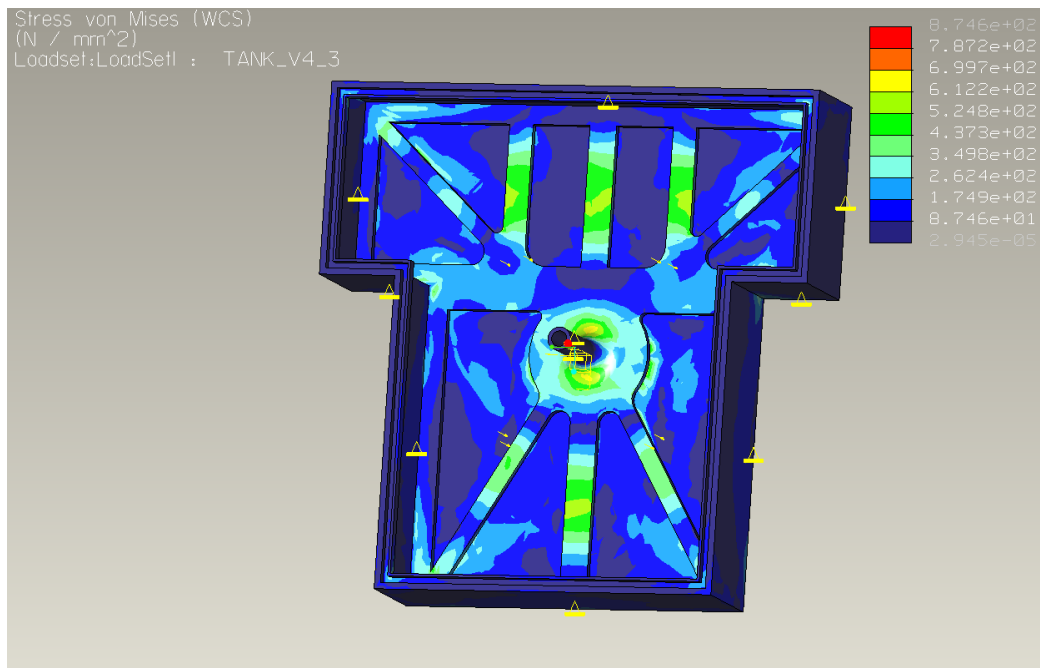


Figure 6.4. Equivalent stress (von Mises): 350 MPa

6.5.3.2.2 Proof Case

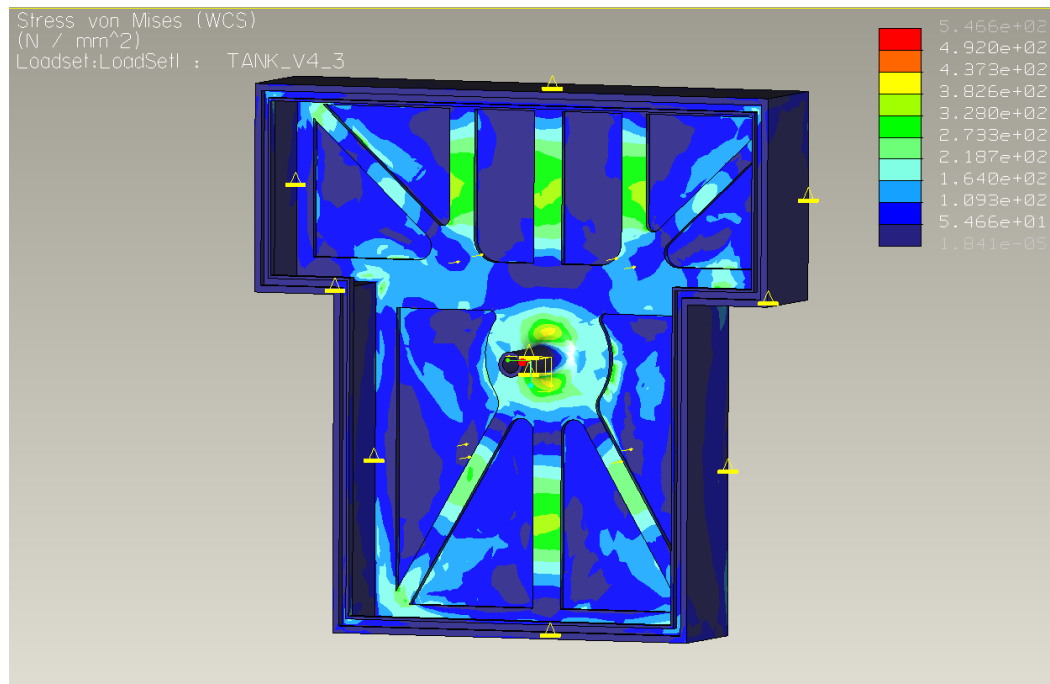


Figure 6.5. Equivalent stress (von Mises): 350 MPa

6.5.3.2.3 MEOP Case

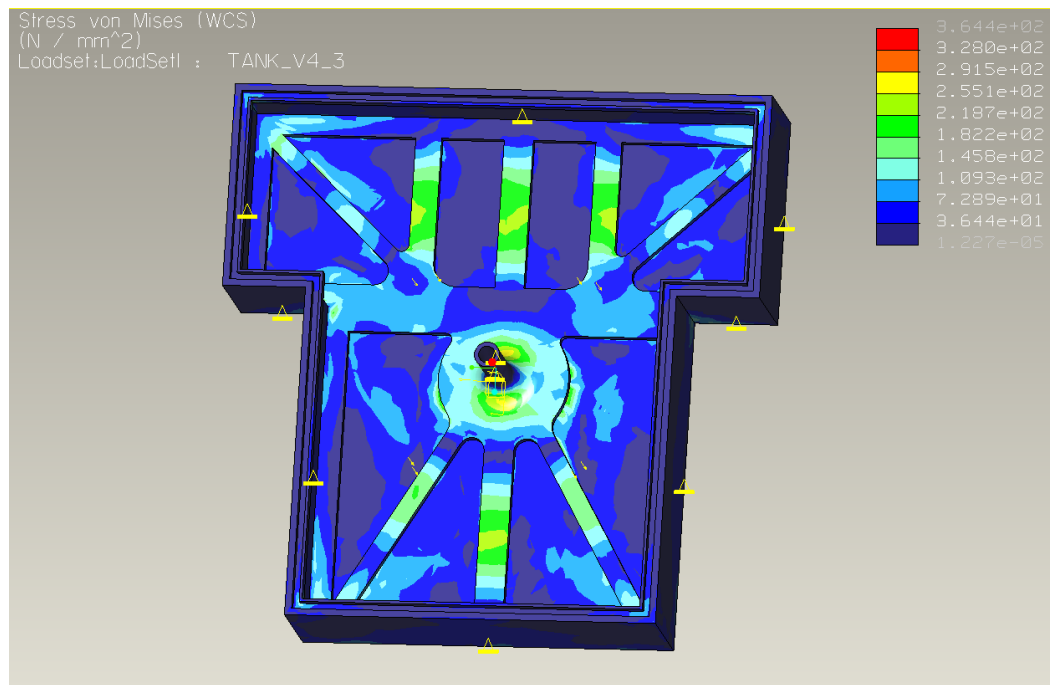


Figure 6.6. Equivalent stress (von Mises): 200 MPa

6.5.3.3 Results

The results of the mechanical analyze and the safety factor for the different load cases is shown in the table below.

Table 6.4. Stress and margin of safety results on the current propellant tank design.

Load Case	Pressure [bar]	Equivalent Stress [MPa]	Max Principle Stress [MPa]	M.O.S.
MEOP	5	220	n/a	94,00%
Proof	7.5	300	n/a	42%
Burst	12.5	350	400	8%

6.6. Gas Thruster Design

The main task for the micropropulsion subsystem with gas thrusters on the RU, is to generate an angular momentum which will deploy the tethers and modify the spin rate. Two thrusters acting on the opposite directions of each others are used to have this functionality. The gas thrusters is positioned with an angle of 15° outward from the tangential spin plane of the ESAIL (see Figure 6.7)

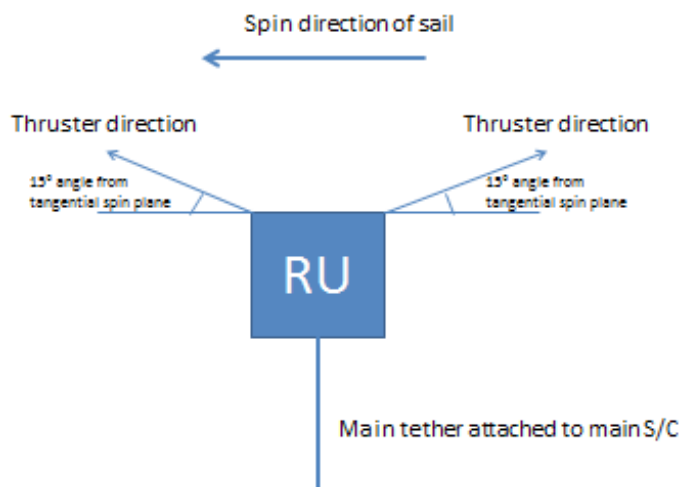


Figure 6.7. Gas thrusters positioned on RU.

The micropropulsion subsystem intended for the RU contains of the following mayor components:

- a propellant tank (incl a propellant fill/vent valve)
- two MEMS thruster modules

A schematic layout of the micropropulsion subsystem is shown in Figure 6.8. The propellant will be stored as a liquid in the tank and degassed by vaporization when

operating one of the valves feeding the gas to the thruster. The feed pressure of the gas will vary depending on the actual tank temperature due to the degassing level of the propellant. Two individual thruster modules are included in the system.

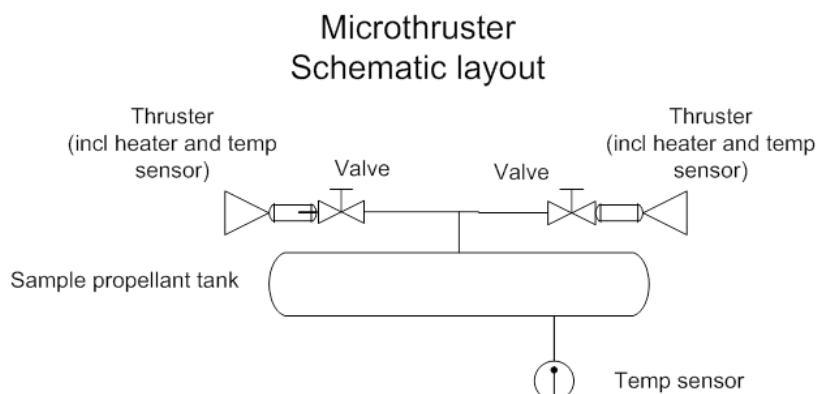


Figure 6.8. Schematic layout of the micropropulsion system.

The propellant tank has a built in temperature sensor monitoring the actual gas pressure in the tank. In the MEMS thruster module also the temperature will be monitored and an internal heater is built in to avoid any condensation of the gas in the thruster. Both the propellant tank and the MEMS thruster module is described further in the components chapter.

The main performance and physical specification of the micropropulsion subsystem is:

- Two 1mN thrusters (Nominal: 1 mN @ 25°C and 2.45 bar)
- Thrust directions 15° outwards from the tangential direction of the ESAIL spin rotation
- Butane as propellant
- Operating pressure: 1.8 - 5 bar
- Total impulse: 40 Ns
- Size: 98*98*17 mm
- Weight: 156.5 g (106.5 g dry weight)

The main electrical and thermal specification of the micropropulsion subsystem is:

- Peak power: 3 W
- Continuous thrust power: 0.6 W
- Thermal management power: 1 W
- Voltage supply: 12 V/2.5 V (Pull in /hold solenoid valve), Battery bus voltage (int heater)
- Operational temperature: 15°C - 50°C
- Non-operational temp: -30°C – 60°C

An overall design 3D-cad drawing of the micropropulsion subsystem is shown in Figure 6.9.

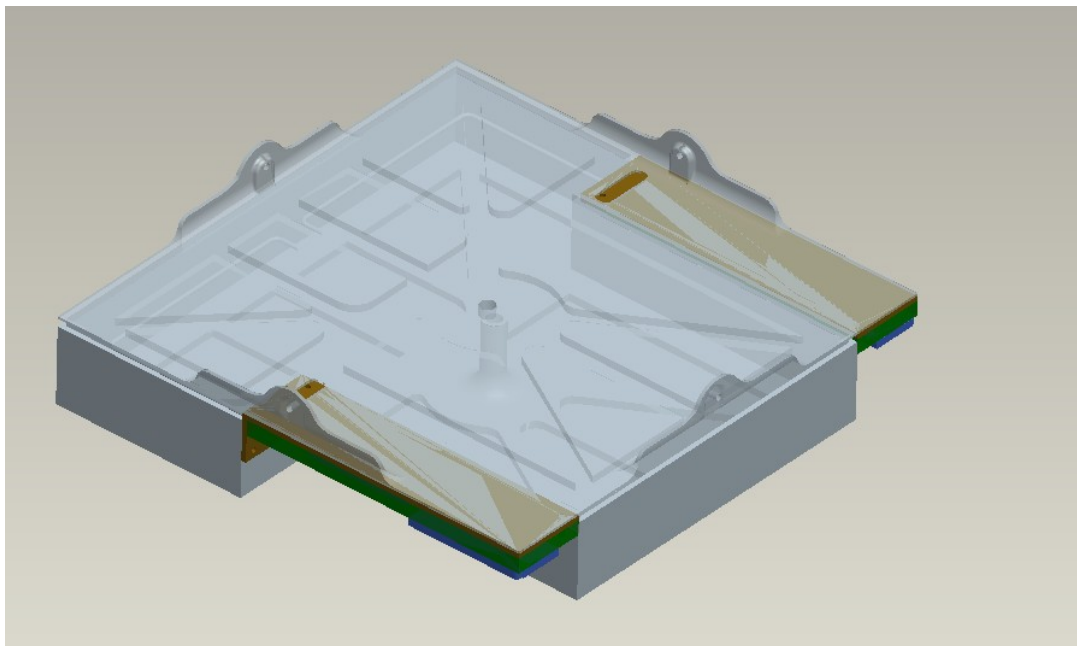


Figure 6.9. 3D-cad drawing of the micropropulsion subsystem.

6.6.1 Interfaces

The different interfaces of the module are described further in this chapter.

6.6.3.1 Mechanical IF

The mechanical interface of the Gas thruster module is the top part of the tank where the adaptor plate is also integrated directly. The top part has the size of 98*98mm, and the module is attached in the mounting “ears”, that has an hole diameter of 1.3mm. They are symmetrically positioned in the center of each side of the top part. The mounting ears has a height of 3mm, see Figure 6.10.

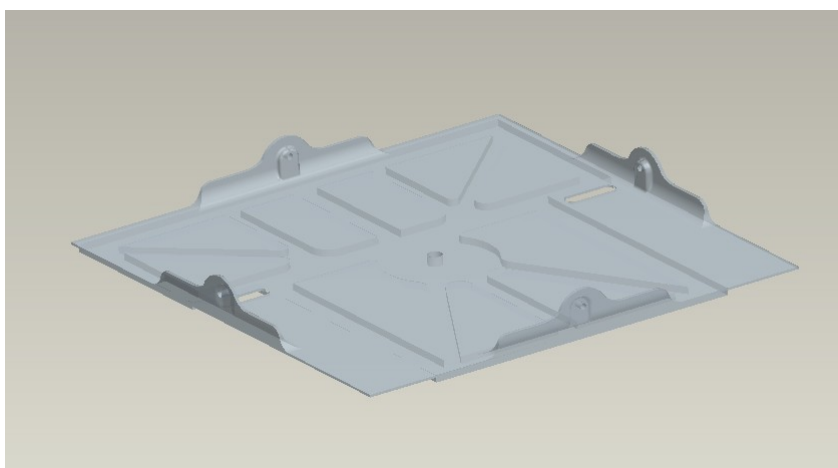


Figure 6.10. Mechanical interface the micropropulsion subsystem.

6.6.3.2 Thermal interface

The thermal interface is the same as the mechanical interface.

6.6.3.3 Electrical interface

The electrical interface from the module will be flying leads from the two MEMS thruster modules electrical interface cards, see Figure 6.11.

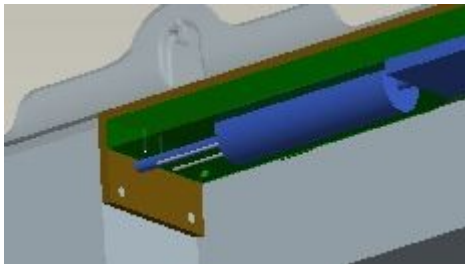


Figure 6.11. Electrical interface the micropropulsion subsystem.

For each thruster module the flying leads will be:

- 2 pins Thruster on/off
- 2 pins heater on/off
- 2 pins temperature read out

And then there will be two additional leads from the tank temperature. In total there will be 14 wires connected to the thruster module.

6.6.2 Components/parts

The mayor components in the micropropulsion subsystem are described in more detail in this chapter.

6.6.2.1 The propellant tank

The propellant tank consists of the following parts:

- Bottom part+top part
- O-ring sealing
- Fill/vent hole, also acting as reinforcement structure with a screw connection
- Liquid storage handling structure walls (to minimize sloshing effect that can give wobbling effects of the RU)

The bottom and top part (shown in Figure 6.12) is made of 1.5mm thick aluminum.

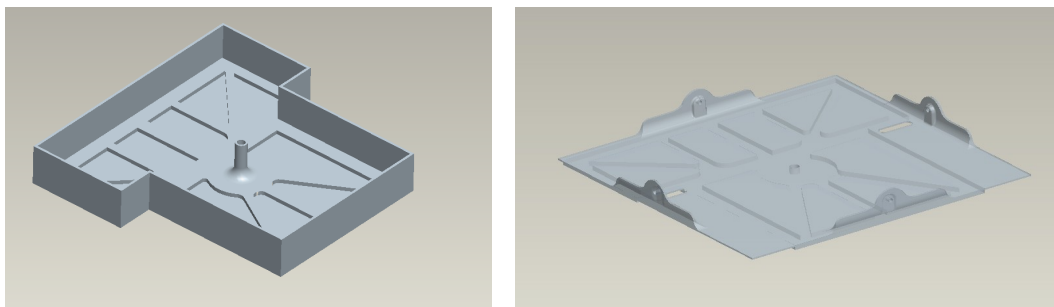


Figure 6.12. Bottom part of the propellant tank to the left, and top part to the right.

Main specification of the propellant tank:

- Volume $\sim 100 \text{ cm}^3$
- Pressure range: 0 - 5 bar (MEOP = 5 bar, Proof = 7.5 bar, Burst: 12.5 bar)
- Size: 98*98*17 mm
- Dry weight: 70.5 g

6.6.2.1.1 Feed pressure for Butane as propellant

The feed pressure of Butane will vary with the actual temperature of the propellant. The operating pressure range for the micropropulsion subsystem is 1.8 – 5 bar which will correspond to an operating temperature range of the Butane between 15 – 50 °C, see also Figure 6.1 in chapter 6.5.1.1.

6.6.2.2 MEMS Thruster module

The MEMS thruster module consists of the following parts:

- MEMS Thrusterchip (incl thruster nozzle and heater)
- Solenoid valve
- Temperature sensor
- Electrical interface card
- Mechanical support and adaptor bracket

The MEMS thruster chip contains of two bonded silicon wafers including a thruster nozzle structure and an internal chip heater. The temperature sensor will be integrated on the thruster chip and then both the solenoid valve and the MEMS thruster chip is mounted on an electrical interface board. The electrical interface board are then mounted on a support bracket with an o-ring sealed gas feed piping for integration with the propellant tank, see Figure 6.13. The size of the MEMS thruster module is 60*15 mm.

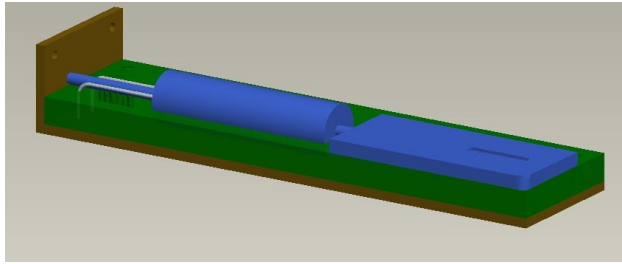


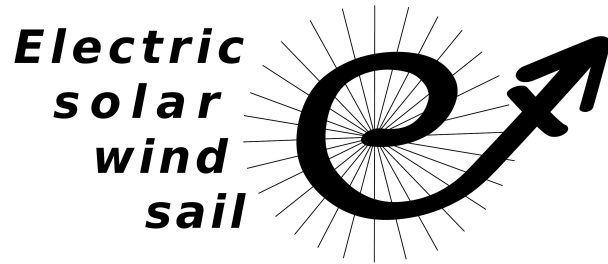
Figure 6.13. MEMS thruster module with support bracket.

6.6.3 Mass breakdown

A mass breakdown of the micropropulsion system is shown in Table 6.5 where the estimated mass of each component is done and the total mass with- and without propellant is listed.

Table 6.5. Mass break down of the micropropulsion subsystem.

Part	Mass (g)
Propellant	50,0
Tank_bottom (0.5/1.5 mm Al)	41,5
Tank_top (0.5/1.5 mm Al)	29,0
Adaptor bracket (integrated in tank top)	0,0
Support_bracket	5,6
Board	4,9
Thruster_chip	1,6
solenoid_valves	8,0
Electric_wires	5,0
Feeding_tube	6,0
Screws and others	5,0
TOTAL MASS (dry mass)	106,6
TOTAL MASS (wet mass)	156,6



7. FEED Thruster

Prepared by:

Alta, Pierpaolo Pergola, Nicola Giusti

Coordinating person:

Salvo Marcuccio, s.marcuccio@alta-space.com

Table of Contents

7.1. Introduction.....	103
7.1.1 Top level Requirements.....	104
7.2. Thruster System.....	105
7.2.1 FEEP working principle.....	105
7.3. Thruster Unit Configuration.....	106
7.3.1 Propellant Mass Estimation.....	106
7.3.2 Thruster Unit Components.....	107
Emitter electrode.....	108
Accelerator electrode.....	108
Insulator between electrodes.....	108
Ground shield and thermal control.....	109
Propellant tank.....	109
Thruster interface.....	109
Tank heater and thermal control.....	109
7.3.3 Thruster Unit Design.....	109
7.4. Power and Control Unit.....	111
Power Unit.....	111
Control Unit.....	112
7.5. Remote Unit and Thruster System Integration.....	113
Plume impingement issue.....	113
Charging issue.....	114
Data exchange.....	115
Reference Documents.....	116

This document describes the design of the ionic liquid FEEP thruster for the Remote Unit in the E-sail project.

7.1. Introduction

The ionic liquid FEEP is a variant of the cesium-fed field emission thruster where the alkali metal propellant is replaced by a molten salt.

Ionic liquids are organic molten salts composed of a mixture of loosely bound cations and anions, with the special property of being liquid at or close to room temperature. Such liquids have been developed by the chemical industry during the last 15 years for their unique properties as process fluids and solvents. Thousands of ionic liquids with different physical and chemical properties have been synthesized and are available commercially. Such liquids are much easier to handle than alkali metals (Cs, Rb) or other liquid metals or alloys (Ga, In, Bi), due to their negligible reactivity with air and water, extremely low vapour tension, and low toxicity. Ionic liquids can be handled in air with no special precautions and are compatible with a large variety of materials.

The use of ionic liquids, with respect to alkali metals, will lead to considerable simplification in space and ground operations and the associated supporting equipment. The possibility of contamination to the host spacecraft, as well as the danger of contamination of the thruster from the environment, are much reduced.

In comparison to liquid metals, ionic liquid propellant have reduced performance in terms of specific impulse and mass efficiency. In principle, operation in either pure ionic or mixed ion/droplet regime is possible, according to the choice of liquid and the operating conditions. The core technology of ionic liquid FEED, i.e. the linear slit emitter, is directly derived from the cesium version, while the remaining components of thruster are the subject of the simplified design here carried out.

7.1.1 Top level Requirements

The simplified FEED system design is driven by a set of requirements imposed by the whole Remote Unit integration and the application conceived.

Ambient Conditions

The Remote Unit is required to operate between 0.9 (ES1-RU-603) and 4 astronomical units (ES1-RU-604) and it has to be properly shielded from the Sun only on a single surface because the fix orientation of the E-sail spacecraft.

Mass

The Remote Unit is required to weight approximately 1 kg (ES1-RU-101) of mass contingency. Accordingly, the simplified FEED system has to be as lightweight as possible. A specific value of the thruster dry mass is not given, however, from preliminary analysis of the whole unit, a target mass of 300 g is considered as requirements.

Total Impulse

Due to its high specific impulse, the simplified FEED system is particularly suitable for missions with demanding total impulse. In this case it is required to provide up to 2040 Ns: 40 Ns during the deployment phase (ES1-RU-212) and approximately 2000 Ns during the E-sail cruising.

Thrust level

During the deployment phase, the Thruster System is necessary for initiating and controlling the rotation of tethers varying the angular speed of the system. In this phase 30 μ N thrust is required. This level is considered the maximum thrust level to be reached and it might be required for the whole deployment phase, up to four weeks.

During the cruise phase the simplified FEED system is considered to compensate any angular velocity variation. The complete mission is designed for 5 years during which the 2000 Ns impulse have to be supplied with an average thrust magnitude of the order of 10 μ N, the minimum value here assumed as requirement.

Power

The Remote Unit is estimate to produce some 4-5 W at 1 astronomical unit (ES1-RU-213) and less than 5 at 4 astronomical units. This tight power budget imposes that the Thruster Unit has to work with the lowest possible power consumption. As target value it is assumed to use less than the minimum of power available on the Remote Unit; i.e. 4 W.

Remote unit thruster arrangement

A single Thruster Unit is required to be placed on each Remote Unit. The thrust vector has to be 30 deg (TBC) oriented with respect to the auxiliary tethers and, in order to assure the capability of changing the angular speed both in clockwise and counter-clockwise direction, two consecutive Remote Units are equipped with thrusters firing in opposite directions.

Temperature

The last requirements here considered for the thruster assembly design is the working temperature range. Due to relatively large interplanetary distance covered and the variety of

operative conditions required, the range is required to be suitable both for ionic liquids (that do not have to freeze, although a dedicated tank heater can be included in the thruster design) and for standard space proven elastomeric components.

Summarizing, the main requirements driving the Thruster Unit design are:

- the total impulse to be delivered:
 - 40 Ns during the deployment phase, 4 weeks (ES1-RU-212)
 - 2000 Ns during the cruise phase, 5 years (ES1-RU-401)
- the thrust level required:
 - 30 μ N during the deployment phase
 - 10 μ N during the cruise phase
- the system constraints:
 - have a maximum dry mass below 300 g
 - operate with less than 4 W
 - have compact dimensions and standard interfaces

7.2. Thruster System

The whole FEED system is composed by three main components, see Fig. 7.1:

- Thruster Unit;
- Power Unit;
- Control Unit.

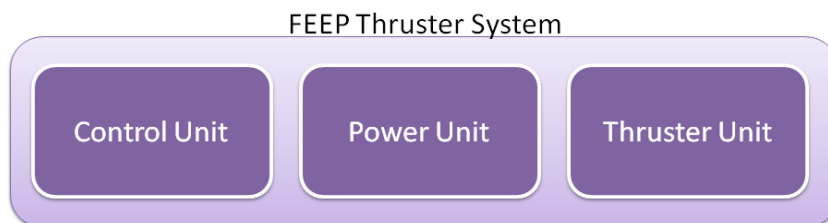


Fig. 7.1: FEED Thruster System main components.

The Thruster Unit is the core of the system and contains the main mechanical elements. In particular, it is composed by:

- the emitter electrode,
- the accelerator electrode,
- an insulator between electrodes,
- a ground shield,
- a propellant tank,
- the thruster interface,
- a tank heater.

The other two FEED system components, the Power and Control Units, have to command the Thruster Unit and to provide the power required to extract ions. A number of connecting cables and sensors is required to interconnecting these components. In the next sections these three thruster subsystem parts will be described more in detail.

7.2.1 FEED working principle

The FEED working principle is rather simple, see Fig. 7.2, and it does not involve any moving component or high temperature part

An accelerating electrode is placed directly in front of the emitter electrode. When the thruster is operating, a strong electric field is generated by the application of a high voltage difference between the electrodes. In this condition, a surface instability takes place on the free surface of the liquid metal due to combined effects of the electrostatic force and surface tension, creating a series of cusps, the so called *Taylor cones*, see Fig. 7.2.

When the electric field reaches a value in the order of 10^9 V/m, the atoms at the tip of the cusps spontaneously ionize and an ion jet is extracted by the electric field, while the electrons are rejected in the bulk of the liquid. In the cesium version of the FEFP thruster, an external source of electrons, the neutralizer, is needed to maintain the global electric neutrality of the spacecraft. While this neutralizer is not required in the ionic liquid case because the Thruster Unit can be run in alternate polarity ejecting both positive and negative ions.

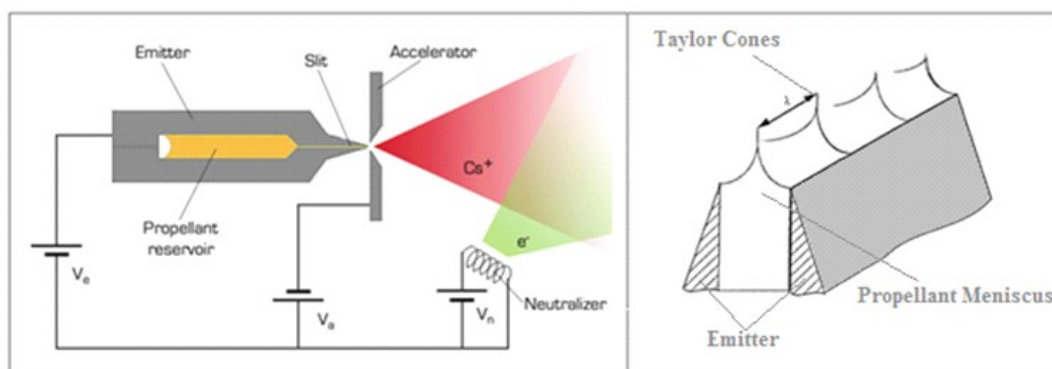


Fig.7.2: Schematic representation for the FEFP concept (left) and Taylor cones formation on the metal meniscus (right).

7.3. Thruster Unit Configuration

This section describes the baseline configuration of the ionic liquid FEFP Thruster Unit, according with the requirements described in the Sec. 7.1.1.

7.3.1 Propellant Mass Estimation

The simplified FEFP thruster for the Remote Unit is based on the heritage of the classical Alta cesium FEFP. The classical FEFP use cesium to continuously feed the emitter. Due to the very low viscosity of this metal, the liquid flows through the emitter by means of capillary gradient. On one hand cesium has several advantages for such application (high atomic mass, low ionization energy, low melting point, good wetting properties, etc.). On the other hand, cesium has several drawbacks (extremely reactivity with air and water, high vapour pressure, quite high cost, toxicity, etc.) making the propellant handling and the thruster assembly complex and expensive.

Nowadays a suitable alternative to cesium is represented by ionic liquids, also known as liquid electrolytes. These are actually salts in the liquid state. They are conductive fluids (fundamental aspect to make the FEFP concept working) composed by polar molecules.

The ionic liquids are generally easy to handle and to store as they are neither hazardous nor toxic and can be manipulated without any specific wariness. There is a huge number of ionic liquids with a broad range of chemical and physical characteristics. Vapour pressure of ionic liquids is generally not appreciable (often neither measurable) and thus these almost do not evaporate. It is possible to find a liquid with very low melting point, or large atomic mass, two fundamental aspects for a candidate alternative to cesium. However, as the average atomic mass of ions of these fluids is smaller than the one of cesium, it is

expected that the simplified FEED has a thrust smaller than the one of the classic FEED, but its specific impulse could be larger.

A trade-off study of possible ionic liquid propellants based on the total impulse requirement and the results of the experimental campaign was performed and accordingly a specific propellant was selected. The tank dimension has been estimated considering a set of reasonable specific impulses and the propellants that show the most promising characteristics. From the total impulse requirement, given a specific impulse it is possible to obtain the propellant mass, see Table. 7.1.

Specific impulse [s]	2000	3000	4000
Propellant mass consumption [g]	100	70	50

Table 7.1: Propellant mass required to realized the mission total impulse based on different specific impulse assumptions.

Ionic liquid propellants with different densities result in different tank volumes. The ionic liquids considered here are the EMI-BF₄, EMIM and BMIM and the resulting tank volumes are summarized in Table 7.2.

Propellant	EMI-BF₄	BMIM	EMIM
Density [g/cm ³]	01.03.00	1.4	1.5
Tank volume [cm ³]	40 - 80	35 - 70	43 - 85

Table 7.2: Propellant tank sizing based on the total impulse required for a number of candidate ionic liquids.

Considering the state of the art of the experimental campaign the EMI-BF₄ is chosen as baseline propellant solution because of its characteristics affecting its propulsive behavior. The main physical properties of the EMI-BF₄ are summarized in Tab. 3.

Density (g/cm³)	Melting point (°C)	Molecular mass (amu)	Mass anion (amu)	Mass cation (amu)	Conductivity (S/m)	Surface tension (N/m)	Viscosity (Pa s)
1.34	15	197.97	86.805	111.165	1.4	0.05	0.0665

Table 7.3: Physical properties of the EMI- BF₄.

In principle, the melting point is a merit figure for the propellant choice. Even though some ionic liquids with lower melting point than EMI-BF₄ exist, these ionic liquids have worse physical properties from the propulsive point of view.

In the following it is assumed to have the thruster operating at 3000 s (conservative values considering the experimental tests) and a tank of about 50 cm³ volume.

7.3.2 Thruster Unit Components

Due to the above mentioned drawbacks of cesium, the configuration of the classical Cs FEED thruster results to be rather complex. The thruster assembly conceived for the Lisa Pathfinder mission is shown in Fig. 7.3

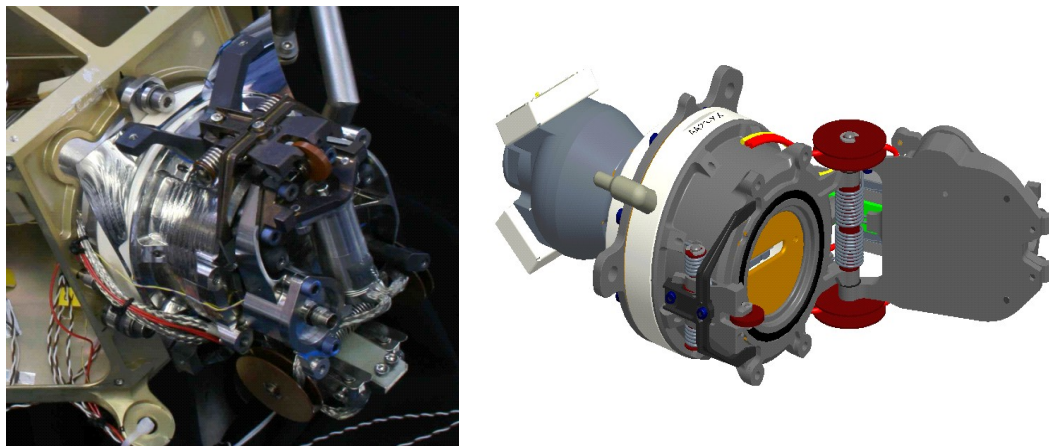


Fig. 7.3: Lisa Pathfinder FEFP thruster assembly.

The Ionic liquids are much more friendly to handle if compared with cesium. This leads to significant simplifications in the thruster design. A number of simplifications in the Cs EEP thruster can be adopted using ionic liquids and the design resulted in a lightweight and simple configuration. The lid and the open mechanism (LOM) present in the Cs FEFP thruster assembly (see Fig. 7.3) , for instance, is not foreseen in the simplified FEFP as the ionic liquid chemical reactivity in air is practically negligible.

Emitter electrode

The linear slit emitter represents the core of the thruster and, in the simplified FEFP, it is one of the heavier component. The emitter is made in Stainless Steel and it is not modified with respect to the classical cesium configuration.

Accelerator electrode

The accelerator is a simple titanium plate 16 x 58 mm and 2 mm thickness machined with a proper slit. The accelerator is grounded to the Remote Unit and is the ground reference of the Power Unit.

Insulator between electrodes

As the thruster is not required to be sealed with an inert gas during the ground operations, besides the simplification introduced by removing the LOM, also the shape of the insulator between electrodes can be simplified. Thus, instead of a cylindrical configuration of the insulator, as the one of Cs FEFP, a simpler double-pillar solution is consider as baseline. In order to further reduce the thruster mass, the machining and manufacturing complexity and the costs, the insulator is made of a polymeric material, i.e. the PolyEtherEther-Ketone (PEEK). Table 7.4 summarizes its main characteristics.

Property	Unit	Value
Density	g/cm ³	1.31
Tensile Strength	GPa	0.11
Tensile Modulus (psi)	Gpa	3.45
Coefficient of Linear Thermal Expansion	m/m/K	1.44 10 ⁻⁵
Melting Temp	°C	340.00
Max Operating Temp	°C	249.00
Thermal Conductivity	W/m/K	0.25
Dielectric Strength short time	V/m	1.89 10 ⁷

Table 7.4: PEEK relevant characteristics.

Ground shield and thermal control

The thruster has to be operated in a controlled environment for temperature and, less important, radiations. The more conservative solution is to place the thruster inside the Remote Unit. Indeed the Remote Unit itself can represent a proper shield for radiation and provides a thermally controlled environment. Anyway the thruster design takes into account a ground shield connected with the accelerator electrode and it encloses the emitter and the electrode insulator. The shield has the same shape of the tank and is realized with a thin aluminum foil.

Propellant tank

The propellant amount required for the whole mission is stored in a not-pressurized tank (however a very low pressure inside the tank can be present due to the outgassing of the propellant). As pointed out in Sec. 7.3.1, the volume of the tank is about 50 cm³. The shape of the tank is elliptic inside and almost rectangular outside to facilitate the Remote Unit assembly. The tank is supposed to be realized in two parts to facilitate the manufacturing and the filling. The maximum tank height is about 30 mm without the MLI covering. To reduce the mass weight of the thruster and to provide electrical insulation between the Remote Unit and the propellant, the tank is made of a polymeric material, i.e. the Poly Ether Ether Ketone (PEEK).

Thruster interface

The thruster physical interface is realized by four screwed attach points on the bottom surface through which the Thruster Unit can be assembled with the Remote Unit by means of 4 M4 screws.

Tank heater and thermal control

The baseline configuration takes into account the whole thruster assembly to be enclosed into the Remote Unit. Otherwise a Multi Layer Insulator (MLI) covering the whole thruster unit is needed as passive thermal control method to avoid potential ionic liquid freezing (this MLI configuration is shown in Fig. 7.4). However, a detailed thermal analysis of the whole system is required to verify if the ionic liquid remains in the liquid state during all the operating conditions. If the Remote Unit thermal analysis shows the possibility of propellant freezing an additional heater placed on the tank can be used to control the temperature of the propellant. In any case, due to the low melting points of ionic liquid, the heater is not considered to require too much power (less than 2 W are conservatively estimated in such a preliminary phase).

Preliminary analyses lead to assume a working temperature between -20 and +60 °C and a survival temperature between -30 and +70. These values are the temperature ranges required at the Thruster Unit interface and are both compliant with the requirements ES1-RU-201, ES1-RU-202.

7.3.3 Thruster Unit Design

Based on the component specifications shown in section 7.3.2, the whole Thruster Unit has been designed following the idea to develop a lightweight, compact and flexible device.

Based on the preliminary design the main properties of the Thruster Unit are summarized in Table 7.5. The reference frame is centred on the accelerator emitter with the z axis along the thruster axis toward the beam, the y axis vertical toward the attach points (bottom surface) and the x axis to complete the coordinate axes. The values in the tables have to be intended as reference values and could be changed according to future design refinements.

Property	Unit	Value
Overall length	mm	125
Overall height	mm	35
Overall width	mm	75
Dry mass	g	165
Wet mass	g	235
Centre of gravity (dry mass)	mm	$X_m = 0$ $Y_m = 0$ $Z_m = -47$
Mass moment of inertia (x axis, dry mass)	kg mm ²	5.4e4
Mass moment of inertia (y axis, dry mass)	kg mm ²	2.6e5
Mass moment of inertia (z axis, dry mass)	kg mm ²	3.0e5
Centre of gravity (wet mass)	mm	$X_m = 0$ $Y_m = 0$ $Z_m = -56$
Mass moment of inertia (x axis, wet mass)	kg mm ²	7.0e4
Mass moment of inertia (y axis, wet mass)	kg mm ²	3.4e5
Mass moment of inertia (z axis, wet mass)	kg mm ²	3.9e5
Materials	-	Stainless Steel, PEEK, Titanium
Interface	-	4 M4 screws (bottom face)

Table 7.5: Simplified FEFP thruster main specifications.

Fig. 7.4 shows the isometric view of the Thruster Unit (completely covered with MLI) and Fig. 7.5 shows the principal views with the overall dimensions.

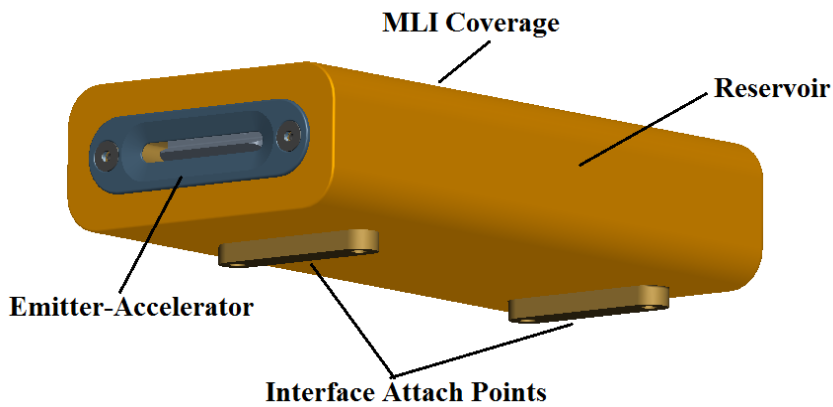


Fig. 7.4: Isometric view of the Thruster Unit.

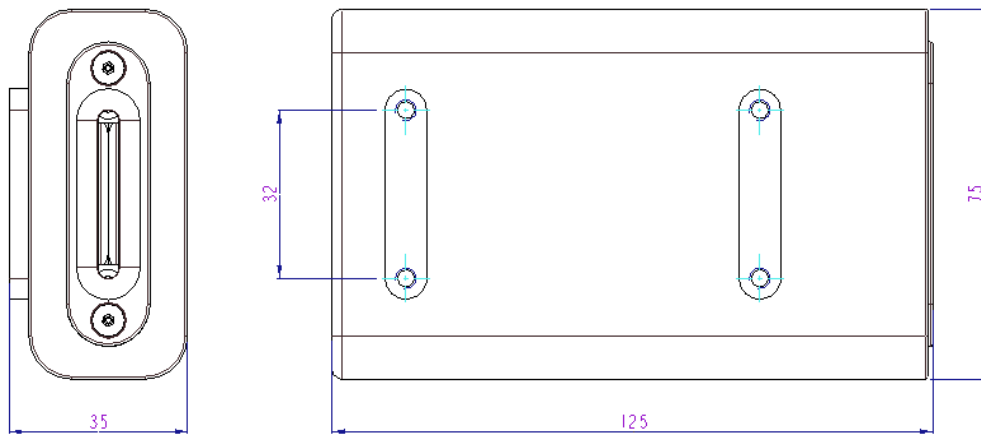


Fig. 7.5: Principal views of the Thruster Unit with overall dimensions.

7.4. Power and Control Unit

The FEFP subsystem is composed of other two main components, the Power Unit and the Control Unit, as described in Sec. 7.2. In the following paragraph, these units are described. The internal structure of the Power and Control Unit, however, is not enough detailed to provide dimensions and mass breakdown, but just to highlight the general architecture and the key components.

Power Unit

The Power Unit is in charge of providing the thruster with a suitable power level to have the FEFP concept working. The high tension required to operate the emitter is supplied by a low tension-high tension converter. This element is the heavier and more power consuming element of the Power Unit and it is the only one considered in this phase.

In order to reduce the thruster overall cost and to assure the maximum reliability of the device a standard off the shelf component has been considered as thruster power supply.

The device selected is the EMCO F-101. This device works with an input tension between 0 and 15 V and returns tensions between 0 and 10 kV. This high voltage range is the one required to have the current lab prototype thruster firing. If the thruster development leads to a reduced emission voltage another model of the EMCO series can be chosen.

The main characteristics of the device are summarized in Table 7.6.

Property	Unit	Value
Mass	g	140
Dimensions	mm	43x71x22
Operating temperature	° C	-10, +50
Efficiency	-	> 70%
Case materials	-	Black Anodized Aluminium
Input voltage	V	0 - 15
Output voltage	V	0 - 10000
Maximum power	W	10
Typical turn-on voltage	V	0.7
Input current (full load)	A	< 1.5
Input current (no load)	A	< 0.5
Output current	A	0.001

Table 7.6: EMCO F-101 series main specifications.

The Power Unit should be placed as close as possible to the Thruster Unit in order to reduce the length of the high voltage cables. However there are not specific constrains on the distance between the two components.

The maximum thruster operating power consumption measured during the lab prototype testing is around 4 W at the rated voltage (+/- 10 kV applied). This value can be very likely reduced by further developments of the thruster.

The power consumption of the heater is estimated to be one order of magnitude smaller than the one of the thruster.

Control Unit

Data exchange between the Remote Unit and the Thruster Unit is handled by the Control Unit. This unit manages the thruster on/off status and receives the signals required to monitoring the thruster (tank temperature, emitter current and voltage). The communication between the Remote Unit and the Thruster System occurs by means of a standard low-speed interface BUS installed on the Control Unit.

The schematic data exchange among the Thruster System components is sketched in Fig.7.6.

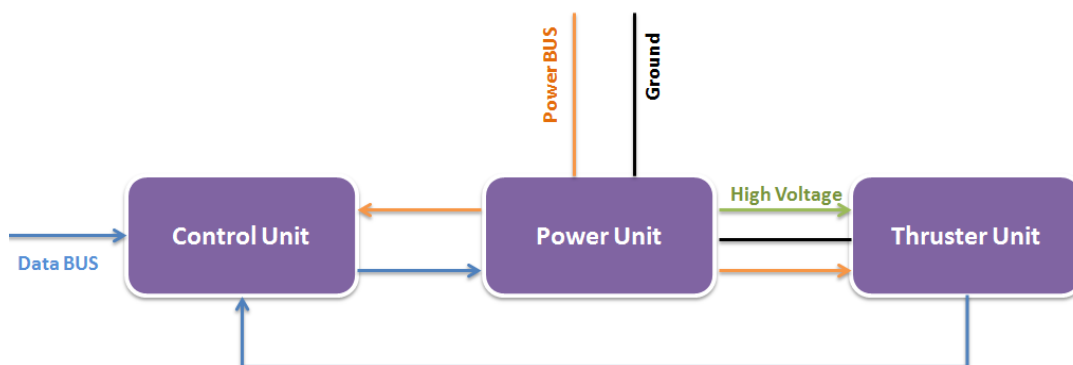


Fig. 7.6: Schematic data exchange among the Thruster Unit components.

The wiring between the Thruster System components includes the following cable types:

- Teledyne Reynolds 187-8781 20 AWG Silicon Coated FEP Wire - 30 kVDC (HV cables between Thruster Unit and EMCO device);
- Axon ESCC 3901.002 polyimide insulated cables (LV cables). If needed shielded cables for signal lines can be used to avoid interference phenomena.

Recent investigations, moreover, suggest that a more sophisticated Control Unit might be considered to satisfy the challenging requirements (e.g. the very high total impulse). For the time being, however, the architecture presented is the one assumed as baseline also based on results of lab experiments.

7.5. Remote Unit and Thruster System Integration

Special attention is required for the thruster integration on the Remote Unit.

There are three main aspects to take care:

- the interaction of the thruster plume with the Remote Unit,
- the potential charging of the Remote Unit,
- the management of data exchange from and to the Thruster System.

Plume impingement issue

The thruster plume should not impact any physical surface to avoid possible damages caused by charged particles.

For this reason any surface of the Remote Unit must be placed outside the thruster plume. Fig. 7.7 shows the definition of the beam divergence half angles.

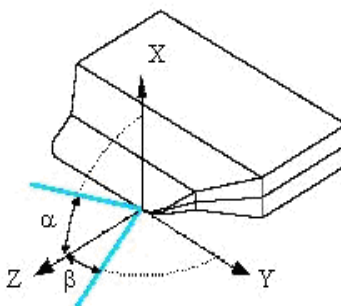


Fig. 7.7: Schematic view of the beam divergence half angles (α , vertical plane; β , horizontal plane).

The plume of ionic liquid FEFP had been characterized by experimental tests on a lab prototype. Typical values resulted to be 10-20 deg in the horizontal plane and 30-40 deg in the vertical plane. The side and frontal view of the plume is shown in Fig. 7.8. In this figure the LV/HV, the larger and heavier component of the Power Unit, is also shown. This component can be placed also at a distance from the thruster body itself.

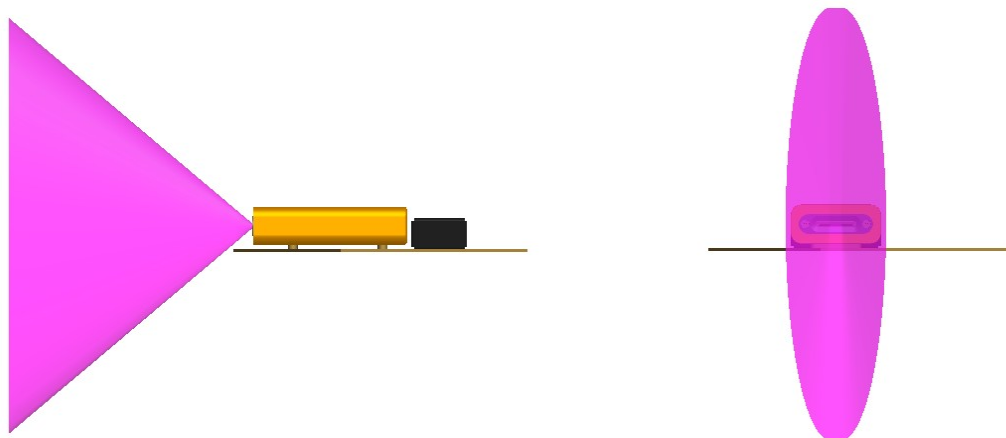


Fig. 7.8: Side and frontal view of the simplified FEED beam plume.

A possible Thruster Unit and EMCO accommodation for two consecutive Remote Unit shield is shown in Fig. 7.9.

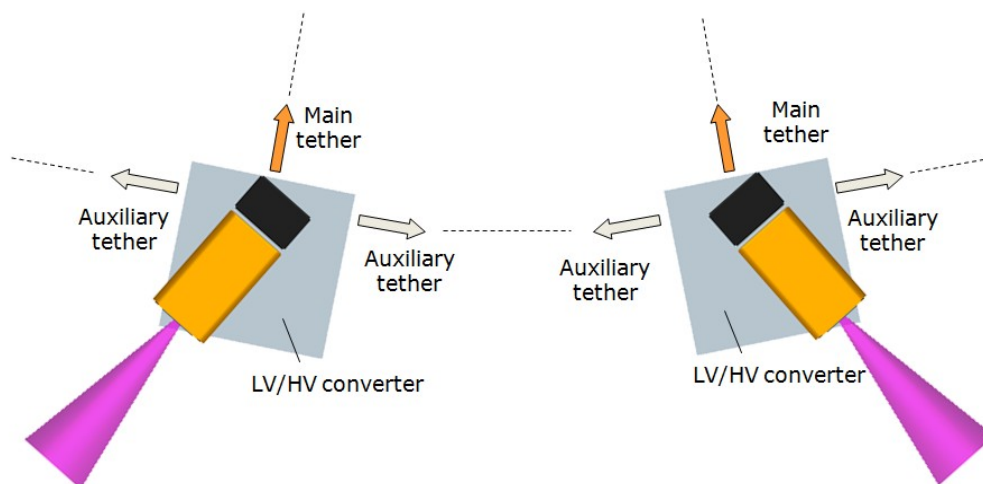


Fig. 7.9: Arrangement of two FEED Thruster Units on two consecutive Remote Units.

Charging issue

The FEED thruster needs a known reference potential for working properly, that is to have a known thrust level. Additionally, the simplified FEED is sought to be operated without a continuous thrust modulation. This implies that the voltage supplied to the Thruster Unit has to be referred to the Remote Unit ground, that is the reference potential.

The FEED thruster produces charge accumulation over the firing time. In the Cs FEED this issue is overcome by using a neutralizer; i.e. an electron source. In the ionic liquids FEED, in principle, this is not necessary if the thruster can be operated in bipolar mode. The switching frequency required, however, is related with the electrical capacitance of the whole system.

A very high switching frequency results if the Remote Unit is electrically insulated from the main spacecraft. Accordingly the Remote Unit could either rely on the rather large capacitance of the long tethers to enable much longer switching periods or it is possible to run different RUs in alternating positive/negative modes (in which case the current would balance mostly through the spacecraft body) to get the switching periods even longer.

A preliminary analysis, with the Remote Unit grounded with the main tethers (ES1-RU-105), leads to consider a switching frequency of the order of 10 Hz that, although not critical for the thruster itself, imposes stringent requirements for the Power and Control Units (larger mass, cost and volume) considering the high voltage levels used for the simplified FEED lab prototype.

Data exchange

Two levels of data exchange is considered to operate the FEED thruster:

- the data exchange between the Thruster Unit and the other components of the Thruster System (Power Unit and Control Unit), see Sec. 7.2;
- the data exchange between the Thruster System and the Remote Unit.

A further level of data exchange for FEED thruster operating is the one between the Remote Unit and the Main Spacecraft. This level is outside of the present study.

A schematic view of the complete data exchange is shown in Fig. 7.10.

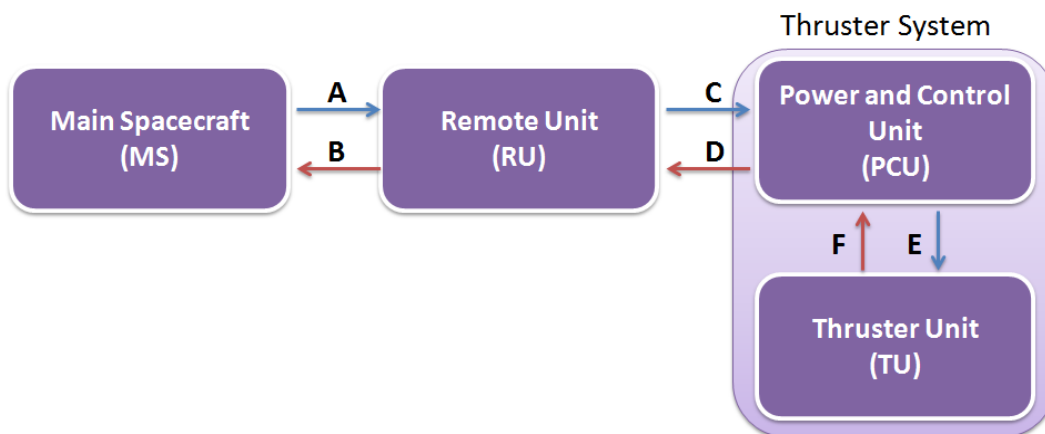


Fig. 7.10: Schematic arrangement of signals between the Thruster System components.

Data exchange between Remote Unit and Thruster System occurs through a standard low-speed interface BUS (I2C, SPI or similar) with a logic level of 0-2.5 V or 0-3.3 V.

Data exchange between Remote Unit and Thruster System is described in Table 7.7.

Index	Components	Data	Type
C	RU - PCU	Thruster on/off	Digital Signals
D	RU - PCU	Thruster status; temperature	Digital Signals
E	PCU - TU	Emitter voltage	Analogical Signals; High Voltage
F	PCU - TU	Thruster temperature; thruster currents, emitter voltage	Analogical Sensors; Low Voltage

Table 7.7: Description of data type within the Thruster System and with the Remote Unit.

In order to minimize the mass impact on the whole Remote Unit, it is assumed that the main bus allows for a voltage regulation at suitable level to have the FEED thruster working at the two thrust level required. Also the temperature regulation is left to the Remote Unit main control. The temperature output given by the thruster is managed by the Remote Unit CPU (ES1-RU-214) to command the FEED tank heater.

FEEP Reference Documents

1. E-sail D41 Requirements specification of the Remote Unit
2. E-sail Design parameters discussion MoM, Tartu, February, 2011
3. E-sail Remote Unit kickoff, MoM, Bremen, April, 2011
4. E-sail Remote Unit component specification, MoM, Uppsala, August, 2011
5. E-sail Remote Unit component design review, MoM, Uppsala, November, 2011
6. E-sail Remote Unit advancement verification, MoM, Uppsala, January, 2012
7. S. Marcuccio, N. Giusti, P. Pergola, "Performance Assessment of Ionic Liquid FEEP", 32nd International Electric Propulsion Conference, Wiesbaden, Germany, September 2011, IEPC-2011-259
8. S. Marcuccio, N. Giusti, P. Pergola, "Development of a Miniaturized Electric Propulsion System for the E-Sail Project", 62nd International Astronautical Federation Congress, Cape Town, South Africa, IAC-11-B4-6A-3-x11311